3

THE SPIN HAMILTONIAN AND THE SPECTRUM

3.1. The spin Hamiltonian

In general a paramagnetic resonance spectrum is rather complex, with lines due to different electronic transitions, which may be further divided into sub-groups of lines by interaction with a nuclear moment. The magnetic fields at which these lines occur alter with the frequency of the applied radiation, and, if anisotropy is present they will also depend on the orientation of the external magnetic field with respect to the crystal axes. Measurement of the spectrum observed under varying conditions of frequency and orientation results in the accumulation of a mass of data, which is bulky and not very meaningful unless some simple interpretation can be found. The solution of this problem lies in the use of a 'spin Hamiltonian', whose form can often be guessed from considerations of crystal symmetry if it cannot be obtained from theory. Such a spin Hamiltonian will contain relatively few terms; its advantage is that a complete description of the experimental data can be presented by giving the size of the coefficients of these terms, together with the directions of the appropriate axes relative to the crystal axes where anisotropy is present. For substances where detailed crystallographic information exists about the paramagnetic ion and its surroundings in the crystal, it is often possible to construct a model and, by carrying through a full treatment of the problem, to derive the spin Hamiltonian, as described in Chapters 16–21. In general the information available is insufficient to give more than rough estimates of the size of the various terms. In other cases crystallographic data may be scanty, but it may be possible to guess a plausible spin Hamiltonian. In either case it is then necessary to relate the spectrum observed under various conditions to a spin Hamiltonian.

As a result of ligand field interaction with the neighbouring diamagnetic ions or atoms in a crystal, the ground state of a paramagnetic ion frequently consists of a group of electronic levels whose separation is a few wave numbers or less, while all other electronic levels lie considerably higher. The behaviour of this group can be represented by defining an 'effective spin' S, such that the total number of levels in the group is $2S+1$, the same as in an ordinary spin multiplet. It is

further required that the matrix elements between the various states determined by the full Hamiltonian that describes the system shall be proportional to those of the effective spin. It is then possible to describe the behaviour of this group of levels by a spin Hamiltonian involving just the effective spin, and where hyperfine interactions are present, the nuclear spins. The use of the symbol S for effective spin may be somewhat misleading at first, but the spin Hamiltonian was initially used for certain cases where the effective spin was the same as the true electronic spin of the ion (for example, the introduction of terms such as S_z^2 to represent splittings due to crystal fields by Van Vleck (1940)). A general form of the spin Hamiltonian (see Chapter 19) for ions of the $3d$ group was derived later, and the use of the symbol S was thus gradually extended. In this chapter no confusion should arise, but in Chapter 1 and later chapters the symbol $\tilde{S}$ is used for the effective spin when it is necessary to distinguish it from the true spin.

The most general form of the spin Hamiltonian contains a large number of terms, representing the Zeeman interaction of the magnetic electrons with an external field, level splittings due to indirect effects of the crystal field (which we shall refer to as 'fine structure'), hyperfine structure due to the presence of nuclear magnetic dipole and electric quadrupole moments in the central ion or in ligand ions, and the Zeeman interaction of the nuclear moment with the external field (which may be modified by induced electronic moments—equivalent to a 'paramagnetic shift'). In this chapter we shall give a fairly detailed but not exhaustive treatment of the relationship between the various terms in the spin Hamiltonian and the observed spectrum, starting with the electronic Zeeman term and including progressively a number of other terms. To keep the complexity within reasonable bounds we shall generally assume some degree of symmetry, for example, that the principal axes of the 'g-tensor' and hyperfine 'tensor' coincide. The extent to which these quantities are justifiably called 'tensors' is discussed in Chapter 15; for simplicity we shall here continue to use the name tensor, omitting the inverted commas but retaining the mental reservations. For example, the electronic Zeeman interaction may be written as

$$\beta\mathbf{H}\,.\,\mathbf{g}\,.\,\mathbf{S} = \beta(g_{xx}H_xS_x+g_{yy}H_yS_y+g_{zz}H_zS_z+g_{xy}H_xS_y+g_{yx}H_yS_x+ \\ +g_{yz}H_yS_z+g_{zy}H_zS_y+g_{zx}H_zS_x+g_{xz}H_xS_z),$$

but if we choose a system where the (x, y, z) axes are the principal

axes this reduces to the form

$$\beta(g_x H_x S_x + g_y H_y S_y + g_z H_z S_z), \tag{3.1}$$

where for shortness g_x has been written for g_{xx}, etc.

3.2. The effect of anisotropy in the g-factor

In order to elucidate the behaviour of a resonance spectrum when anisotropy is present we shall consider first the case of an ion with an anisotropic g-factor, but without any initial splitting of the electronic levels and without any hyperfine structure. A suitable spin Hamiltonian then contains only the terms given in eqn (3.1). If the field **H** is in such a direction that it has direction cosines (l, m, n) with respect to the principal axes (x, y, z) of the g-tensor, the Hamiltonian is

$$\mathscr{H} = \beta H(l g_x S_x + m g_y S_y + n g_z S_z). \tag{3.2}$$

If g were isotropic we could change to a new set of axes (x_e, y_e, z_e) where z_e is parallel to the field **H**, and the Hamiltonian would reduce (using primes to denote components of **S** relative to the new axes) to

$$\mathscr{H} = g\beta H(l S_x + m S_y + n S_z) = g\beta H S'_z \tag{3.3}$$

where $g = g_x = g_y = g_z$. The energy levels are then clearly a set of $(2S+1)$ levels equally spaced in energy by $g\beta H$, and the allowed transitions are those in which the component S'_z changes by one unit, so that they require a quantum

$$h\nu = g\beta H. \tag{3.4}$$

When anisotropy is present, we cannot eliminate the terms off-diagonal in the energy matrix by changing to a set of axes where z_e is parallel to **H**. It is obvious, however, that our Hamiltonian can be written in the form

$$\mathscr{H} = g\beta H(l' S_x + m' S_y + n' S_z),$$

where $gl' = g_x l$, etc. If we now make $(l'^2 + m'^2 + n'^2) = 1$, the Hamiltonian is identical with that for an ion with a spectroscopic splitting factor g, in a field **H** with direction cosines (l', m', n'). Hence the energy levels will be just as given above, and the resonance condition will be given by eqn (3.4), where, from the normalization of the apparent direction cosines (l', m', n') we have

$$g^2 = l^2 g_x^2 + m^2 g_y^2 + n^2 g_z^2. \tag{3.5}$$

In essence, we have diagonalized the energy matrix by changing to a

new set of axes where the z_e-axis has direction cosines (l', m', n') with respect to the principal axes (x, y, z) of the g-tensor.

Evaluation of the transition probability is rather more complicated than in the case of a simple ion with an isotropic g-factor. In the latter case it is possible to choose the z-axis as that of the steady magnetic field $\mathbf{H}$, and the analysis of § 2.9 can be applied, if $\gamma\hbar$ is replaced by $-g\beta$. Then the operator components in eqn (2.56) such as $-l_1\mu_x$ are replaced by $l_1 g\beta S_x$, etc., and for the transition $M \leftrightarrow M-1$ we have, instead of eqn (2.57),

$$\begin{aligned} |\mu_{M,M-1}|^2 &= \tfrac{1}{4}(l_1^2+m_1^2)g^2\beta^2\langle M-1|\, S_-\, |M\rangle^2 \\ &= \tfrac{1}{4}g_1^2\beta^2\langle M-1|\, S_-\, |M\rangle^2 \end{aligned} \tag{3.6}$$

where

$$g_1^2 = (l_1^2+m_1^2)g^2. \tag{3.7}$$

The value of g_1 is clearly a maximum if $\mathbf{H}_1$ is normal to $\mathbf{H}$, when $(l_1^2+m_1^2) = 1$ and $g_1 = g$.

To analyze the position when anisotropy is present, we assume that we have a linearly polarized oscillatory field $H_1 \cos \omega t$, which is in a direction with cosines (l_1, m_1, n_1) with respect to the principal axes of the g-tensor. The 'oscillatory Hamiltonian' is then

$$\mathscr{H}_1 = \beta(l_1 g_x S_x + m_1 g_y S_y + n_1 g_z S_z)H_1 \cos \omega t. \tag{3.8}$$

This must be referred to the system of axes (x_e, y_e, z_e) in which the Hamiltonian (3.2) is diagonal. We can write the result formally as

$$\mathscr{H}_1 = \beta H_1(g_{1x}S'_x + g_{1y}S'_y + g_{1z}S'_z) \cos \omega t \tag{3.8a}$$

$$= \beta H_1\{\tfrac{1}{2}(g_{1x} - \mathrm{i}g_{1y})S'_+ + \tfrac{1}{2}(g_{1x} + \mathrm{i}g_{1y})S'_- + g_{1z}S'_z\} \cos \omega t. \tag{3.8b}$$

The square of the matrix element for the transition $M \leftrightarrow M-1$ is

$$|\mu_{M,M-1}|^2 = \tfrac{1}{4}g_1^2\beta^2\langle M-1|\, S'_-\, |M\rangle^2 \tag{3.9}$$

where, after some reduction, it can be shown that one obtains a value of g_1 analogous to that given above (eqn (3.7)) given by

$$g_1^2 = (g_{1x})^2 + (g_{1y})^2 \tag{3.10}$$

$$= (l_1^2 g_x^2 + m_1^2 g_y^2 + n_1^2 g_z^2) - g^{-2}(l_1 l g_x^2 + m_1 m g_y^2 + n_1 n g_z^2)^2, \tag{3.10a}$$

where g is given by eqn (3.5). An alternative form of this is

$$g_1^2 g^2 = g_x^2 g_y^2 (l_1 m - l m_1)^2 + g_y^2 g_z^2 (m_1 n - m n_1)^2 + g_z^2 g_x^2 (n_1 l - n l_1)^2. \tag{3.10b}$$

To find the optimum direction of $\mathbf{H}_1$ from these equations we note

that, from eqn (3.10b), g_1 vanishes if $l_1 = l$, $m_1 = m$, $n_1 = n$; that is, if $\mathbf{H}_1$ is parallel to $\mathbf{H}$ (this follows also from the fact that (3.8) would then transform like (3.3) into a single term containing only S'_z). Thus we conclude that $\mathbf{H}_1$ should be normal to $\mathbf{H}$ to have the maximum effect, since any component parallel to $\mathbf{H}$ would be ineffective. (Note that this does not in general mean that the coefficient of $H_1 S'_z$ is then zero.) The value of g_1 will still depend on the orientation of $\mathbf{H}_1$ in the plane normal to $\mathbf{H}$, so that there will be a specific orientation of $\mathbf{H}_1$ which gives the greatest intensity.

This behaviour can be understood more clearly by considering a special case. Let us suppose that $\mathbf{H}$ is confined to the plane $y = 0$, and that it is at an angle θ with the z-axis. We retain the general condition that g_x, g_y, g_z are all unequal, but if $g_x = g_y = g_\perp$, so that the z-axis is a symmetry axis, the treatment will apply generally since we can then always choose our x-axis so that $\mathbf{H}$ lies in the zx-plane.

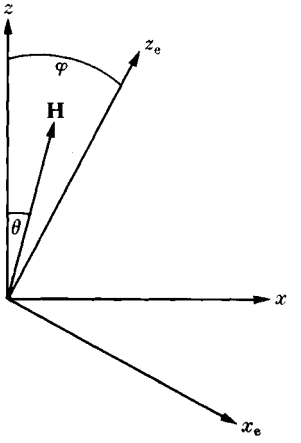

FIG. 3.1. Rotation of axes (z_e, x_e) from axes (z, x) through angle ϕ about y-axis, where $\tan\phi = (g_x/g_z)\tan\theta$. Note that unless g_x, g_z are both positive, z_e lies in a different quadrant from $\mathbf{H}$. The equations relating the two systems (where primes indicate components in the x_e, z_e system) are (see eqns (3.11), (3.13), (3.13a), (3.14)).

$$S_z = S'_z\cos\phi - S'_x\sin\phi = (g_z/g)S'_z\cos\theta - (g_x/g)S'_x\sin\theta,$$
$$S_x = S'_z\sin\phi + S'_x\cos\phi = (g_x/g)S'_z\sin\theta + (g_z/g)S'_x\cos\theta,$$
$$S_y = S'_y.$$

If we change to a set of axes (x_e, y_e, z_e) rotated about the y-axis by an angle ϕ (see Fig. 3.1), this requires the transformation

$$\begin{aligned} S_z &= S'_z\cos\phi - S'_x\sin\phi, \\ S_x &= S'_z\sin\phi + S'_x\cos\phi. \end{aligned} \tag{3.11}$$

Then

$$\begin{aligned}\mathscr{H} &= \beta H(g_x S_x \sin\theta + g_z S_z \cos\theta) \\ &= \beta H \begin{Bmatrix} S'_x(g_x \sin\theta\cos\phi - g_z \cos\theta \sin\phi) + \\ + S'_z(g_x \sin\theta \sin\phi + g_z \cos\theta\cos\phi) \end{Bmatrix}\end{aligned} \tag{3.12}$$

and we can make the coefficient of S'_x vanish by choosing the angle ϕ such that

$$\tan\phi = (g_x/g_z)\tan\theta. \tag{3.13}$$

If we define g by the equation

$$g^2 = g_x^2 \sin^2\theta + g_z^2 \cos^2\theta, \tag{3.14}$$

which is clearly a special case of eqn (3.5), then we have

$$\sin\phi = (g_x/g)\sin\theta, \quad \cos\phi = (g_z/g)\cos\theta \tag{3.13a}$$

and the Hamiltonian reduces to the form $\mathscr{H} = g\beta H S'_z$.

Suppose now that $\mathbf{H}_1$ is applied in a direction making an angle η with the y-axis, and that its projection on the xz-plane makes an angle θ_1 with the z-axis. Then the components of $\mathbf{H}_1$ are $H_x = H_1 \sin\eta \sin\theta_1$, $H_y = H_1 \cos\eta$ and $H_z = H_1 \sin\eta \cos\theta_1$. On transforming to the (x_e, y_e, z_e) axes the oscillatory Hamiltonian becomes

$$\mathscr{H}_1 = \beta H_1 \cos\omega t \begin{Bmatrix} S'_x(g_x g_z/g)\sin\eta \sin(\theta_1 - \theta) + \\ + S'_y g_y \cos\eta + \\ + S'_z g^{-1}(g_x^2 \sin\theta \sin\theta_1 + g_z^2 \cos\theta\cos\theta_1)\sin\eta \end{Bmatrix}. \tag{3.15}$$

From this the value of g_1 is found to be given by

$$g_1^2 = (g_x g_z/g)^2 \sin^2\eta \sin^2(\theta_1 - \theta) + g_y^2 \cos^2\eta. \tag{3.16}$$

It is clear from this equation that the best value of θ_1 is $\theta \pm \pi/2$, i.e. the oscillatory field should be in the plane normal to $\mathbf{H}$. The best value of η is then either 0 or $\pi/2$, depending on whether $|g_y|$ is greater or less than $|(g_x g_z/g)|$. With axial symmetry ($g_x = g_y = g_\perp$, $g_z = g_\parallel$) this condition reduces to making $\eta = 0$ if $|g_\perp| > |g_\parallel|$, and $\eta = \pi/2$ if $|g_\perp| < |g_\parallel|$, since g always lies between $|g_\parallel|$ and $|g_\perp|$.

Note that if $g_x = g_y = 0$ then $g_1 = 0$, corresponding to the fact that there are no allowed transitions.

Determination of the sign of the g-values

Though g is essentially positive for a free electron, the signs of the principal g-values in the spin Hamiltonian using an effective spin are

not known *a priori*, and the question arises, how far can they be determined experimentally? The spectrum is not changed by reversing the direction of $\mathbf{H}$, and reversal of $\mathbf{H}_1$ is equivalent to a simple phase change if $\mathbf{H}_1$ is linearly polarized. If circularly polarized radiation is used, however, a comparison of the relative intensities of a given transition using right- and left-handed senses can be used to obtain information about signs. This will be discussed for the special case where $\mathbf{H}$ lies in the xz-plane at an angle θ to the z-axis just considered.

The oscillatory Hamiltonian for a field $\mathbf{H}_1$ (perpendicular to $\mathbf{H}$) rotating in the right-handed sense about $\mathbf{H}$ is

$$\mathscr{H} = \beta H_1\{(+g_x S_x \cos\theta - g_z S_z \sin\theta)\cos\omega t + g_y S_y \sin\omega t\}. \quad (3.17)$$

(By changing the sign of ω a field rotating in the opposite sense would be obtained.) On transforming to the (x_e, y_e, z_e) axes in which the static Zeeman energy is diagonalized, the oscillatory Hamiltonian becomes (using eqns (3.11), (3.13a) and $S'_{\pm} = S'_x \pm iS'_y$),

$$\mathscr{H} = \tfrac{1}{4}\beta H_1 \left[\begin{array}{l} S'_+\left\{\left(\frac{g_x g_z}{g} - g_y\right)e^{i\omega t} + \left(\frac{g_x g_z}{g} + g_y\right)e^{-i\omega t}\right\} + \\ +S'_-\left\{\left(\frac{g_x g_z}{g} + g_y\right)e^{i\omega t} + \left(\frac{g_x g_z}{g} - g_y\right)e^{-i\omega t}\right\} + \\ +S'_z\left\{\left(\frac{g_x^2 - g_z^2}{g}\right)\sin 2\theta(e^{i\omega t} + e^{-i\omega t})\right\} \end{array}\right]. \quad (3.18)$$

We now assume that the sign of g is always positive, thereby resolving the sign ambiguity in eqns (3.5) and (3.14). (If either g_x, g_z or both have negative signs, this means that the z_e-axis lies in a different quadrant from $\mathbf{H}$ in Fig. 3.1.) It then follows that the level with $S'_z = M$ lies higher in energy than $M-1$, and on calculating the intensity of the transition between these two levels by the methods of § 2.3 it is found to be proportional to $\{(g_x g_z/g)+g_y\}^2$ for radiation that is right-hand circularly polarized about $\mathbf{H}$, and to $\{(g_x g_z/g)-g_y\}^2$ for the opposite sense. Since g is taken to be always positive, experimental observation of which sense gives the higher intensity yields the sign of $g_x g_z$ relative to g_y, i.e. it determines whether the quantity $(g_x g_y g_z)$ is positive or negative. In § 15.6 it is shown that this quantity is invariant.

3.3. Multipole fine structure

When $S = 1$ or more, an additional splitting of the energy levels may appear due to indirect effects of the crystal field. This may be represented by adding to the spin Hamiltonian terms of higher powers

in S_x, S_y, S_z. It is convenient to group such terms into combinations of spin operators, each such operator being the equivalent of a combination of spherical harmonics. This has the advantage that the appropriate spin Hamiltonian can generally be written down without detailed calculation, since it must reflect the symmetry of the crystal field. If the latter has trigonal symmetry, for example, it is only necessary to include the spin operators corresponding to spherical harmonics with threefold or higher symmetry about the trigonal axis. The number of such spin operators is further limited by the more general restriction that spin operators of odd degree are excluded because they are not invariant under time reversal. Also operators of degree higher than $2S$ can be omitted since they have zero matrix elements; thus for $S = 1$ or $\frac{3}{2}$, only terms of the second degree are required; for $S \geqslant 2$, terms of the fourth degree must be included, and for $S \geqslant 3$, terms of the sixth degree. In general, the spin Hamiltonian may be written (in the absence of hyperfine structure) as

$$\mathscr{H} = \beta(\mathbf{H} \cdot \mathbf{g} \cdot \mathbf{S}) + \sum_{k,q} B_k^q O_k^q, \tag{3.19}$$

where O_k^q is a spin operator. The more important equivalent operators are listed in Table 16 in terms of angular momentum J; expressions identical with these, except for the replacement of J by S, are required in eqn (3.19).

The use of spin operators of this form has several advantages. The matrix elements of such operators are tabulated; these elements are diagonal for operators with $q = 0$, and off-diagonal when $q \neq 0$. Thus in a very strong magnetic field parallel to the z-axis of the spin operators only the matrix elements of the operators with $q = 0$ are required for a first order perturbation calculation. When the magnetic field is applied in a different direction, it is sometimes convenient to use the standard formulae for the rotation of axes of spherical harmonics to transform to a system where **H** is again along the 'polar' axis. This means that the corresponding combination of spherical harmonics can be transformed to the new axes, after which the new set of spin operators can be written down to correspond with the new combination of spherical harmonics (see, for example, Bleaney, Scovil, and Trenam (1954); Baker and Williams (1961)). (In this procedure it must be remembered that the spherical harmonics contain normalizing coefficients that unfortunately have not been included in a systematic way in the spin operators.) Then in strong magnetic fields the spectrum is determined by the new set of coefficients of the operators O_k^0, which

are of course related to the original set of coefficients B_k^q in a known way. Thus by observation of the spectrum at a sufficient variety of angles, all the coefficients B_k^q can be determined.

In a case where a number of multipole spin operators are required, there will in general be more than one interpretation depending on the identification of the observed lines with the various allowed transitions. However, the fact that different transitions have different intensities is of considerable help in the identification. For example, in strong magnetic fields (Zeeman energy $\gg$ multipole energy), the strongly allowed transitions are those for which $\Delta M = \pm 1$, and the intensity of the $M \leftrightarrow M-1$ transition is proportional to $S(S+1)-M(M-1)$.

When measurements of the positions of the spectral lines as a function of angle have been completed, the *relative* signs of the coefficients B_k^q are determined as well as the magnitudes. There is, however, an ambiguity in the overall sign, which arises as follows. The reversal of the direction of flow of time ('time reversal') is an operation which does not change the energy spectrum of a Hermitian operator since, as shown in Chapter 15, time reversal is an antiunitary operator. However, under such an operation the spin components S_x, S_y, S_z change their sign and the Hamiltonian (3.19), in which all the indices k are even, becomes

$$\mathscr{H}' = -\beta(\mathbf{H} \,.\, \mathbf{g} \,.\, \mathbf{S}) + \sum_{k,q} B_k^q O_k^q. \tag{3.19a}$$

The Hamiltonian (3.19a) must have the same energy spectrum as (3.19) and, since in a resonance experiment only differences of energy are measured, (3.19a) must have the same *resonance* spectrum as

$$-\mathscr{H}' = \beta(\mathbf{H} \,.\, \mathbf{g} \,.\, \mathbf{S}) - \sum_{k,q} B_k^q O_k^q. \tag{3.19b}$$

A comparison of (3.19) and (3.19b), which differ only in the reversed signs of all the B_k^q but correspond to the same resonance spectrum, shows that the absolute signs of the B_k^q remain undetermined.

This ambiguity can be resolved by observation of the relative intensities of the different lines as the temperature is reduced towards the region where kT is comparable with the overall splitting of the energy levels. The population of the lower levels will then be increased at the expense of that of the higher levels, and transitions between the lowest levels will gain in intensity noticeably over transitions between the highest levels; from this the order of the levels can be found. With

this information, the absolute signs of the spin operator terms can be found; an example of this is given in § 3.6.

3.4. Fine structure in cubic fields ($S = \frac{5}{2}, \frac{7}{2}$)

The highest degeneracy left in a crystal field even of cubic symmetry is usually only fourfold, corresponding to an effective spin of $S = \frac{3}{2}$. Hence magnetic resonance spectra corresponding to $S = 2$ or more occur normally only for ions with half-filled electron shells, where the free ion is in an S-state that is split in the solid state by rather small amounts through higher-order effects of the crystalline field. Examples are $3d^5$, ${}^6S_{\frac{5}{2}}$, (Mn^{2+}, Fe^{3+}) and $4f^7$, $5f^7$, ${}^8S_{\frac{7}{2}}$, (Eu^{2+}, Gd^{3+}, Cm^{3+}). In these cases g is isotropic and very close to the free-spin value; a special case of some interest is that of cubic symmetry, and this will be considered first.

Formulae for $S = \frac{5}{2}$

In terms of Cartesian coordinates, the potential term of the fourth degree with cubic symmetry that satisfies Laplace's equation is

$$x^4+y^4+z^4-\tfrac{3}{5}r^4. \tag{3.20}$$

This has the operator equivalent

$$\tfrac{1}{6}a\{S_x^4+S_y^4+S_z^4-\tfrac{1}{5}S(S+1)(3S^2+3S-1)\}. \tag{3.21}$$

The coefficient a is that used in early work on paramagnetic salts with spin $S = \frac{5}{2}$. In terms of the operator equivalents listed in Table 16 the fourth degree cubic operator may be written as

$$B_4\{O_4^0+5O_4^4\} \tag{3.22a}$$

$$= -\tfrac{2}{3}B_4\{O_4^0+20\sqrt{(2)}O_4^3\}, \tag{3.22b}$$

where the first form is referred to the fourfold axes and the second to the threefold axes. The numerical relation between these and the earlier form is expressed by the relation

$$a = 120B_4.$$

The matrix elements of the spin operators are given in Table 17. For either (3.22a) or (3.22b) there is only one off-diagonal element, so that the energy levels are given by quadratic expressions. The matrix elements of the Zeeman interaction are diagonal if we take its direction to be the z-axis, and if the magnetic field is directed along either a fourfold or threefold axis we again have only one off-diagonal element

TABLE 3.1

Energy levels and states for $S = \frac{5}{2}$, cubic field, magnetic field along fourfold axis

$$\mathscr{H} = g\beta HS_z + (a/120)\{O_4^0 + 5O_4^4\} \tag{3.22c}$$

Energy matrix

$$\begin{array}{l|cc|} \pm\frac{5}{2} & \pm\frac{5}{2}g\beta H + \frac{1}{2}a, & \frac{1}{2}\sqrt{(5)}a \\ \mp\frac{3}{2} & \frac{1}{2}\sqrt{(5)}a & \mp\frac{3}{2}g\beta H - \frac{3}{2}a \\ \pm\frac{1}{2} & \pm\frac{1}{2}g\beta H + a & \end{array}$$

States	*Energy levels*
$\cos\alpha\,\lvert\pm\frac{5}{2}\rangle + \sin\alpha\,\lvert\mp\frac{3}{2}\rangle$	$\frac{1}{2}(\pm g\beta H - a) + \{(a \pm 2g\beta H)^2 + 5a^2/4\}^{\frac{1}{2}}$
$\sin\alpha\,\lvert\pm\frac{5}{2}\rangle - \cos\alpha\,\lvert\mp\frac{3}{2}\rangle$	$\frac{1}{2}(\pm g\beta H - a) - \{(a \pm 2g\beta H)^2 + 5a^2/4\}^{\frac{1}{2}}$
$\lvert\pm\frac{1}{2}\rangle$	$\pm\frac{1}{2}g\beta H + a$

Here the upper signs must be taken with $\tan 2\alpha = \sqrt{(5)}\,a/(2a + 4g\beta H)$ and the lower signs with $\tan 2\alpha = \sqrt{(5)}\,a/(2a - 4g\beta H)$.

of the cubic field, provided we use the operator expression whose 'polar' axis is the direction of **H**. The energy matrices, energy levels, and states are given in Tables 3.1 and 3.2.

In zero magnetic field the levels reduce to a quadruplet state at $+a$, and a doublet at $-2a$; these are just the fourfold Γ_8 and twofold Γ_7 levels into which a level with angular momentum $\frac{5}{2}$ splits in a cubic field (see § 14.4). We shall evaluate the zero-field states, from which we also obtain the first-order weak-field Zeeman effect for a magnetic field along the fourfold and threefold axes. A complete series expansion including the second-order Zeeman effect in weak fields ($g\beta H \ll a$)

TABLE 3.2

Energy levels and states for $S = \frac{5}{2}$, cubic field, magnetic field along threefold axis

$$\mathscr{H} = g\beta HS_z - (a/180)\{O_4^0 + 20\sqrt{(2)}O_4^3\} \tag{3.22d}$$

Energy matrix

$$\begin{array}{l|cc|} \pm\frac{5}{2} & \pm\frac{5}{2}g\beta H - \frac{1}{3}a & \mp\frac{1}{3}\sqrt{(20)}a \\ \mp\frac{1}{2} & \mp\frac{1}{3}\sqrt{(20)}a & \mp\frac{1}{2}g\beta H - \frac{2}{3}a \\ \pm\frac{3}{2} & \pm\frac{3}{2}g\beta H + a & \end{array}$$

States	*Energy levels*
$\cos\alpha\,\lvert\pm\frac{5}{2}\rangle + \sin\alpha\,\lvert\mp\frac{1}{2}\rangle$	$\pm g\beta H - \frac{1}{2}a + \frac{1}{6}\{(a \pm 9g\beta H)^2 + 80a^2\}^{\frac{1}{2}}$
$\sin\alpha\,\lvert\pm\frac{5}{2}\rangle - \cos\alpha\,\lvert\mp\frac{1}{2}\rangle$	$\pm g\beta H - \frac{1}{2}a - \frac{1}{6}\{(a \pm 9g\beta H)^2 + 80a^2\}^{\frac{1}{2}}$
$\lvert\pm\frac{3}{2}\rangle$	$\pm\frac{3}{2}g\beta H + a$

Here the upper signs must be taken with $\tan 2\alpha = -\sqrt{(80)}a/(a + 9g\beta H)$ and the lower signs with $\tan 2a = \sqrt{(80)}a/(a - 9g\beta H)$.

for an arbitrary direction of the magnetic field is given by Kronig and Bouwkamp (1939).

Weak-field Zeeman effect ($g\beta H \ll a$)

We consider first the Γ_7 doublet at energy $-2a$. The states referred to the fourfold and threefold axes, and the energy in a weak field along these axes are given in Table 3.3. We see at once that the Zeeman

TABLE 3.3

Energy levels and states for $S = \frac{5}{2}$, Γ_7 *doublet in weak magnetic field* ($g\beta H \ll a$)

States (fourfold axis)	Energy	States (threefold axis)
$\sqrt{(\frac{1}{6})}\,\vert+\frac{5}{2}\rangle-\sqrt{(\frac{5}{6})}\,\vert-\frac{3}{2}\rangle$	$-2a-\frac{5}{6}g\beta H$	$\sqrt{(\frac{4}{5})}\,\vert-\frac{5}{2}\rangle+\sqrt{(\frac{5}{5})}\,\vert+\frac{1}{2}\rangle$
$\sqrt{(\frac{1}{6})}\,\vert-\frac{5}{2}\rangle-\sqrt{(\frac{5}{6})}\,\vert+\frac{3}{2}\rangle$	$-2a+\frac{5}{6}g\beta H$	$\sqrt{(\frac{4}{5})}\,\vert+\frac{5}{2}\rangle-\sqrt{(\frac{5}{5})}\,\vert-\frac{1}{2}\rangle$

splitting is the same along the fourfold and threefold axes; in fact the Γ_7 doublet has an isotropic g-factor, as we would expect for a doublet in a cubic field. In representing the doublet by a spin-Hamiltonian with an effective spin $\tilde{S} = \frac{1}{2}$, we must identify the state $\tilde{S}_z = +\frac{1}{2}$ with that on the upper line, and $\tilde{S}_z = -\frac{1}{2}$ with that on the lower line, since we need the operator $\tilde{S}_-$ to take us from the former to the latter in the one representation and S_- in the other. This means that the effective g-factor for the weak-field Zeeman effect (and hence for the representation $\tilde{S} = \frac{1}{2}$) is $-\frac{5}{3}g$; this is a simple example of a case where the effective g-factor is negative.

We consider now the Γ_8 quadruplet at energy $+a$. The unusual behaviour of such a quadruplet will be discussed for the general case in Chapter 18, where it is shown that the fourfold manifold of states can be fitted with a spin Hamiltonian of the form

$$\mathscr{H} = g'\beta(H_x\tilde{S}_x+H_y\tilde{S}_y+H_z\tilde{S}_z)+g''\beta(H_x\tilde{S}_x^3+H_y\tilde{S}_y^3+H_z\tilde{S}_z^3) \quad (3.22e)$$

with $\tilde{S} = \frac{3}{2}$. This Zeeman interaction is a special case of the general vector **V** discussed in Chapter 18 where the matrix elements of V_z are

$$\langle+\tfrac{3}{2}|\,V_z\,|+\tfrac{3}{2}\rangle = -\langle-\tfrac{3}{2}|\,V_z\,|-\tfrac{3}{2}\rangle = P = \beta H_z(\tfrac{3}{2}g'+\tfrac{27}{8}g'')$$
$$\langle+\tfrac{1}{2}|\,V_z\,|+\tfrac{1}{2}\rangle = -\langle-\tfrac{1}{2}|\,V_z\,|-\tfrac{1}{2}\rangle = Q = \beta H_z(\tfrac{1}{2}g'+\tfrac{1}{8}g'').$$

Here the (x, y, z) axes are the fourfold cubic axes, so that the matrix elements of V_z give the Zeeman interaction for a field along one of the fourfold axes in the weak field case where $\beta H \ll a$. The energy levels of the Γ_8 quadruplet of $S = \frac{5}{2}$ for this case are shown in Fig. 3.2(a),

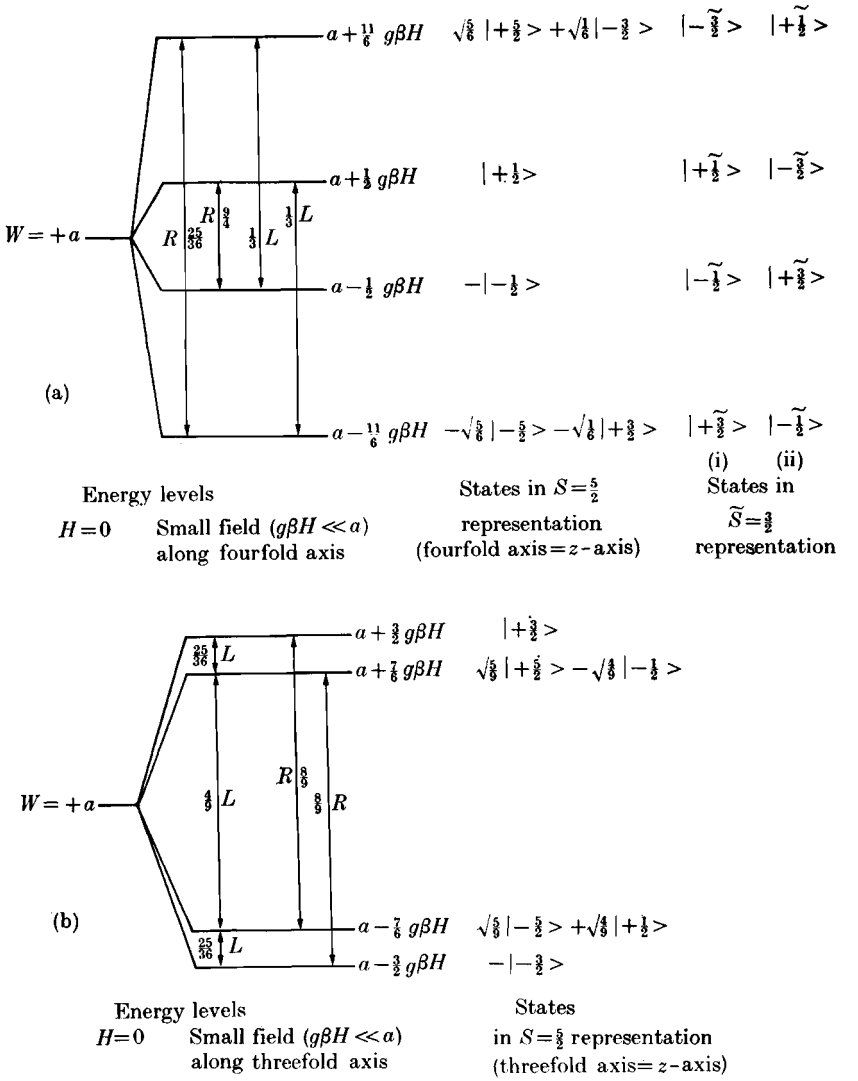

FIG. 3.2. (a) Energy levels in weak magnetic field along the fourfold axis for the Γ_8 quadruplet of $S=\frac{5}{2}$ in a strong cubic crystal field. The states have two alternative representations in $\widetilde{S}=\frac{3}{2}$; in the nomenclature of Chapter 18, eqn (18.16), the choice labelled (i) above requires $P=-(\frac{11}{6})g\beta H, Q=+\frac{1}{2}g\beta H$, while (ii) requires $P=-\frac{1}{2}g\beta H$, $Q=+(\frac{11}{6})g\beta H$. The symbol R by a transition indicates that it requires right-handed circular polarization, while L requires left-handed polarization, if circularly polarized radiation is used. The numbers indicate the relative intensities. (b) Energy levels in weak magnetic field along threefold axis for the Γ_8 quadruplet of $S=\frac{5}{2}$ in a strong cubic crystal field. The symbols R, L indicate whether right- or left-handed polarization is required, if circularly polarized radiation is used. The numbers indicate the relative intensities. The Zeeman splittings agree with those calculated from eqn (18.36), using either of the two sets of values for P, Q given above.

together with the states calculated from eqn (3.22c). These can be identified with the four states of $\tilde{S} = \frac{3}{2}$ in two ways, as shown on the diagram. These require either $P = -(\frac{11}{6})g\beta h$, $Q = +\frac{1}{2}g\beta H$ or $P = -\frac{1}{2}g\beta H$, $Q = +(\frac{11}{6})g\beta H$, where g is of course the parameter in eqn (3.22c) and not either of those in eqn (3.22e).

The Zeeman interaction is anisotropic; its value for an arbitrary direction of the magnetic field can be found from eqn (18.30) or from the expressions given by Kronig and Bouwkamp. For the particular case of a field along a threefold axis the levels are shown in Fig. 3.2(b), together with the states calculated from eqn (3.22d) where the threefold axis is taken as the z- or polar axis. It is readily verified that the Zeeman splittings agree with those calculated from eqn (18.36).

If circularly polarized radiation is used, some of the transitions require right-handed polarization and some left-handed polarization. In terms of the states formed from $S = \frac{5}{2}$, all transitions are of the type $\Delta M = \pm 1$, that is they are allowed (as we should expect) between levels whose states contain values of S_z differing by one unit. The polarization rule can be stated as follows; in a transition of the form $M \leftrightarrow M-1$, right-handed polarization is required if the level $M-1$ lies lower in energy than M, and left-handed polarization if it lies higher. The polarization rules and the relative intensities are also shown in Figs. 3.2(a) and 3.2(b).

Strong-field Zeeman effect ($g\beta H \gg a$)

To the second order in perturbation theory, the energy levels in a strong magnetic field (see also Kronig and Bouwkamp) with direction cosines (l, m, n) are given in Table 3.4, and the strong transitions in

TABLE 3.4

Energy levels for $S = \frac{5}{2}$, *cubic field, with strong magnetic field* H *along direction* (l, m, n) *with respect to the fourfold axes*

States	Energy levels
$\pm\frac{5}{2}$	$\pm\frac{5}{2}g\beta H + \frac{1}{2}pa \pm (212 - 24p - 113p^2)(a^2/240g\beta H)$
$\pm\frac{3}{2}$	$\pm\frac{3}{2}g\beta H - \frac{3}{2}pa \pm (12 + 8p - 15p^2)(a^2/16g\beta H)$
$\pm\frac{1}{2}$	$\pm\frac{1}{2}g\beta H + pa \pm (-2 - 3p + 5p^2)(a^2/3g\beta H)$

Table 3.5. In these tables $p = 1 - 5(l^2m^2 + m^2n^2 + n^2l^2)$; the quantum numbers labelling the states, and the relative intensities, are exact only in the strong field limit $(a/g\beta H) \to 0$.

TABLE 3.5

Resonance transitions ($\Delta M = \pm 1$) *and approximate relative intensities for* $S = \frac{5}{2}$, *cubic field, in strong magnetic field* ($g\beta H \gg a$)

Transition	Position	Relative intensity
$+\frac{5}{2} \leftrightarrow +\frac{3}{2}$	$h\nu = g\beta H + 2pa + (2 - 9p + 7p^2)(a^2/15g\beta H)$	5
$+\frac{3}{2} \leftrightarrow +\frac{1}{2}$	$g\beta H - \frac{5}{2}pa + (68 + 72p - 125p^2)(a^2/48g\beta H)$	8
$+\frac{1}{2} \leftrightarrow -\frac{1}{2}$	$g\beta H + (-2 - 3p + 5p^2)(2a^2/3g\beta H)$	9
$-\frac{1}{2} \leftrightarrow -\frac{3}{2}$	$g\beta H + \frac{5}{2}pa + (68 + 72p - 125p^2)(a^2/48g\beta H)$	8
$-\frac{3}{2} \leftrightarrow -\frac{5}{2}$	$g\beta H - 2pa + (2 - 9p + 7p^2)(a^2/15g\beta H)$	5

In sufficiently strong fields, where terms of order $a^2/g\beta H$ can be neglected, the resonance spectrum consists just of the five lines for which $\Delta M = \pm 1$. Their relative intensities follow from the square of the matrix elements, which is just $S(S+1) - M(M-1)$ for the transition $M \leftrightarrow M-1$. The lines form a symmetrical pattern, as shown in Fig. 3.3(a); the spectrum retains the same form for all directions of **H**, but with varying displacements of the outer lines depending on the quantity p. This displacement varies with angle in the same way as the cubic potential, since p can be written in the form

$$2p/5 = l^4 + m^4 + n^4 - \tfrac{3}{5}.$$

The extreme values of p are $+1$ along a $\langle 100 \rangle$ axis and $-\frac{2}{3}$ along a $\langle 111 \rangle$ axis, with another stationary value of $-\frac{1}{4}$ along an $\langle 011 \rangle$ axis. In the important cube planes p varies as follows:

$\{111\}$ plane: $p = -\frac{1}{4}$ (invariant).

$\{001\}$ plane: $p = 1 - \frac{5}{4}\sin^2 2\theta$, where $\theta = 0$ along a $\langle 100 \rangle$ axis.

$\{01\bar{1}\}$ plane: $p = 1 - 5\sin^2\theta + \frac{15}{4}\sin^4\theta$, where $\theta = 0$ along a $\langle 100 \rangle$ axis.

The last plane is important, as it contains the $\langle 100 \rangle$, $\langle 111 \rangle$, and $\langle 011 \rangle$ axes.

Formulae for $S = \frac{7}{2}$

For ions where $S = 3$ or more, terms of the sixth degree must also be included. The full operator equivalent for the case of cubic symmetry then becomes

$$B_4(O_4^0 + 5O_4^4) + B_6(O_6^0 - 21O_6^4)$$
$$= -\tfrac{2}{3}B_4\{O_4^0 + 20\sqrt{(2)}O_4^3\} + (\tfrac{1}{9}\tfrac{6})B_6[O_6^0 - \{35/\sqrt{(8)}\}O_6^3 + (\tfrac{7}{8}\tfrac{7})O_6^6], \quad (3.23)$$

where the first form is that referred to the four fold axes and the second that referred to the three fold axes. The case most generally

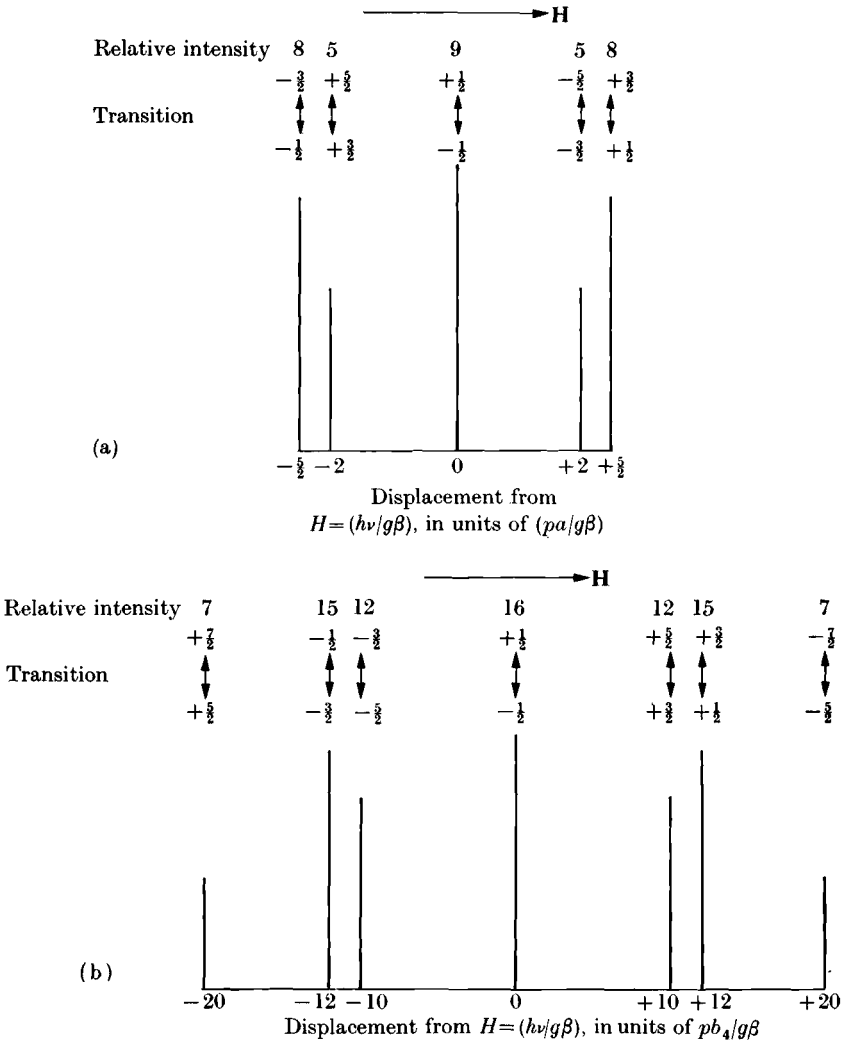

FIG. 3.3. (a) Spectrum for $S = \frac{5}{2}$, cubic field splitting, in strong magnetic field. (b) Spectrum for $S = \frac{7}{2}$ cubic crystal field splitting of fourth degree only, in strong magnetic field. In each case constant frequency and variable field are assumed.

encountered is that of $S = \frac{7}{2}$, for the ions with configuration f^7. For this case closed formulae for the levels can be given only when the magnetic field is directed along one of the $\langle 001 \rangle$ axes (see Table 3.6).

These results show that the values of α, β when $H = 0$ become independent of b_4, b_6 so that the states are uniquely determined. In a cubic field $S = \frac{7}{2}$ splits into two doublets Γ_6, Γ_7 and a quadruplet Γ_8;

TABLE 3.6

Energy levels and states for $S = \frac{7}{2}$, cubic field, with magnetic field **H** *along an* $\langle 001 \rangle$ *axis*

States	Levels
$\cos\alpha \mid \pm\frac{7}{2}\rangle + \sin\alpha \mid \mp\frac{1}{2}\rangle$	$\pm\frac{3}{2}g\beta H + 8b_4 - 2b_6 + \{(\pm 2g\beta H - b_4 + 3b_6)^2 + 35(b_4 - 3b_6)^2\}^{\frac{1}{2}}$
$\sin\alpha \mid \pm\frac{7}{2}\rangle - \cos\alpha \mid \mp\frac{1}{2}\rangle$	$\pm\frac{3}{2}g\beta H + 8b_4 - 2b_6 - \{(\pm 2g\beta H - b_4 + 3b_6)^2 + 35(b_4 - 3b_6)^2\}^{\frac{1}{2}}$
$\cos\beta \mid \pm\frac{5}{2}\rangle + \sin\beta \mid \mp\frac{3}{2}\rangle$	$\pm\frac{1}{2}g\beta H - 8b_4 + 2b_6 + \{(\pm 2g\beta H - 5b_4 - 7b_6)^2 + 3(5b_4 + 7b_6)^2\}^{\frac{1}{2}}$
$\sin\beta \mid \pm\frac{5}{2}\rangle - \cos\beta \mid \mp\frac{3}{2}\rangle$	$\pm\frac{1}{2}g\beta H - 8b_4 + 2b_6 - \{(\pm 2g\beta H - 5b_4 - 7b_6)^2 + 3(5b_4 + 7b_6)^2\}^{\frac{1}{2}}$

Here the abbreviations $b_4 = 60B_4$, $b_6 = 1260B_6$ have been used, while the values of α and β are given by

$$\tan 2\alpha = \sqrt{(35)}(b_4 - 3b_6)/(\pm 2g\beta H - b_4 + 3b_6),$$
$$\tan 2\beta = \sqrt{(3)}(5b_4 + 7b_6)/(\pm 2g\beta H - 5b_4 - 7b_6).$$

since these occur only once, the states are independent of the cubic field parameters. The energy levels in a weak field parallel to a fourfold axis, and the zero field states are given in Table 3.7.

More general expressions for the energy levels in a magnetic field, including series expansions for arbitrary directions of the magnetic field in both strong and weak magnetic fields, are given by Lacroix (1957). He uses a different nomenclature (as also does Low (1960)), whose connection with that used here can be seen from a comparison of the formulae for the levels in zero magnetic field given in Table 3.8.

In strong magnetic fields the only allowed transitions are those in which $\Delta M = \pm 1$, and the states are fairly accurately represented by single values of M, where M is the component of angular momentum about an axis parallel to the magnetic field. There are then seven

TABLE 3.7

Energy levels and states for $S = \frac{7}{2}$, cubic field, in a weak magnetic field **H** *along an* $\langle 001 \rangle$ *axis*

	States	Energy levels
Γ_6	$\sqrt{(\frac{5}{12})} \mid \pm\frac{7}{2}\rangle + \sqrt{(\frac{7}{12})} \mid \mp\frac{1}{2}\rangle$	$14b_4 - 20b_6 \pm \frac{7}{6}g\beta H$
Γ_7	$\sqrt{(\frac{3}{4})} \mid \pm\frac{5}{2}\rangle - \frac{1}{2} \mid \mp\frac{3}{2}\rangle$	$-18b_4 - 12b_6 \pm \frac{3}{2}g\beta H$
Γ_8	$\sqrt{(\frac{7}{12})} \mid \pm\frac{7}{2}\rangle - \sqrt{(\frac{5}{12})} \mid \mp\frac{1}{2}\rangle$	$2b_4 + 16b_6 \pm \frac{11}{6}g\beta H$
	$\frac{1}{2} \mid \pm\frac{5}{2}\rangle + \sqrt{(\frac{3}{4})} \mid \mp\frac{3}{2}\rangle$	$2b_4 + 16b_6 \mp \frac{1}{2}g\beta H$

In this Γ_8 quadruplet the values of P, Q are the same as for the Γ_8 quadruplet of $S = \frac{5}{2}$.

TABLE 3.8

Comparison of nomenclatures for $S = \frac{7}{2}$ in cubic field

	(This notation)	Lacroix	Low
Doublet_6	$32b_4 - 8b_6$	$(8+\epsilon)\delta$	$8c - 2d$
Quadruplet_8	$20b_4 + 28b_6$	5δ	$5c + 7d$
Doublet_7	0	0	0

allowed transitions, whose position and relative intensities are given in Table 3.9. Here the abbreviations $b_4 = 60B_4$, $b_6 = 1260B_6$ have again been used; p is as defined above for $S = \frac{5}{2}$, while q is the equivalent expression of the sixth degree

$$q = (\tfrac{2}{2}\tfrac{1}{1})\{11l^2m^2n^2 - (l^2m^2 + m^2n^2 + n^2l^2) + \tfrac{2}{2\,1}\}$$

whose angular variation is similar to that of the sixth degree cubic potential

$$11x^2y^2z^2 - (x^2y^2 + y^2z^2 + z^2x^2)r^2 + 2r^6/21.$$

Values of q for specific directions are $+1$, $+\frac{1\,6}{9}$ along $\langle 100 \rangle$ and $\langle 111 \rangle$ axes respectively. In a $\{111\}$ plane

$$q = \tfrac{7\,7}{7\,2} \cos 6\theta - \tfrac{5}{9}.$$

where θ is measured from a $\langle 11\bar{2} \rangle$ direction. Since p is invariant at $-\frac{1}{4}$ in this plane the sixth degree term can be measured directly by rotating H in a $\{111\}$ plane. These results follow also from eqn (3.23) since both O_4^3 and O_6^3 have zero expectation values in this plane, and if

TABLE 3.9

Resonance transitions ($\Delta M = \pm 1$) and relative intensities for $S = \frac{7}{2}$, cubic field, in a strong magnetic field $\mathbf{H}$ *($g\beta H \gg b_4, b_6$)*

Transition	Position	Intensity
$+\frac{7}{2} \leftrightarrow +\frac{5}{2}$	$h\nu = g\beta H + 20pb_4 + 6qb_6$	7
$+\frac{5}{2} \leftrightarrow +\frac{3}{2}$	$g\beta H - 10pb_4 - 14qb_6$	12
$+\frac{3}{2} \leftrightarrow +\frac{1}{2}$	$g\beta H - 12pb_4 + 14qb_6$	15
$+\frac{1}{2} \leftrightarrow -\frac{1}{2}$	$g\beta H$	16
$-\frac{1}{2} \leftrightarrow -\frac{3}{2}$	$g\beta H + 12pb_4 - 14qb_6$	15
$-\frac{3}{2} \leftrightarrow -\frac{5}{2}$	$g\beta H + 10pb_4 + 14qb_6$	12
$-\frac{5}{2} \leftrightarrow -\frac{7}{2}$	$g\beta H - 20pb_4 - 6qb_6$	7

eqn (3.23) is rotated through 90° (cf. eqns (5.78), (5.79)) we have for the diagonal part just

$$-\tfrac{1}{4}B_4O_4^0+B_6O_6^0(\tfrac{77}{72}\cos 6\theta-\tfrac{5}{8}). \tag{3.23a}$$

In an {001} plane we have

$$g = 1-\tfrac{21}{8}\sin^2 2\theta$$

and in an $\{01\bar{1}\}$ plane (which contains the ⟨100⟩, ⟨111⟩, and ⟨011⟩ axes)

$$g = 1-\tfrac{21}{8}(4\sin^2\theta - 14\sin^4\theta + 11\sin^6\theta),$$

the angle θ being measured in each case from the ⟨100⟩ axis.

Measurements of line positions in the spectrum do not yield the absolute signs of any of the splitting parameters, though the relative signs of b_4, b_6 can be found when both fourth and sixth degree terms are present. The absolute signs can, however, be determined by observing the change in relative intensities of the lines as the temperature is reduced, because of the depopulation of the states with positive values of M, just as in the case of a second degree splitting (see § 3.6). In practice the splitting due to b_6 is usually small compared with that due to b_4. The spectrum in a strong magnetic field ($g\beta H \gg b_4$) with $b_6 = 0$ is shown in Fig. 3.3(b).

The results quoted in this section are based on the assumption that the spectroscopic splitting factor g is isotropic; in a cubic field g would be expected to be rigorously isotropic. In fact with very few exceptions no anisotropy in g has been detected outside the experimental error for an ion in an S-state.

3.5. Electronic 'quadrupole' fine structure ($S = 1, \frac{3}{2}$)

When the symmetry is less than cubic, fine structure terms of the second degree will generally be present. This is an effect of more common occurrence than higher multipole fine structure, and hence we shall consider it separately, another reason for so doing being that it occurs in cases when g may be anisotropic.

In terms of the spin operators O_2^0, O_2^2 listed in Table 16, the second degree or 'quadrupole' terms are

$$B_2^0O_2^0+B_2^2O_2^2 = B_2^0\{3S_z^2-S(S+1)\}+\tfrac{1}{2}B_2^2(S_+^2+S_-^2). \tag{3.24}$$

These may be expressed in an alternative form, which can be written as a single term $\mathbf{S}\,.\,\mathbf{D}\,.\,\mathbf{S}$. where $\mathbf{D}$ is a tensor quantity. Referred to the principal axes, this term is

$$D_xS_x^2+D_yS_y^2+D_zS_z^2, \tag{3.25}$$

where it is convenient to take the sum of the three coefficients as zero, i.e. $D_x+D_y+D_z = 0$. If this sum is not zero, it can be made so by subtracting the quantity

$$\tfrac{1}{3}(D_x+D_y+D_z)(S_x^2+S_y^2+S_z^2) = \tfrac{1}{3}(D_x+D_y+D_z)S(S+1),$$

which is just a constant that moves all the levels up or down by the same amount, and so does not affect the resonance spectrum. The fact that one can set the sum of the three coefficients equal to zero means that there are really only two independent coefficients, as in eqn (3.24). The connection between the two forms is revealed by manipulation of eqn (3.25) as follows:

$$\begin{aligned} D_xS_x^2+D_yS_y^2+D_zS_z^2 &\\ &= \tfrac{1}{2}(D_x+D_y)(S_x^2+S_y^2)+\tfrac{1}{2}(D_x-D_y)(S_x^2-S_y^2)+D_zS_z^2 \\ &= D\{S_z^2-\tfrac{1}{3}S(S+1)\}+\tfrac{1}{2}E(S_+^2+S_-^2), \end{aligned} \tag{3.26}$$

where $D = \frac{3}{2}D_z = 3B_2^0$, $\frac{1}{2}(D_x-D_y) = E = B_2^2$.

The form (3.25) is often convenient when all the coefficients are unequal, since the energy levels can be computed for the case of a magnetic field along one axis, and the formulae for the other axes obtained by cyclic permutation of the subscripts. The permutation required is (moving from column to column):

g_x	g_y	g_z
$\frac{3}{2}D_x$	$\frac{3}{2}D_y$	$\frac{3}{2}D_z$
$= \frac{1}{2}(3E-D)$	$= -\frac{1}{2}(3E+D)$	$= D$
$\frac{1}{2}(D_y-D_z)$	$\frac{1}{2}(D_z-D_x)$	$\frac{1}{2}(D_x-D_y)$
$= -\frac{1}{2}(D+E)$	$= \frac{1}{2}(D-E)$	$= E$

When axial symmetry is present, $D_x = D_y$ and $E = 0$. The forms (3.24) or (3.26) are then to be preferred since they contain only one parameter. Even when $E \neq 0$ they have the advantage of containing only two parameters instead of three (which are not all independent).

Formulae for $S = 1$

The quadrupole terms have no effect on the energy of a doublet ($S = \frac{1}{2}$) but with larger values of S they produce a splitting of the levels when no magnetic field is present. For the cases of $S = 1$ and $S = \frac{3}{2}$, the energy levels can be expressed in a closed form when a magnetic field is applied, so long as it is parallel to one of the three principal axes of the tensor **D**. We shall examine the first of these ($S = 1$) fairly completely, as it illustrates in a simple fashion the effects that occur.

The spin Hamiltonian, when an external magnetic field is applied along the z-axis, is

$$\mathscr{H} = g_z\beta H S_z + D\{S_z^2 - \tfrac{1}{3}S(S+1)\} + E(S_x^2 - S_y^2). \tag{3.27}$$

The energy matrix is

$$\begin{array}{c|ccc} |+1\rangle & \frac{1}{3}D+G & 0 & E \\ |0\rangle & 0 & -\frac{2}{3}D & 0 \\ |-1\rangle & E & 0 & \frac{1}{3}D-G \end{array}$$

and the quantum states and energy levels can be written as

$$\left.\begin{array}{ll} |+\rangle = \cos\alpha\,|+1\rangle + \sin\alpha\,|-1\rangle, & W_+ = +\frac{1}{3}D + (G^2+E^2)^{\frac{1}{2}}, \\ |0\rangle = |0\rangle, & W_0 = -\frac{2}{3}D, \\ |-\rangle = \sin\alpha\,|+1\rangle - \cos\alpha\,|-1\rangle, & W_- = +\frac{1}{3}D - (G^2+E^2)^{\frac{1}{2}}, \end{array}\right\} \tag{3.28}$$

where $\tan 2\alpha = E/G$ and $G = g_z\beta H$. The allowed transitions between these levels have varying intensity according to the orientation of the oscillatory magnetic field, as shown in Table 3.10. The behaviour of

TABLE 3.10

Transitions and relative intensities for $S = 1$, rhombic field, **H** *along z-axis*

Transition	Quantum required	Intensity (value of $g_i^2\,\lvert S_{ij}\rvert^2$) H_1 along x-axis	y-axis	z-axis
$\lvert+\rangle \leftrightarrow \lvert 0\rangle$	$D+(G^2+E^2)^{\frac{1}{2}}$	$\frac{1}{2}g_x^2(1+\sin 2\alpha)$	$\frac{1}{2}g_y^2(1-\sin 2\alpha)$	0
$\lvert 0\rangle \leftrightarrow \lvert-\rangle$	$-D+(G^2+E^2)^{\frac{1}{2}}$	$\frac{1}{2}g_x^2(1-\sin 2\alpha)$	$\frac{1}{2}g_y^2(1+\sin 2\alpha)$	0
$\lvert+\rangle \leftrightarrow \lvert-\rangle$	$2(G^2+E^2)^{\frac{1}{2}}$	0	0	$g_z^2 \sin^2 2\alpha$

the energy levels for the special case of $E = \frac{1}{2}D$ are shown in Fig. 3.4, together with the transitions requiring a quantum equal to $\frac{5}{2}D$.

In zero magnetic field $\alpha = 45°$ and the three states are

$$2^{-\frac{1}{2}}\{|+1\rangle \pm |-1\rangle\};\ |0\rangle,$$

each of which is an eigenstate with $\langle S_x\rangle = \langle S_y\rangle = \langle S_z\rangle = 0$. Thus the system has no permanent magnetic moment, and the line width due to spin-spin interaction is extremely small. This makes it possible to measure the zero-field transitions with very high accuracy, a result that has been applied in the measurement of the spectrum of the photoexcited triplet state of phenanthrene (see Brandon, Gerkin, and Hutchison (1962)). Another curiosity of the zero field spectrum is that

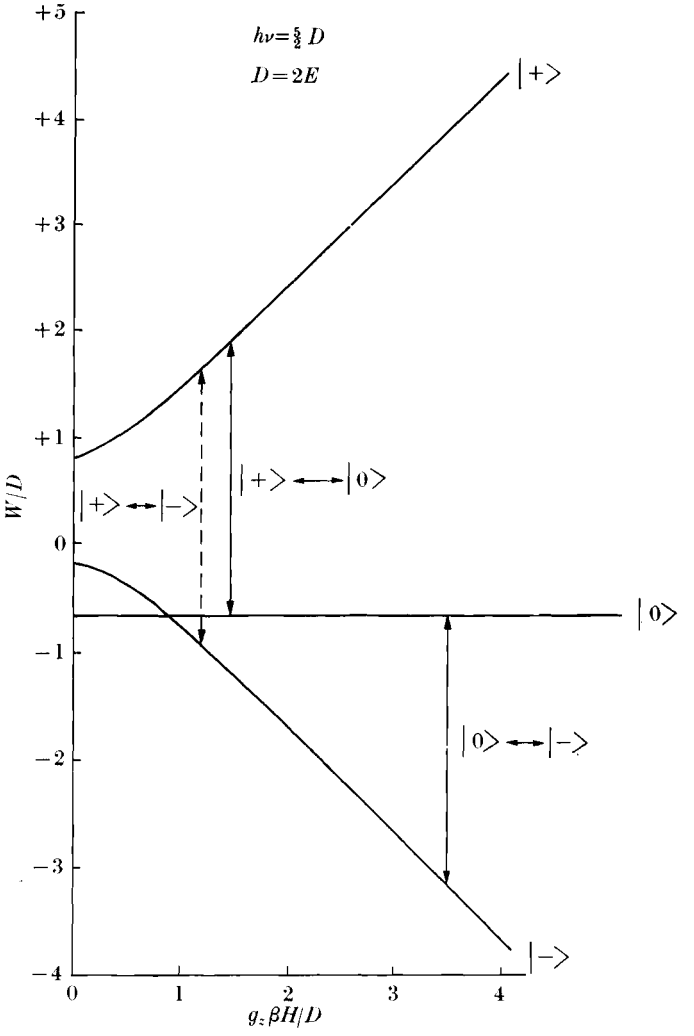

FIG. 3.4. Energy levels for $S = 1$ with rhombic splitting ($D = 2E$), in units of ($g_z\beta H/D$), with magnetic field along the z-axis. The vertical arrows indicate the allowed transitions for a quantum $h\nu = \frac{5}{2}D$.

each of the transitions is strongest for an oscillatory magnetic field linearly polarized along a different principal axis.

When a magnetic field of increasing size is applied along the z-axis, the value of α decreases towards zero; the three quantum states approach the simple description $|+1\rangle$, $|0\rangle$, and $|-1\rangle$, and the energy levels eventually diverge linearly with slopes $g_z\beta H$ times $+1$, 0, and -1 respectively. This shows that in strong fields the magnetic moment

simply precesses about the axis determined by the magnetic field, whereas in zero field its motion can be regarded as consisting of three mutually perpendicular linear vibrations of different frequencies; in intermediate fields its motion is more complicated. In strong fields the transition $|+\rangle \leftrightarrow |-\rangle$ becomes smaller and smaller in intensity; it is often loosely referred to as a '$\Delta M = \pm 2$' transition, but this assumes that the states are labelled by their strong field description as $|+1\rangle$ and $|-1\rangle$. This nomenclature is only accurate in infinitely strong fields, and the two states $|+\rangle$, $|-\rangle$ at finite fields are each an admixture of the two states $|+1\rangle$, $|-1\rangle$. It would be more correct to call it a $\Delta M = 0$ transition, since it is allowed only because the same values of M occur in the two states. This agrees with the simple polarization rule, that $\Delta M = 0$ transitions require an oscillatory field parallel to the axis used to specify the components M of angular momentum while $\Delta M = \pm 1$ transitions in strong fields require an oscillatory field normal to this axis.

Although these formulae have been given only for a field along the z-axis, they can be applied for fields along the x- and y-axes by making the substitutions $D = \frac{3}{2}D_z$, $E = \frac{1}{2}(D_x - D_y)$ and using cyclic permutations. They can also be used for the case of an axial fine structure term with the magnetic field normal to the axis of symmetry by taking the field direction as the z-axis, and the fine structure term as

$$\begin{aligned} D'\{S_x^2 - \tfrac{1}{3}S(S+1)\} &= \tfrac{1}{3}D'(2S_x^2 - S_y^2 - S_z^2) \\ &= -\tfrac{1}{2}D'\{S_z^2 - \tfrac{1}{3}S(S+1)\} + \tfrac{1}{2}D'(S_x^2 - S_y^2), \end{aligned}$$

which is equivalent to $D = -\frac{1}{2}D'$, $E = +\frac{1}{2}D'$.

Formulae for $S = \frac{3}{2}$

Using the spin Hamiltonian (3.27) but with $S = \frac{3}{2}$, the energy matrix is

$$\begin{array}{c|cc} & \pm\frac{3}{2} & \mp\frac{1}{2} \\ \hline \pm\frac{3}{2} & D \pm \frac{3}{2}G & \sqrt{(3)}E \\ \mp\frac{1}{2} & \sqrt{(3)}E & -D \mp \frac{1}{2}G \end{array}$$

from which the states and energy levels are

States	*Energy*
$\lvert\pm\bar{\frac{3}{2}}\rangle = \cos\alpha\,\lvert\pm\frac{3}{2}\rangle + \sin\alpha\,\lvert\mp\frac{1}{2}\rangle$	$\pm\frac{1}{2}G + \{(D \pm G)^2 + 3E^2\}^{\frac{1}{2}}$
$\lvert\mp\bar{\frac{1}{2}}\rangle = -\sin\alpha\,\lvert\pm\frac{3}{2}\rangle + \cos\alpha\,\lvert\mp\frac{1}{2}\rangle$	$\pm\frac{1}{2}G - \{(D \pm G)^2 + 3E^2\}^{\frac{1}{2}}$

where $G = g_z\beta H$ and $\tan 2\alpha = \sqrt{(3)}E/(D \pm G)$. The nomenclature $|\bar{M}\rangle$ is a useful shorthand which is a correct description of the states only

TABLE 3.11

Transitions and relative intensities for $S = \frac{3}{2}$, rhombic field, **H** *along z-axis*

Transition	Orientation of H_1	Intensity (value of $g_1^2 \lvert S_{ij} \rvert^2$)
$\lvert +\frac{3}{2}\rangle \leftrightarrow \lvert -\frac{1}{2}\rangle$	z-axis	$g_z^2 \sin^2 2\alpha$
$\lvert -\frac{3}{2}\rangle \leftrightarrow \lvert +\frac{1}{2}\rangle$	z-axis	$g_z^2 \sin^2 2\alpha$
$\lvert +\frac{3}{2}\rangle \leftrightarrow \lvert -\frac{3}{2}\rangle$	$\begin{matrix} x \\ y \end{matrix}$-axis	$g_{\substack{x \\ y}}^2 \{\sin^2 \alpha \pm \sqrt{(3)} \cos \alpha \sin \alpha\}^2$
$\lvert +\frac{1}{2}\rangle \leftrightarrow \lvert -\frac{1}{2}\rangle$	$\begin{matrix} x \\ y \end{matrix}$-axis	$g_{\substack{x \\ y}}^2 \{\cos^2 \alpha \mp \sqrt{(3)} \cos \alpha \sin \alpha\}^2$
$\lvert +\frac{3}{2}\rangle \leftrightarrow \lvert +\frac{1}{2}\rangle$	$\begin{matrix} x \\ y \end{matrix}$-axis	$\frac{1}{4} g_{\substack{x \\ y}}^2 \{\sin 2\alpha \pm \sqrt{(3)} \cos 2\alpha\}^2$
$\lvert -\frac{3}{2}\rangle \leftrightarrow \lvert -\frac{1}{2}\rangle$	$\begin{matrix} x \\ y \end{matrix}$-axis	$\frac{1}{4} g_{\substack{x \\ y}}^2 \{\sin 2\alpha \pm \sqrt{(3)} \cos 2\alpha\}^2$

In the limit of strong magnetic fields $\alpha \to 0$ and only three transitions with relative intensity 3:4:3 are allowed, with the oscillatory field normal to the steady field.

in the limit of very strong magnetic field. The transition probabilities for various orientations of the oscillatory field are given in Table 3.11.

3.6. Electronic 'quadrupole' fine structure in a strong magnetic field

For values of $S > \frac{3}{2}$, or if the external field is in an arbitrary direction, calculation of the energy levels is cumbersome and no simple formulae can be given. In cases where the Zeeman energy is very large or very small compared with the fine structure energy, perturbation methods can be used. The former case is the one more commonly encountered in practice, and the following discussion is restricted to this case.

When the symmetry is rhombic, measurements at arbitrary field directions are useful in finding the positions of the principal axes, if not already known; precise measurements can then be made in the directions of the principal axes, where the theory is more amenable to simple calculation. For intermediate directions the formulae are therefore carried only as far as first order perturbation theory. On transforming to the new set of axes (x_e, y_e, z_e) to diagonalize the Zeeman energy, as in § 3.2, the quadrupole term

$$D_x S_x^2 + D_y S_y^2 + D_z S_z^2$$

transforms into a mixture of all possible products of the second degree in the spin components. Using the relation $D_x + D_y + D_z = 0$, the

diagonal term becomes

$$\tfrac{1}{2}D''\{S_z'^2-\tfrac{1}{3}S(S+1)\}, \tag{3.29}$$

where

$$g^2D'' = 3(l^2g_x^2D_x+m^2g_y^2D_y+n^2g_z^2D_z) \tag{3.30}$$

and g is given by eqn (3.5).

The transition $M \leftrightarrow M-1$ occurs at

$$h\nu = g\beta H+D''(M-\tfrac{1}{2})+\ldots, \tag{3.31}$$

and, in this approximation where terms of order $D^2/h\nu$ are neglected, the spectrum consists of $2S$ lines equally spaced at intervals of D'' about the position corresponding to $D = 0$. The splitting interval D'' varies with angle, reaching extreme values along the principal axes, but becoming zero at certain intermediate directions since not all the coefficients D_x, D_y, D_z can have the same sign. This equal spacing is upset by the second-order terms, but these will be evaluated only for the case of axial symmetry.

Axial symmetry

When axial symmetry is present,

$$g_z = g_\parallel, \quad g_x = g_y = g_\perp, \quad D_x = D_y = -\tfrac{1}{2}D_z = -\tfrac{1}{3}D, \quad (E = 0).$$

The calculations will be carried to second order of perturbation theory, assuming that the Zeeman energy $\gg$ electronic quadrupole energy, and that the external field is at an angle θ with the z-axis in the xz-plane. Then the spin Hamiltonian becomes

$$\mathscr{H} = \beta H(g_\perp S_x \sin\theta+g_\parallel S_z\cos\theta)+D\{S_z^2-\tfrac{1}{3}S(S+1)\}. \tag{3.32}$$

The Zeeman energy is first diagonalized as in § 3.2 by a rotation about the y-axis through an angle ϕ given by eqn (3.13). Then the spin Hamiltonian becomes

$$\mathscr{H} = g\beta HS_z'+\tfrac{1}{2}D\{S_z'^2-\tfrac{1}{3}S(S+1)\}(3\cos^2\phi-1)- \\ -D(S_x'S_z'+S_z'S_x')\cos\phi\sin\phi+\tfrac{1}{4}D(S_+'^2+S_-'^2)\sin^2\phi. \tag{3.32a}$$

The last two terms are off-diagonal, and on evaluation by second-order perturbation theory the energy of the state $S_z' = M$ is found to be

$$W = g\beta HM+\tfrac{1}{2}D\{(3g_\parallel^2/g^2)\cos^2\theta-1\}\{M^2-\tfrac{1}{3}S(S+1)\}+ \\ +(g_\parallel^2g_\perp^2/g^4)(D^2\cos^2\theta\sin^2\theta/2G)M\{8M^2+1-4S(S+1)\}+ \\ +(g_\perp^4/g^4)(D^2\sin^4\theta/8G)M\{2S(S+1)-2M^2-1\}. \tag{3.33}$$

Here g is given by eqn (3.14), and $G = g\beta H$. The ratios $g_\perp/g$, $g_\parallel/g$

that occur arise from the relations between $\sin\phi$, $\cos\phi$ and $\sin\theta$, $\cos\theta$.

The diagonal term in eqn (3.33) is of course just a special case of (3.29) with

$$D'' = D\{(3g_{\parallel}^2/g^2)\cos^2\theta - 1\}, \tag{3.34}$$

and to a first approximation the spectrum is given by eqn (3.31) with this special value of D''. The angular variation of D'' is just $(3\cos^2\phi - 1)$, corresponding to the fact that $3S_z'^2 - S(S+1)$ transforms like

$$3z_e^2 - r^2 = r^2(3\cos^2\phi - 1)$$

and ϕ is the angle made by z_e, the spin axis, with the symmetry axis. The variation with angle is shown in Fig. 3.5 for the case of isotropic

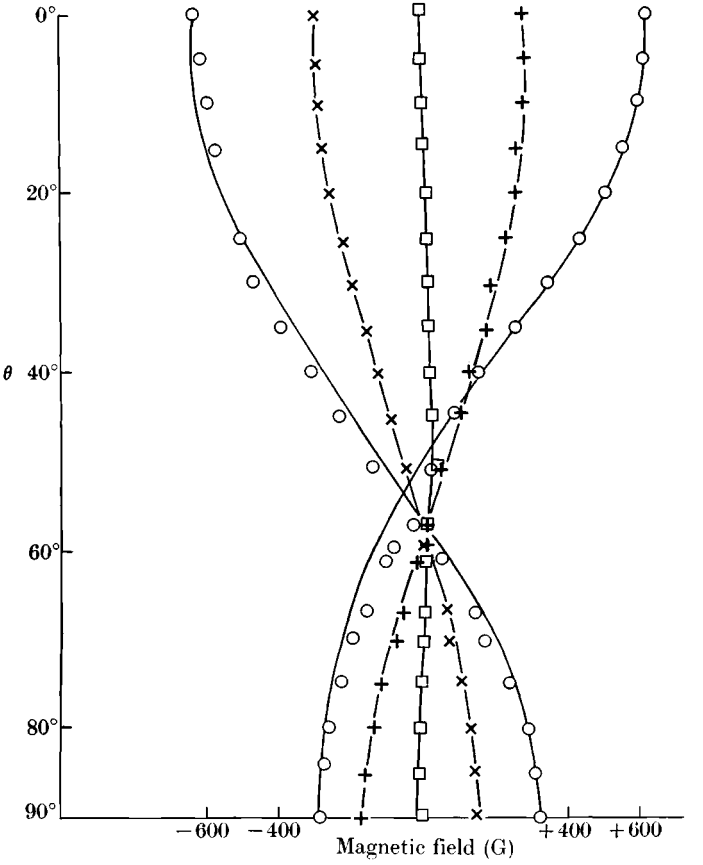

FIG. 3.5. Variation of the fine structure with angle (showing the experimental points and the calculated curves). Dilute manganese fluosilicate, $S = \frac{5}{2}$, at 3·3-cm wave-length, and 90°K (Bleaney and Ingram 1951*a*).

g and $S = \frac{5}{2}$. At $\theta = \pi/2$ the splitting is just half of that for $\theta = 0$, and the lines occur in the reverse order; the first-order splitting is zero at $3\cos^2\theta = 1$, or $\theta = 54° 44'$. If g is anisotropic, this zero occurs at $3\cos^2\phi = 1$.

The effect of off-diagonal terms in the energy matrix which were neglected in eqn (3.31) but included in eqn (3.33) is to give small shifts in the energy levels of order D^2/G. There are corresponding shifts in the lines, which for the transition $M \leftrightarrow M-1$ is given by adding to eqn (3.31) the quantity

$$(g_\parallel^2 g_\perp^2/g^4)(D^2\cos^2\theta\sin^2\theta/2G)\{24M(M-1)+9-4S(S+1)\}+ \\ +(g_\perp^4/g^4)(D^2\sin^4\theta/8G)\{2S(S+1)-6M(M-1)-3\}. \quad (3.35)$$

These shifts account for the departure from a simple $(3\cos^2\theta-1)$ variation shown in Fig. 3.5.

The off-diagonal matrix elements are of two kinds: elements between $|M\rangle$ and $|M-1\rangle$, whose magnitudes vary with $\sin 2\theta$ and which therefore vanish both parallel and perpendicular to the symmetry axis; elements between $|M\rangle$ and $|M-2\rangle$, which vary with $\sin^2\theta$ and hence vanish only parallel to the symmetry axis. Elements of these two kinds give rise to and determine the intensity of the so-called 'forbidden' transitions with $\Delta M = \pm 2$ or higher. When the external field is along the symmetry axis such transitions are forbidden entirely; when **H** is normal to this axis they are allowed only if the oscillatory field $\mathbf{H}_1$ is parallel to **H**; but for intermediate directions they are allowed with $\mathbf{H}_1$ either parallel or perpendicular to **H**. The transition $M+1 \leftrightarrow M-1$ occurs at

$$h\nu = 2G+2D''M+ \\ +(g_\parallel^2 g_\perp^2/g^4)(D^2\cos^2\theta\sin^2\theta/G)\{24M^2+9-4S(S+1)\}+ \\ +(g_\perp^4/g^4)(D^2\sin^4\theta/4G)\{2S(S+1)-6M^2-3\}. \quad (3.36)$$

When the spectrum is observed at constant frequency these lines occur at roughly half the field required for the normal transitions but the average separation in field between successive lines is the same; the intensity is smaller by a factor of order $(D/G)^2$. Also, for intermediate directions of the magnetic field **H** the intensity of the normal transitions ($\Delta M = \pm 1$) does not vanish when $\mathbf{H}_1$ is parallel to **H** but falls only by a factor of order $(D/G)^2$.

The number of strong transitions of the form $\Delta M = \pm 1$ is just $2S$, and the intensity of the transition $M \leftrightarrow M-1$ is proportional to $\{S(S+1)-M(M-1)\}$ in the first approximation. Unlike the cases of

higher multipole splitting discussed in § 3.4 the intensity is highest in the centre and smallest for the outside lines of the spectrum. This intensity variation makes it possible to identify the transition corresponding to a given line, except for an ambiguity in the sign of the values of M involved. This ambiguity can be resolved by observing the change in the relative intensity of the lines as the temperature is reduced as mentioned in § 3.3. The way in which this can be done is readily understood from the energy levels shown in Fig. 3.6 for the

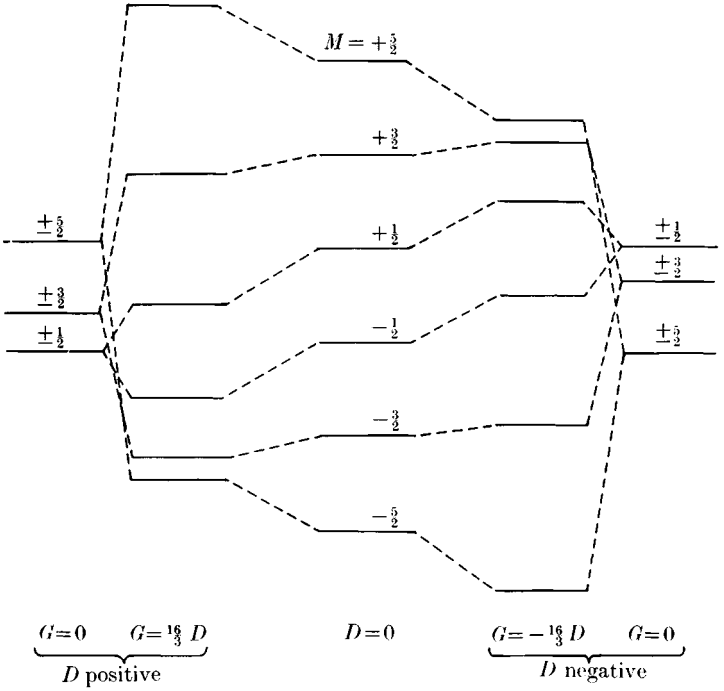

FIG. 3.6. Energy levels with electronic 'quadrupole' splitting, for $S=\frac{5}{2}$, with magnetic field H along symmetry axis ($G=g_z\beta H$), for the spin Hamiltonian,

$$\mathscr{H}=g_z\beta HS_z+D\{S_z^2-\tfrac{1}{3}S(S+1)\}.$$

case of $S=\frac{5}{2}$ in a strong field. The diagram shows positive and negative values of D respectively and it will be seen that one set of levels is just inverted from the other. At low temperatures when kT is comparable with the overall splitting the population of the highest levels will be noticeably smaller than that of the lowest levels, and the intensity of the transitions between the higher levels will decrease relative to those between the lower levels. Comparison of the intensity of these transitions is easiest in strong fields working at constant

frequency, when the different transitions can be traversed by varying the field. It is readily seen that if D is positive the transition between the highest two levels, which has the lower intensity at lower temperatures, comes at highest frequency in a given field or at lowest field for a given frequency; if D is negative the reverse is the case. In this way the order of the levels can be identified, and the sign of D established.

This is possible in measurements at zero field, for which the energy levels are shown to the right and left of the diagram, but then the splittings are much smaller and the difference in populations will be much lower than that for the transitions compared in strong fields. In addition it would be necessary to compare the relative strengths of transitions at different frequencies when working in zero field, which is experimentally much more difficult to do accurately.

The strength of this method is illustrated by inserting some numerical values. For an ion with $S = \frac{5}{2}$, $g = 2$ in a field of about 10 kG the allowed transitions occur near 1 cm wavelength. The intensity ratio between the extreme transitions $+\frac{5}{2} \leftrightarrow +\frac{3}{2}$ and $-\frac{3}{2} \leftrightarrow -\frac{5}{2}$ is very nearly $\exp(-4h\nu/kT)$. Even at 14°K, a temperature readily obtained with pumped hydrogen, this intensity ratio is about 1·5, which is easily discernible in the spectrum. This makes it possible to label the transitions and determine the sign of D; it should be noted that the method can be used for quite small values of D, the only limitation being that D must be larger than the line width so that the various transitions are resolved.

The method outlined above for determining the sign of D can be used for multipole splittings of any degree. Figure 3.7 shows an example where it is used for a splitting that is predominantly due to the cubic term of eqn (3.21). As remarked in § 3.3, measurements of the line positions in the spectrum at a sufficient number of directions will give the values of the coefficients of all the multipole splitting terms, together with their relative signs. Thus only one observation of the change of intensity with temperature is required to determine all the signs. This may be illustrated, using as an example, a rhombic splitting of the second degree. Measurements of the fine structure of the spectrum observed with a magnetic field along each of the three principal axes of the tensor $\mathbf{D}$ determine the three quantities $|D_x|$, $|D_y|$, $|D_z|$, but since $D_x+D_y+D_z = 0$ there is only one choice of the relative signs of the three coefficients which is possible. We may summarize this situation by saying that only the sign of the product $(D_xD_yD_z)$ is unknown,

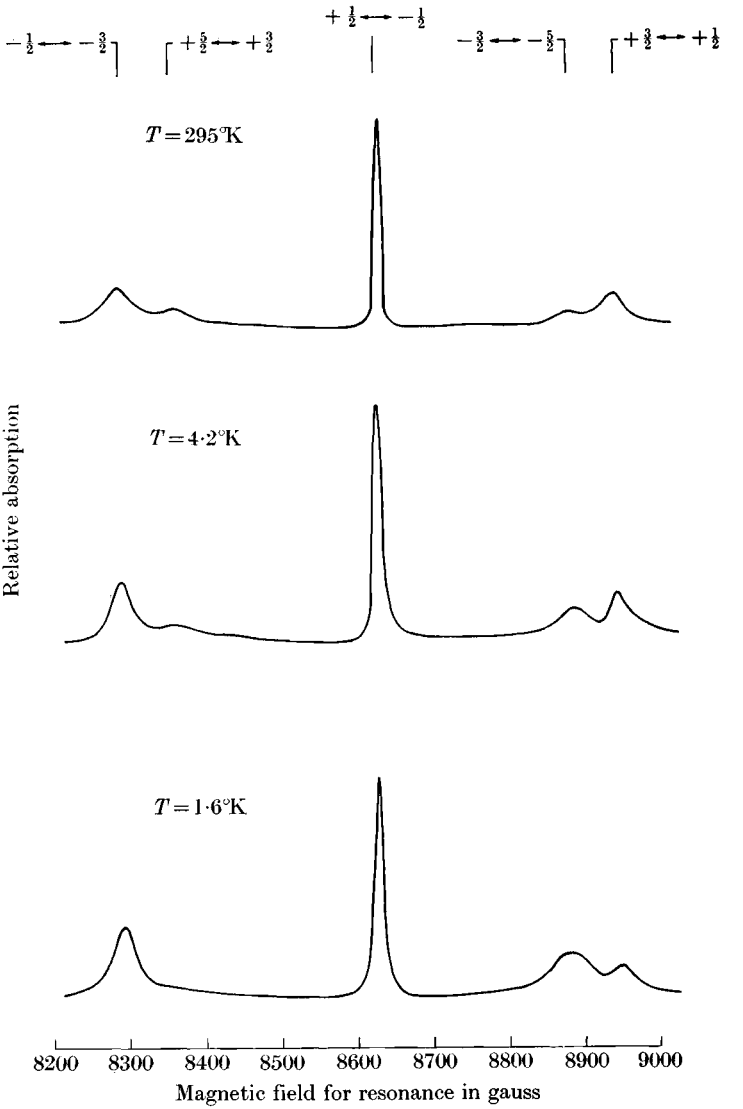

FIG. 3.7. Paramagnetic resonance at 24000 MHz of Fe^{3+} in rubidium aluminium sulphate with **H** parallel to ⟨100⟩ direction. The change of intensity at low temperatures shows that the cubic field parameter a is positive, since the transitions which gain in relative intensity must be those between the states of low Zeeman energy (negative values of M); cf. Fig. 3.3(a)). (Geschwind 1959).

and a knowledge of the sign of any one of the three individual parameters is sufficient to determine the overall sign. In a strong field along the x-axis, for example, the energy levels will approximately be as shown in Fig. 3.6 except that the parameter D would be replaced by $3D_x/2$. Observation of the change of relative intensity with temperature would then give the sign of D_x. It may be remarked here that the change in population of the levels with temperature also gives a term in T^{-2} in the susceptibility whose sign is related to that of D (see eqn (A.34), Appendix A); hence in some cases the sign of D can be found from anisotropy measurements (see, for example, Bleaney and Ingram 1951*a*). This is not such a good method, since it can only be used when g is quite isotropic, and for non-cubic crystals.

These last limitations apply generally to susceptibility measurements as compared with paramagnetic resonance measurements. Also the information obtained from a resonance measurement in strong fields is very much greater than that in zero field. For example, in zero field for $S = \frac{3}{2}$, the energy levels reduce to two doublets separated by an energy $(D^2+3E^2)^{\frac{1}{2}}$, so that a measurement in zero field would yield a value only for this quantity. On the other hand, by measurements in a strong field one can find the values of D and E separately, and also determine the directions of the axes associated with these quantities, together with the principal g-values.

3.7. Hyperfine structure I (introductory remarks)

The effects of hyperfine structure in free atoms are well known, and can usually be described by a Hamiltonian of the form

$$\mathscr{H}_{\mathrm{n}} = a_J \mathbf{J}.\mathbf{I} + \frac{b}{2I(2I-1)J(2J-1)}\{3(\mathbf{I}.\mathbf{J})^2+\tfrac{3}{2}(\mathbf{I}.\mathbf{J})-I(I+1)J(J+1)\}- \\ -g_I\beta\mathbf{H}.\mathbf{I}, \qquad (3.37)$$

where the first term represents the interaction between the nuclear magnetic moment and the electronic magnetic field (whose steady component is parallel to the electronic angular momentum vector $\mathbf{J}$); the second term the interaction between the nuclear electric quadrupole moment and the electronic electric field gradient (also parallel to $\mathbf{J}$) at the nucleus, and the third the Zeeman interaction between the nuclear magnetic moment and the external magnetic field. In an external magnetic field we have also the electronic Zeeman interaction $\mathscr{H}_{\mathrm{Z}} = g_J\beta\mathbf{H}.\mathbf{J}$, but none of the fine structure terms discussed earlier in this chapter. In a strong field ($g_J\beta H \gg a_J$), the allowed

electronic transitions are those in which the nuclear magnetic quantum number m does not change, and the diagonal part of the quadrupole interaction term is

$$\frac{b}{4I(2I-1)J(2J-1)}\{3J_z^2-J(J+1)\}\{3I_z^2-I(I+1)\}, \qquad (3.37a)$$

where the z-axis is parallel to the external field. The quantum required for a transition $(M,m) \leftrightarrow (M-1, m)$ is

$$h\nu = g_J\beta H + a_J m + \frac{3b}{4I(2I-1)J(2J-1)}(2M-1)\{3m^2-I(I+1)\} \qquad (3.38a)$$

and by measuring a sufficient number of such transitions the parameters can be determined except g_I, which does not appear in eqn (3.38a).

In strong magnetic fields **L** and **S** may be partially decoupled, a result that is expressed quantum mechanically by the admixture of the first excited state $J\pm1$ into the ground state J. Amongst other effects this modifies the apparent nuclear Zeeman interaction through cross terms of the form

$$\frac{\langle J|\ \mathscr{H}_Z\ |J+1\rangle\langle J+1|\ \mathscr{H}_n\ |J\rangle + \langle J|\ \mathscr{H}_n\ |J+1\rangle\langle J+1|\ \mathscr{H}_Z\ |J\rangle}{W_J - W_{J+1}}, \qquad (3.38b)$$

where J is the ground state and $J+1$ the excited state. This may be written in the form

$$\frac{2a_{J,J+1}\beta H\langle J+1\|\ \Lambda\ \|J\rangle\{(J+1)^2-M^2\}m}{W_J - W_{J+1}}, \qquad (3.38c)$$

where

$$a_{J,J+1} = 2g_I\beta^2\langle r^{-3}\rangle\langle J+1\|\ N\ \|J\rangle$$

and $\langle J+1\|\ N\ \|J\rangle$, $\langle J+1\|\ \Lambda\ \|J\rangle$ are numbers such as those tabulated for the $4f$ group in Table 20. This gives an additional energy for the transition $(M,\ m) \leftrightarrow (M-1,\ m)$ of

$$-\frac{2a_{J,J+1}\beta H\langle J+1\|\ \Lambda\ \|J\rangle(2M-1)m}{W_J - W_{J+1}}, \qquad (3.38d)$$

which gives useful additional information about the atomic structure (see, for example, Harvey (1965)). It will be seen that the additional energy given by eqn (3.38c) is of the form $\mathbf{H}\,.\,\mathbf{I}$; it is essentially the same effect as gives rise to the 'paramagnetic shift' in nuclear resonance. The atomic state is modified by the applied field by an amount which is linear in H, making the field seen by the nucleus different from the external field by a constant fraction varying as $(2M-1)$.

In a weak magnetic field ($g_J\beta H \ll a_J$) the off-diagonal terms in eqn (3.37) cannot be neglected and the behaviour of the energy levels is correspondingly somewhat more complicated. In zero field **I** and **J** may be vectorially combined to give a resultant **F**, whose motion in a weak magnetic field is a precession about **H**. This gives a weak field Zeeman interaction that can be expressed in terms of a magnetic quantum number $m_F = M+m$. We shall not consider the possible transitions in detail but note that transitions in which m_F changes by ± 1 require an oscillatory magnetic field perpendicular to the steady magnetic field, while those in which $\Delta m_F = 0$ require an oscillatory field parallel to the external field. In the strong magnetic field limit the latter have vanishing intensity, while the former fall into two classes: those in which $\Delta M = \pm 1$, which have an intensity determined by the electronic magnetic moment, and those in which $\Delta m = \pm 1$, whose intensity is determined by the nuclear magnetic moment and are therefore very weak in comparison.

The method of electron paramagnetic resonance has been applied to free atoms in a gaseous mixture, and has produced a number of significant results. These form rather a separate field, more related to the results of atomic beam and other methods of precision hyperfine structure measurement than to solid state paramagnetism, and we shall not discuss them further. Our main purpose in writing down the equations given above is for convenience in introducing the more complex subject of hyperfine interactions in the solid state, and later to draw some useful comparisons with atomic hyperfine structure.

In the solid state the electronic magnetic moment is often highly anisotropic, and we would expect its interaction with the nuclear moment also to be anisotropic. The electronic charge cloud is far from spherical in shape, and the electric field gradient at the nucleus must be expressed by a tensor whose principal axes are fixed in the crystal. Before considering the main results of these effects on the hyperfine structure, we mention the case of cubic symmetry. For a Γ_8 quadruplet the hyperfine magnetic dipole and electric quadrupole terms require drastic modification; this may also occur for Γ_4, Γ_5 triplet states, and even the Γ_3 doublet, as discussed in Chapter 18. Minor modifications may also be needed for ions with half-filled shells in S-states with $S = \frac{5}{2}, \frac{7}{2}$; the corrections are usually so small that they can be detected only in Endor experiments, and will be discussed in Chapter 5. The following discussion applies mainly to ions where the crystal field leaves a doublet ground state, or to states with a higher multiplicity

where the complications just mentioned do not occur or are so small that they can be neglected.

In the presence of anisotropy the interaction between the magnetic moment of a nucleus of spin **I** with the electronic field of an ion whose effective spin is **S**, may be written in the form **S . A . I**. The nature of the quantity **A** is discussed in Chapter 15; for brevity we shall still refer to it as a 'tensor' with a mental reservation similar to that for the g 'tensor'. When referred to its principal axes the term takes the form

$$A_x S_x I_x + A_y S_y I_y + A_z S_z I_z, \tag{3.39a}$$

but when axial symmetry is present we may use the form

$$A_\perp (S_x I_x + S_y I_y) + A_\parallel S_z I_z \tag{3.39b}$$

(in the literature the nomenclature A, B has generally been used for $A_\parallel$, $A_\perp$).

When the nucleus has a spin $I \geqslant 1$, and there is also an electric field gradient at the nucleus, an interaction with the nuclear electric quadrupole moment may arise whose form for an ion with effective spin $S = \frac{1}{2}$ may be written as **I . P . I**. Here **P** is a tensor quantity. The electric field gradient is set up by the anisotropic distribution of electric charge on the paramagnetic ion and its immediate neighbours, and the tensor **P** generally has the same principal axes as the quantities **g**, **D**, **A**. The general form of the interaction is

$$\begin{aligned} \mathbf{I \cdot P \cdot I} = {} & P_{xx} I_x^2 + P_{yy} I_y^2 + P_{zz} I_z^2 + \\ & + P_{xy} I_x I_y + P_{yx} I_y I_x + \\ & + P_{yz} I_y I_z + P_{zy} I_z I_y + \\ & + P_{zx} I_z I_x + P_{xz} I_x I_z, \end{aligned} \tag{3.40a}$$

but when referred to its principal axes it has the simpler form

$$P_x I_x^2 + P_y I_y^2 + P_z I_z^2, \tag{3.40b}$$

which is similar to that of the tensor **D** (eqn (3.25)). Thus by analogous reasoning, we can set $P_x + P_x + P_z = 0$, so that there are only two independent parameters. Then we can transform (3.40b) into an expression analogous to (3.26):

$$P_\parallel [\{I_z^2 - \tfrac{1}{3} I(I+1)\} + \tfrac{1}{3} \eta (I_x^2 - I_y^2)], \tag{3.40c}$$

where $P_\parallel = 3P_z/2$, $\eta = (P_x - P_y)/P_z$. This form is particularly useful if axial symmetry is present, when $\eta = 0$.

Since the nomenclature adopted here is somewhat different from that in other branches of radio-frequency spectroscopy, we note that

$$P_{\parallel} = \frac{3eQq}{4I(2I-1)} = \frac{3eQ}{4I(2I-1)} \frac{\partial^2 V}{\partial z^2}, \tag{3.41}$$

where $q = (\partial^2 V/\partial z^2)$ is the electric field gradient at the nucleus.

Finally, we have a term $-\beta \mathbf{H} \cdot \mathbf{g}^{(I)} \cdot \mathbf{I}$, which represents the interaction between the nuclear magnetic moment and the external field **H**. If this were a simple direct interaction, $\mathbf{g}^{(I)}$ would be a scalar quantity, equal to the ordinary nuclear g-factor. However, when an external magnetic field is applied the electronic wave-function is changed by an amount that is in first approximation proportional to H, and the electronic field at the nucleus is similarly modified, producing the equivalent of paramagnetic shielding (or anti-shielding). An atomic example of this is given in eqn (3.38c). In the solid state this effect can be quite large; when low-lying excited electronic states are present so that the electronic wave-function is appreciably modified in a magnetic field, and the (anti-)shielding correction may outweigh the direct interaction. For example, Lewis and Sabisky (1963) find that for the Ho^{2+} ion in CaF_2 the apparent value of $\mathbf{g}^{(I)}$ is forty times larger than the true value. Also, when the electronic ground state is anisotropic the (anti-)shielding will be anisotropic, so that $\mathbf{g}^{(I)}$ becomes a 'tensor' usually with the same principal axes as the g-factor.

3.8. Hyperfine structure II—strong external field

In general the energy levels of a system with hyperfine structure must be evaluated either by numerical or by perturbation methods. In most cases the electron Zeeman energy is the largest term in the Hamiltonian, and perturbation methods can be used if this term is diagonalized first. These methods are adequate for many purposes, and also give qualitatively the behaviour of the spectrum in the general case.

The hyperfine terms in the spin Hamiltonian are

$$\mathscr{H}_{\mathrm{n}} = \mathbf{S} \cdot \mathbf{A} \cdot \mathbf{I} + \mathbf{I} \cdot \mathbf{P} \cdot \mathbf{I} - \beta \mathbf{H} \cdot \mathbf{g}^{(I)} \cdot \mathbf{I}. \tag{3.42}$$

If the electronic Zeeman term $\beta \mathbf{H} \cdot \mathbf{g} \cdot \mathbf{S}$ is the largest interaction term, then it must be diagonalized first. This is accomplished by changing to new axes, as in § 3.2; if the magnetic field **H** has direction cosines (l, m, n) with respect to the principal axes of the g-tensor, then the z_{e}-axis of the new system must have direction cosines $(lg_x/g, mg_y/g, ng_z/g)$.

When the new system of axes is introduced for **S** in the magnetic hyperfine term **S . A . I**, where **A** is assumed to have the same principal axes as the g-tensor and to be a symmetric tensor (see below), terms involving products of all possible pairs of the components of **S** and **I** appear. Those containing S'_x, S'_y are off-diagonal and connect levels separated by the electronic Zeeman energy; they can be treated by second-order perturbation theory. The term in S'_z is

$$S'_z(lg_xA_xI_x+mg_yA_yI_y+ng_zA_zI_z)/g. \tag{3.43}$$

The coefficients of I_x, I_y, I_z, if suitably normalized, can be regarded as a set of direction cosines; this normalization requires that

$$g^2A^2 = l^2g_x^2A_x^2+m^2g_y^2A_y^2+n^2g_z^2A_z^2. \tag{3.44}$$

Then by changing to a set of axes (x_n, y_n, z_n) for **I**, where z_n has the direction cosines (lg_xA_x/gA), (mg_yA_y/gA), (ng_zA_z/gA), the first order hyperfine term given by eqn (3.43) reduces to

$$AS'_zI'_z, \tag{3.45}$$

where the primes indicate that S'_z refers to the 'electronic' coordinate system (x_e, y_e, z_e) and I'_z refers to the 'nuclear' coordinate system (x_n, y_n, z_n). From eqn (3.45) it is obvious that in the first order the energy of a state (M, m) is displaced by an amount AMm, where A is given by eqn (3.44). The strongly allowed transitions are of the type $(M, m) \leftrightarrow (M-1, m)$, and these are displaced in energy by an amount Am. Thus each electronic transition is divided into $2I+1$ hyperfine lines, which are equally spaced in this approximation (see Fig. 3.8). Since at ordinary temperatures all nuclear orientations are equally probable, the hyperfine lines in each electronic transition have equal intensity; this makes it readily possible to distinguish a hyperfine splitting from an electronic 'fine splitting', where the lines have unequal intensity (see § 3.3).

In physical terms these results arise as follows. In a sufficiently strong external magnetic field the magnetic electrons may be regarded as giving rise to a magnetic field H_e at the centre of the ion, whose direction and (to some extent) magnitude depend on the direction of the external field. H_e is usually much stronger than the external field (and here we have assumed that this is so); its direction defines the axis denoted by z_n above, so that it is natural to take this axis in labelling the $2I+1$ nuclear quantum states. In this approximation their energy is just $-g_I\beta H_e m$, where g_I is the true nuclear g-factor. In an electronic transition the value of H_e changes; it is proportional to M, and in the

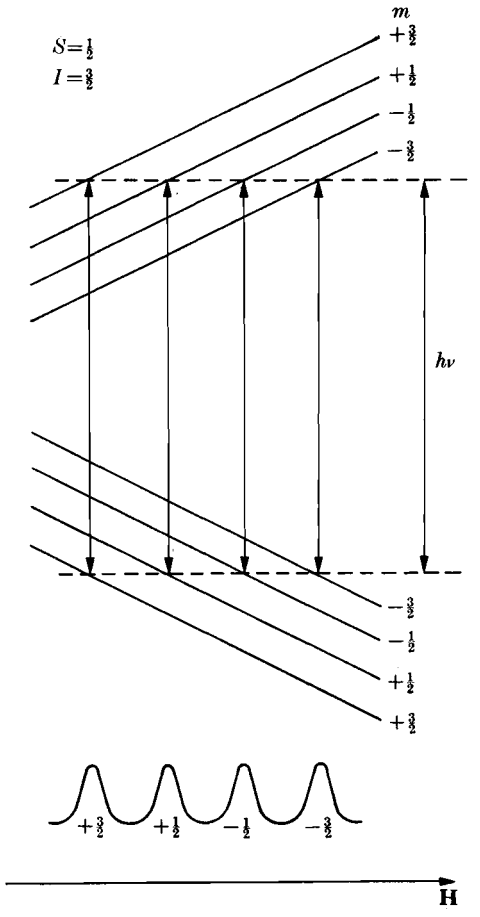

FIG. 3.8. Energy levels and allowed transitions for $S = \frac{1}{2}, I = \frac{3}{2}$ with magnetic hyperfine splitting, observed at constant frequency in strong magnetic field.

transition $M = +\frac{1}{2} \leftrightarrow -\frac{1}{2}$ it simply changes sign. The energy difference between each electronic state is therefore different for the $2I+1$ nuclear orientations, and this gives rise to $2I+1$ lines. Alternatively we may regard the electronic transition as taking place in a net field $H+H_n$, where H_n is the mean magnetic field produced by the nucleus and acting on the electronic magnetic moment; the value of H_n is proportional to the nuclear magnetic quantum number m.

In the treatment given above we have assumed that the quantity **A** has the same principal axes as **g**. This is not necessarily true in cases of low symmetry (see, for example, Bleaney and O'Brien (1956)) when, if x, y, z are the principal axes of the **g** 'tensor', the magnetic hyperfine

structure term will have the general form

$$A_{xx}S_xI_x+A_{yy}S_yI_y+A_{zz}S_zI_z+A_{xy}S_xI_y+A_{yx}S_yI_x+ \\ +A_{yz}S_yI_z+A_{zy}S_zI_y+A_{zx}S_zI_x+A_{xz}S_xI_z. \quad (3.45a)$$

Then on transforming to a new set of axes (x_e, y_e, z_e) where the z_e-axis has direction cosines $(g_xl/g, g_ym/g, g_zn/g)$, in order to diagonalize the electronic Zeeman interaction when a field **H** is applied with direction cosines (l, m, n), we obtain a term in S'_z

$$S'_z\begin{bmatrix} I_x\{A_{xx}(lg_x/g)+A_{yx}(mg_y/g)+A_{zx}(ng_z/g)\}+ \\ +I_y\{A_{xy}(lg_x/g)+A_{yy}(mg_y/g)+A_{zy}(ng_z/g)\}+ \\ +I_z\{A_{xz}(lg_x/g)+A_{yz}(mg_y/g)+A_{zz}(ng_z/g)\} \end{bmatrix} \quad (3.45b)$$

of which eqn (3.43) is clearly a special case. This can be diagonalized by changing to a set of axes (x_n, y_n, z_n) for **I**, where the direction cosines of z_n are just the coefficients of I_x, I_y, I_z in eqn (3.45b), whose normalization condition gives

$$g^2A^2 = (lg_xA_{xx}+mg_yA_{yx}+ng_zA_{zx})^2+(lg_xA_{xy}+mg_yA_{yy}+ng_zA_{zy})^2+ \\ +(lg_xA_{xz}+mg_yA_{yz}+ng_zA_{zz})^2. \quad (3.45c)$$

This is the equation of an ellipsoid in (l, m, n) space whose projection on a plane is an ellipse. If the quantity g^2A^2 is plotted as a function of angle while the magnetic field is rotated in any given plane, a sinusoidal variation is obtained repeating every 180°. If the angle θ is measured from an axis corresponding to an extremum of g^2A^2, then a plot of g^2A^2 against $\cos^2\theta$ or $\sin^2\theta$ will give a straight line. If the plane contains one of the principal axes (assumed to coincide) of **g** and **A**, such a plot (cf. Pryce (1949)) can be used to extrapolate the hyperfine constants to axes along which resonance cannot be observed.

The method of diagonalization we have used above depends on the fact that we can use different sets of axes as a reference for **S** and for **I**, a technique that would not be possible if **A** were a genuine tensor quantity. This is a particular illustration of a result that is discussed more generally for **A** and for **g** in Chapter 15; in contrast, quantities like **D** and **P** are tensors whose components multiply two components of the same vector quantity, **S** and **I** respectively.

The results obtained above are not changed in the first approximation by the inclusion of the second and third terms in $\mathscr{H}_n$, eqn (3.42), provided that they are small compared with the first term, as is usually the case. (Other possibilities are considered in § 3.11.) When this

condition is satisfied, we diagonalize the magnetic hyperfine structure by transforming to the axes (x_n, y_n, z_n) for $\mathbf{I}$; then the diagonal terms of $\mathscr{H}'_n$ are (assuming all 'tensor' quantities to have the same principal axes)

$$\mathscr{H}'_n = AS'_zI'_z+P\{I'^2_z-\tfrac{1}{3}I(I+1)\}- \\ -G_II'_z\ (+\text{second order terms}), \quad (3.46)$$

where

$$g^2A^2P = \tfrac{3}{2}\{l^2g_x^2A_x^2P_x+m^2g_y^2A_y^2P_y+n^2g_z^2A_z^2P_z\} \quad (3.47)$$

and

$$gAG_I = \beta H(l^2g_xA_xg_x^{(I)}+m^2g_yA_yg_y^{(I)}+n^2g_zA_zg_z^{(I)}), \quad (3.48)$$

while A is given by eqn (3.44). These diagonal terms in P and G_I change the energy levels but not, in a first approximation, the transitions, since only levels with the same value of m are involved in a strong transition, and these levels are displaced equally by such terms. Hence to the first order, the transition $|M, m\rangle \leftrightarrow |M-1, m\rangle$ is still displaced from the position at which the transition $M \leftrightarrow M-1$ would have occurred in the absence of the hyperfine structure by an amount Am. The quantity A, like g, must be taken to be positive.

The derivation of eqns (3.47), (3.48) is as follows. In the transformation to axes (x_n, y_n, z_n) the term $P_xI_x^2+P_yI_y^2+P_zI_z^2$ gives rise to a term

$$\{(lg_xA_x/gA)^2P_x+(mg_yA_y/gA)^2P_y+(mg_zA_z/gA)^2P_z\}I'^2_z = P'_zI'^2_z$$

together with terms in I'^2_x, I'^2_y and cross terms. The diagonal terms are

$$P'_zI'^2_z+\tfrac{1}{2}(P'_x+P'_y)(I'^2_x+I'^2_y) = \tfrac{1}{2}P'_z(2I'^2_z-I'^2_x-I'^2_y) = \tfrac{3}{2}P'_z\{I'^2_z-\tfrac{1}{3}I(I+1)\}$$

since $P'_x+P'_y+P'_z = P_x+P_y+P_z = 0$. Similarly the term

$$\beta H(lg_x^{(I)}I_x+mg_y^{(I)}I_y+ng_z^{(I)}I_z)$$

transforms to

$$\beta HI'_z(l^2g_xA_xg_x^{(I)}+m^2g_yA_yg_y^{(I)}+n^2g_zA_zg_z^{(I)})/(gA)$$

plus terms in I'_x, I'_y. It will be seen that a general advantage of the method of approximate diagonalization used in this chapter is that the first-order terms can be extracted from the directions of z_e and z_n without determining the directions of the axes x_e, y_e or x_n, y_n.

Off-diagonal terms

The effect of the off-diagonal terms in the magnetic *hfs* is twofold: (1) they allow transitions in which the nuclear magnetic quantum

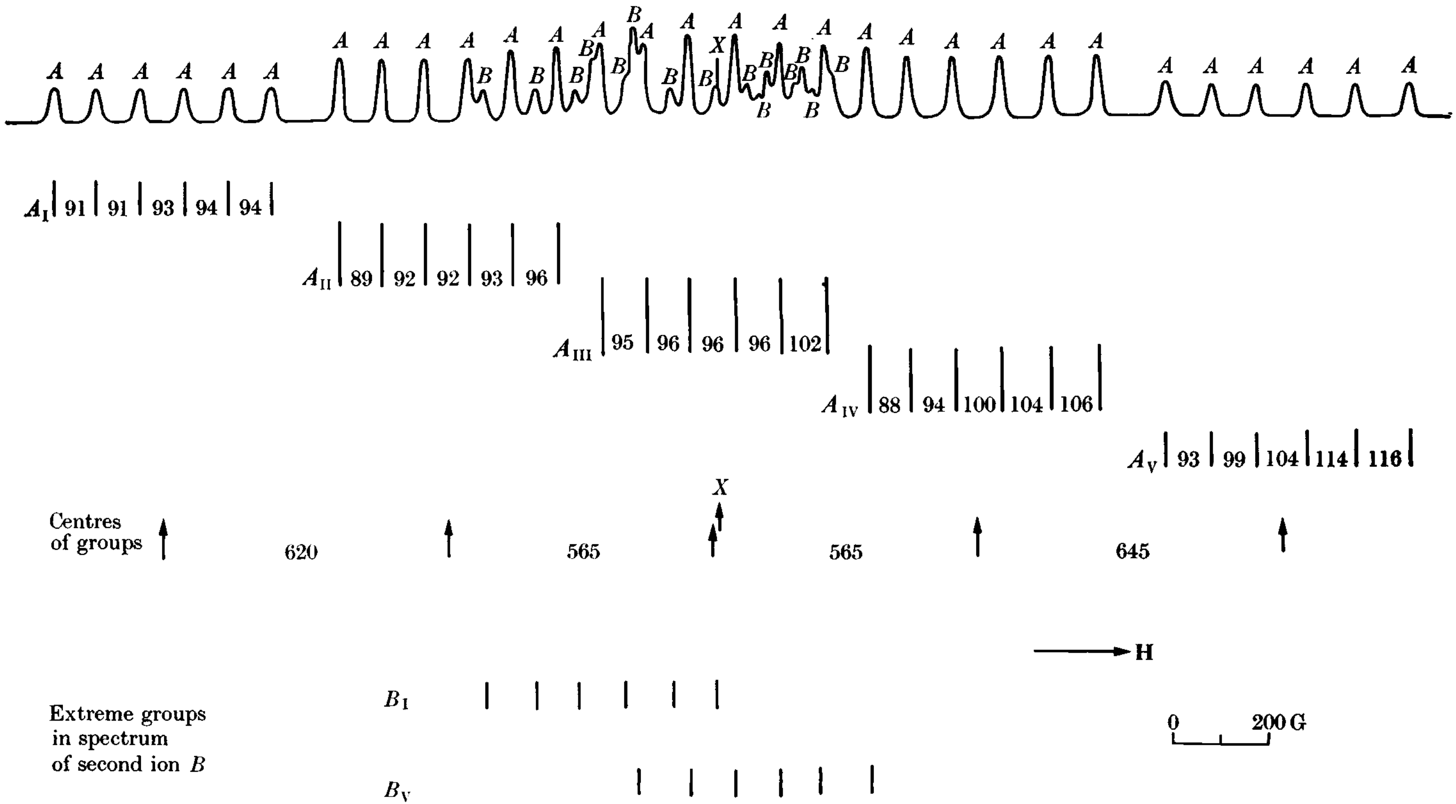

FIG. 3.9. Spectrum, at 20°K and 3·3 cm wavelength, of dilute manganese ammonium sulphate, with magnetic field parallel to the tetragonal axis of ion *A*. The hyperfine structure and fine-structure separations are given in gauss. Only two groups of lines for ion *B* are resolved; *X* is the narrow line of the organic radical used to determine *g*. Note that within each hyperfine group (I to V) splittings increase to the right (increasing magnetic field), and that different groups have different mean hyperfine splittings; the latter can be used for determining relative signs (see text) (Bleaney and Ingram 1951*a*).

number m changes by ± 1, smaller in intensity than the strong transitions by a factor $\sim(A/h\nu)^2$; (2) they introduce energy terms of order $A^2/(h\nu)$ which involve m^2, and hence make the hyperfine lines unequally spaced; (3) for $S > \frac{1}{2}$, they introduce terms in Mm which change the spacing of the hyperfine lines in different electronic transitions by amounts of the order $A^2/(h\nu)$. These effects are illustrated in Fig. 3.9. The effect of terms of this order can be eliminated by taking the average of all the separations between successive hyperfine lines to find A.

The effect of the off-diagonal terms arising from $\mathbf{I} \cdot \mathbf{P} \cdot \mathbf{I}$ is also to make transitions allowed in which m changes, smaller in intensity by a factor $\sim(P/A)^2$. The positions of the strong transitions are affected by amounts of order P^2/A. The off-diagonal terms in $\beta\mathbf{H} \cdot \mathbf{g}^{(I)} \cdot \mathbf{I}$ are usually too small to have an observable effect.

In general we shall evaluate these second-order effects only in the case of axial symmetry.

Axial symmetry—magnetic hyperfine interaction only

In order to look at the behaviour of hyperfine structure in some detail, it is more profitable to restrict the discussion to the case of axial symmetry, and to omit at first the nuclear electric quadrupole interaction as well as the electronic fine structure terms. With axial symmetry we can choose the direction of the x-axis so that the external magnetic field lies in the xz-plane. Then the Hamiltonian may be written as

$$\begin{aligned}\mathscr{H} = {} & \beta H(g_{\parallel} S_z \cos\theta + g_{\perp} S_x \sin\theta) + \\ & + A_{\parallel} S_z I_z + A_{\perp}(S_x I_x + S_y I_y) - \\ & - \beta H(g_{\parallel}^{(I)} I_z \cos\theta + g_{\perp}^{(I)} I_x \sin\theta), \quad (3.49)\end{aligned}$$

where the effective nuclear g-factor $\mathbf{g}^{(I)}$ is assumed also to have axial symmetry. The electronic Zeeman term, which we again assume to be much the largest, is first diagonalized, as in § 3.2, by changing to a new set of axes for $\mathbf{S}$ which are rotated from the original set by an angle ϕ about the y-axis. This leaves terms in the hyperfine structure involving $S'_z I_x$, as well as terms such as $S'_x I_x$ and $S'_y I_y$; the latter connect levels that differ in energy by $g\beta H$ and can be treated by second-order perturbation theory if $|A| \ll g\beta H$. However a term such as $S'_z I_x$ cannot, and must be eliminated by changing to a new set of axes for $\mathbf{I}$. If this system is rotated from the original system (as in Fig. 3.10) by an angle ψ about the y-axis, then the coefficient of $S'_z I'_x$ after this

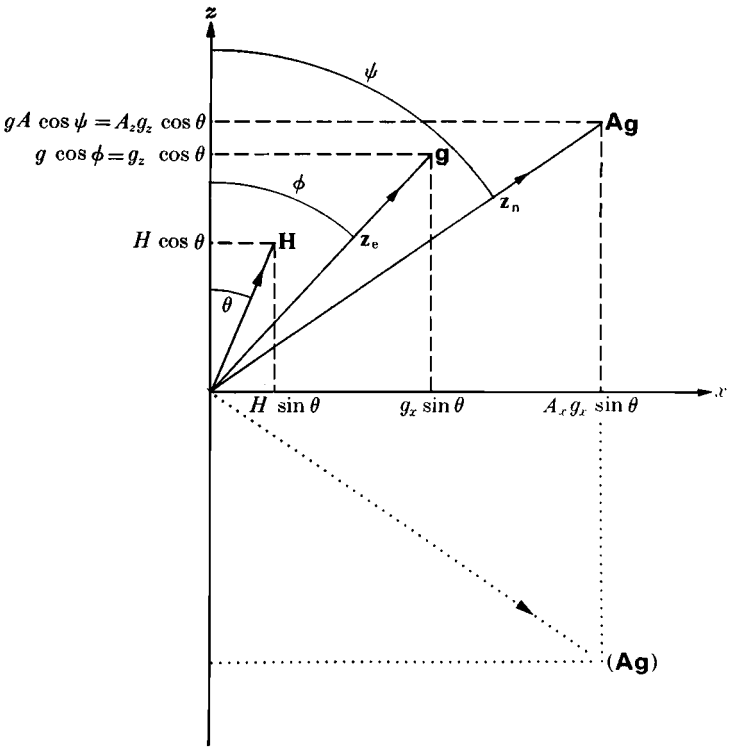

FIG. 3.10. Orientation of magnetic field **H**, electron spin ($\mathbf{z}_e$) and nuclear spin ($\mathbf{z}_n$) when anisotropy is present. The figure is drawn for $g_x > g_z$, $A_x > A_z$ (all positive). The dotted vector is appropriate to a negative value of A_z, the other parameters remaining positive. The equations relating the components of **I** in the two systems eqns (3.49), (3.51) and Fig. 3.1.) are (primes refer to the x_n, y_n, z_n system):

$$I_z = I'_z \cos\psi - I'_x \sin\psi,$$
$$I_x = I'_z \sin\psi + I'_x \cos\psi,$$
$$I_y = I'_y,$$

with

$$\cos\psi = (A_z/A)\cos\phi = (g_z A_z/gA)\cos\theta,$$
$$\sin\psi = (A_x/A)\sin\phi = (g_x A_x/gA)\sin\theta.$$

transformation is found to be

$$A_\perp \sin\phi\cos\psi - A_\parallel \cos\phi\sin\psi, \tag{3.50}$$

which vanishes if we choose ψ so that

$$\tan\psi = (A_\perp/A_\parallel)\tan\phi = (A_\perp g_\perp/A_\parallel g_\parallel)\tan\theta.$$

The term in $S'_z I'_z$ can now be written as $AS'_z I'_z$, where

$$g^2A^2 = g_\parallel^2 A_\parallel^2 \cos^2\theta + g_\perp^2 A_\perp^2 \sin^2\theta. \tag{3.51}$$

This is clearly the special form of eqn (3.44) appropriate to axial symmetry.

The spin Hamiltonian now becomes

$$\begin{aligned}\mathscr{H} = {} & g\beta HS'_z + AS'_zI'_z + \\ & + S'_x[(A_\parallel A_\perp/A)I'_x - \tfrac{1}{2}\{(A_\parallel^2 - A_\perp^2)/A\}(g_\parallel g_\perp/g^2)\sin 2\theta\, I'_z] + \\ & + A_\perp S'_y I'_y - \\ & - \beta H\begin{bmatrix} I'_z(g_\perp^{(I)} \sin\theta \sin\psi + g_\parallel^{(I)} \cos\theta \cos\psi) + \\ + I'_x(g_\perp^{(I)} \sin\theta \cos\psi - g_\parallel^{(I)} \cos\theta \sin\psi)\end{bmatrix}. \end{aligned} \tag{3.52}$$

If $g^{(I)}$ is isotropic, the last term reduces to

$$-g^{(I)}\beta H\{I'_z \cos(\theta-\psi) + I'_x \sin(\theta-\psi)\}, \tag{3.53}$$

corresponding to the fact that the angle between **H** and the z_n-axis is just $(\theta-\psi)$. The angle ψ can be eliminated using the relations

$$\sin\psi = (g_\perp A_\perp/gA)\sin\theta,\ \cos\psi = (g_\parallel A_\parallel/gA)\cos\theta.$$

In most cases the nuclear Zeeman term is so small that we need retain only its diagonal part, and using first- and second-order perturbation theory the energy of the state (M, m) is found to be

$$\begin{aligned} W_{M,m} = {} & g\beta HM + Am[M + (A_\parallel A_\perp^2/2A^2G)\{M^2 - S(S+1)\}] + \\ & + (A_\parallel^2 + A^2)(A_\perp^2/4A^2G)M\{I(I+1) - m^2\} - \\ & - [\{(A_\parallel^2 - A_\perp^2)^2/8A^2G\}(g_\parallel g_\perp/g^2)^2 \sin^2 2\theta]Mm^2 - G_I m, \end{aligned} \tag{3.54}$$

where $G = g\beta H$ and G_I is given by the relation

$$gAG_I = \beta H(g_\parallel^{(I)} g_\parallel A_\parallel \cos^2\theta + g_\perp^{(I)} g_\perp A_\perp \sin^2\theta). \tag{3.55}$$

Hence the transition $(M, m) \leftrightarrow (M-1, m)$ requires a quantum

$$\begin{aligned} h\nu = {} & g\beta H + Am\{1 + (A_\parallel A_\perp^2/2A^2G)(2M-1)\} + \\ & + (A_\parallel^2 + A^2)(A_\perp^2/4A^2G)\{I(I+1) - m^2\} + \\ & + [\{(A_\parallel^2 - A_\perp^2)^2/8A^2G\}(g_\parallel g_\perp/g^2)^2 \sin^2 2\theta]m^2. \end{aligned} \tag{3.56}$$

The significance of the angle ψ is similar to that of ϕ, and can be pictured as follows. The steady component of the electronic moment lies along z_e, and has components proportional to $\cos\phi = (g_\parallel/g)\cos\theta$ and $\sin\phi = (g_\perp/g)\sin\theta$ parallel and perpendicular to the symmetry axis respectively. Owing to the anisotropy in the hyperfine interaction, the corresponding components of the magnetic field $\mathbf{H}_e$ which the electrons produce at the nucleus are proportional to $A_\parallel(g_\parallel/g)\cos\theta$ and $A_\perp(g_\perp/g)\sin\theta$ respectively, and the nucleus therefore precesses

about the direction $\mathbf{z}_n$ given by the resultant of these two components, in a field $\mathbf{H}_e$ proportional to $(g_\parallel^2 A_\parallel^2 \cos^2\theta + g_\perp^2 A_\perp^2 \sin^2\theta)^{\frac{1}{2}}/g$. It is convenient to call this direction the 'nuclear spin axis', though the nucleus does not precess in a simple manner about this axis.

The second-order terms vary as $(g\beta H)^{-1}$ or $(h\nu)^{-1}$ and so vanish in strong fields. They are of two kinds, and we consider first those which vary as m^2. These cause a departure from equal spacing in the hyperfine structure; under normal conditions the lines observed at lower field, when working at constant frequency, are closer together than those at higher field, as illustrated in Fig. 3.9. This may be reversed at certain angles if $|A_\parallel| > |A_\perp|$ because the term in $\sin^2 2\theta$ in eqn (3.56) has the opposite sign to the term in which θ does not occur explicitly (there is an implicit variation with angle in both terms through the variation in A). This effect is shown in Fig. 3.11.

The second type of second order term is linear in m, and has been

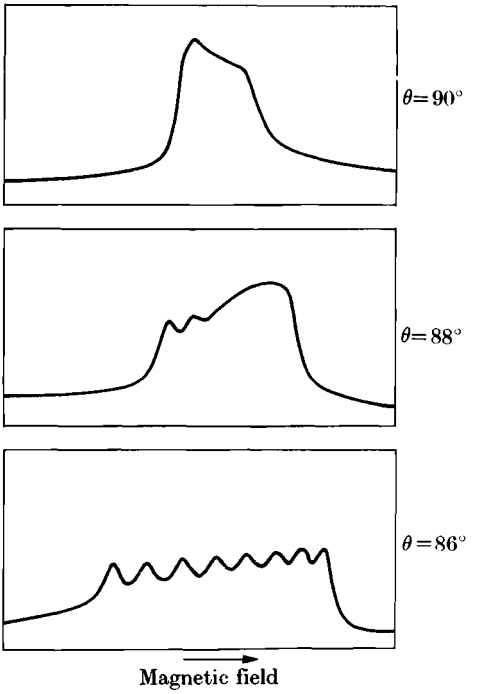

FIG. 3.11. Spectra of dilute cobalt ammonium sulphate near the perpendicular to the tetragonal axis at $T = 20°\text{K}$, $\bar{\nu} = 0{\cdot}8\ \text{cm}^{-1}$. Normally the second-order terms make the hyperfine lines closer together at the high field end, but in cases of high anisotropy this may be reversed near $\theta = 90°$ by the term in $\sin^2 2\theta$ in eqn (3.56) (Bleaney and Ingram 1951*b*).

combined with the principal term Am. It is present only when $S > \frac{1}{2}$. Its effect is to produce a variation in the spacing of the hyperfine components in different electronic transitions. If these are not split by a fine structure interaction, then the hyperfine lines belonging to different electronic transitions are slightly split by an amount increasing with $|m|$; this is greatest at the two ends of the hyperfine structure pattern, and if not resolved, may appear as a broadening of the outside lines. If there is a fine structure, then the appropriate terms from §§ 3.3–3.6 must be included in the spin Hamiltonian and in a first approximation the consequent displacements of the lines can be added linearly to eqn (3.56). It is then possible to observe experimentally whether the transitions occurring at higher frequencies in a constant field (i.e. in lower fields at constant frequency) have greater or smaller mean separations between the hyperfine lines. From this some information can be obtained about the signs of A_x, etc., provided that the signs of the g-values and of the fine structure terms have been determined, as described earlier.

For simplicity we consider only a quadrupole-like electronic splitting, but the argument is readily extended; initially we also assume axial symmetry. Then, if **H** is along the axis of symmetry, it is readily seen from Fig. 3.6 that if D is positive, the transitions between levels with positive values of M occur at higher frequencies in constant field (lower fields at constant frequency), and vice versa if D is negative. Then from eqn (3.56) the hyperfine structures in the transitions with positive values of M have a larger mean spacing if $A_\parallel$ is positive; thus the sign of $A_\parallel$ relative to that of D is determined. If **H** is perpendicular to the symmetry axis, the electronic transitions occur in the reverse order (see Fig. 3.5) and so also does the change in the mean spacing. However it is clear from eqn (3.56) that this still yields only the sign of $A_\parallel$ relative to that of D, since $A_\perp$ occurs only in the square in the second-order terms.

If there is only rhombic symmetry, the coefficient of $(2M-1)$ in eqn (3.56) becomes $(A_xA_yA_z/2A^2G)$, where the value of A is A_x, A_y, A_z according as the external field is directed along the corresponding axis (the coefficient has not been evaluated for intermediate directions, though its form suggests that it is still correct if the appropriate value of A is used). Thus in this case observation of the variation of the mean hyperfine spacing between different electronic transitions determines the sign of $(A_xA_yA_z)$ relative to that of D_x, D_y, D_z if the external field is directed along the three axes in turn. The situation is

rather similar to that for the g-values: with rhombic symmetry the use of a circularly polarized oscillatory field yields the sign of $(g_x g_y g_z)$, while from the fine structure one finds the sign of $(D_x D_y D_z)$ provided a relative intensity measurement can be made at low temperatures; from the hyperfine structure the sign of $(A_x A_y A_z)$ is determined if the signs of the principal values of the **D**-tensor are known (if not, only the sign of $(A_x A_y A_z)$ relative to that of $(D_x D_y D_z)$ can be found). With axial symmetry, circularly polarized radiation yields the sign of $g_\parallel$ uniquely, and the hyperfine structure gives the sign of $A_\parallel$ relative to that of D. No information about the signs of A_x, A_y, A_z is obtained if only one electronic transition is observed, as in the case of $S = \frac{1}{2}$.

At first sight it might appear that the argument given above might have to be reversed if one of the g-values were negative, since G appears in the denominator of the second-order terms in eqn (3.56). However the labelling of the transitions would also have to be reversed in sign, and the argument is still correct. This illustrates the advantage of always taking g and A to be positive quantities; the actual signs of the principal values of the **g**, **A** tensors then only affect the quadrants in which the angles ϕ, ψ lie, and appear automatically in equations such as (3.56) where functions of ϕ, ψ have been translated back into functions of θ.

3.9. Hyperfine structure III—nuclear electric quadrupole interaction

We discuss first a special case where explicit formulae can be obtained for the energy levels, and which shows some similarity to a free atom: an ion with $S = \frac{1}{2}$, and axial symmetry. If the external magnetic field **H** is applied along the axis of symmetry, the spin Hamiltonian is

$$\mathscr{H} = g_\parallel \beta H S_z + A_\parallel S_z I_z + A_\perp (S_x I_x + S_y I_y) + P_\parallel \{I_z^2 - \tfrac{1}{3} I(I+1)\} - g_\parallel^{(I)} \beta H I_z. \tag{3.57}$$

The effect of the term in $A_\perp$ is to admix the states $(M = +\frac{1}{2}, m)$ and $(M = -\frac{1}{2}, m+1)$, where m is the nuclear magnetic quantum number. These two states both have the same component of total angular momentum along the z-axis; this component is $m+\frac{1}{2}$ (in units of $\hbar$), which we may write as m_F, where $m_F = M+m$. It is similar to the magnetic quantum number m_F used in the hyperfine structure of free atoms (see Fig. 3.12), being the component of the total angular momentum along the z-axis, but with the difference that the symmetry axis of **A** and $\overline{\mathbf{P}}$ (the z-axis) is fixed in the crystal, whereas in the free

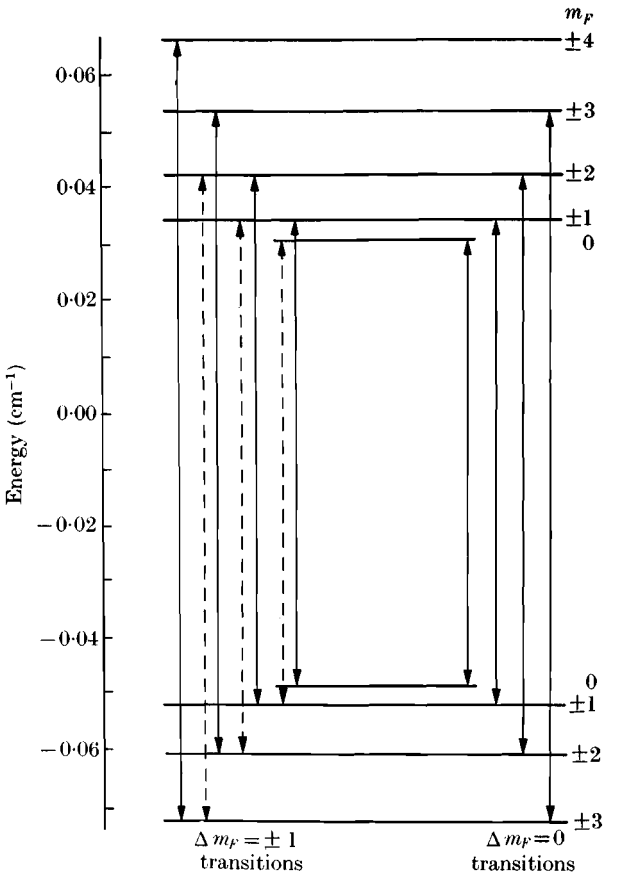

FIG. 3.12. Hyperfine levels of ^{143}Nd in lanthanum ethyl sulphate in zero magnetic field. The Nd^{3+} ion in this salt has axial symmetry, so that the levels $\pm m_F$ are degenerate, giving doublets except for the levels $m_F = 0$. The transitions corresponding to $\Delta m_F = \pm 1$ are shown on the left, the broken lines indicating rather weak transitions; the transitions $\Delta m_F = 0$ are shown on the right. If there were no anisotropy ($A_\parallel = A_\perp$, $P_\parallel = 0$), the upper and lower groups of levels would each be unsplit, corresponding to $F = 4$ and $F = 3$ respectively.

atom there is no restriction and the z-axis can be taken as that of the external magnetic field. In the present instance we restrict the discussion to the case where **H** is along the z-axis, in order to obtain a simple closed form for the energy levels. Then the energy of the two states with the same value of m_F is

$$W = -g_\parallel^{(I)}\beta H m_F - \tfrac{1}{4}A_\parallel + P_\parallel\{m_F^2 + \tfrac{1}{4} - \tfrac{1}{3}I(I+1)\} \pm$$
$$\pm \tfrac{1}{2}[\{\beta H(g_\parallel + g_\parallel^{(I)}) + (A_\parallel - 2P_\parallel)m_F\}^2 + A_\perp^2\{I(I+1) + \tfrac{1}{4} - m_F^2\}]^{\frac{1}{2}}, \quad (3.58)$$

where the positive sign must be taken for the state where the electronic spin moment is parallel to the field and the negative sign when it is anti-parallel.

The transitions that are allowed within this set of energy levels are of two kinds. If the oscillatory field $\mathbf{H}_1$ is normal to the z-axis, only transitions of the type $\Delta m_F = \pm 1$ are allowed, but we must distinguish between transitions of the form $|M, m\rangle \leftrightarrow |M \pm 1, m\rangle$ and of the form $|M, m\rangle \leftrightarrow |M, m \pm 1\rangle$. In strong external fields where $h\nu \gg A_\perp$ the admixture of states for a given value of m_F becomes very small, so that each state is rather accurately specified as just $|M, m\rangle$. Then the transitions in which $\Delta M = \pm 1$, $\Delta m = 0$ are strong ones, involving the electronic moments, and require a quantum of the order

$$|g_\parallel \beta H + A_\parallel m|.$$

The transitions in which $\Delta M = 0$, $\Delta m = \pm 1$ are weak transitions involving (in the strong field limit) only the nuclear moments, and require a quantum of the order $A_\parallel M + P_\parallel(2m \pm 1) \mp g_\parallel^{(I)} \beta H$.

In intermediate fields these latter transitions gain in intensity because some electronic magnetic moment is involved through the mixture of states.

If the oscillatory field is parallel to the z-axis, the selection rule is $\Delta m_F = 0$. Hence the only allowed transitions are those between the two energy levels with the same value of m_F, and from eqn (3.58),

$$h\nu = [\{\beta H(g_\parallel + g_\parallel^{(I)}) + (A_\parallel - 2P_\parallel)m_F\}^2 + A_\perp^2\{I(I+1) + \tfrac{1}{4} - m_F\}^2]^{\frac{1}{2}}. \tag{3.59}$$

The matrix element for these transitions has the squared value (neglecting the nuclear magnetic moment)

$$|\mu_{ij}|^2 = \tfrac{1}{4} g_\parallel^2 \beta^2 (A_\perp / h\nu)^2 \{I(I+1) + \tfrac{1}{4} - m_F^2\}. \tag{3.60}$$

It depends on the value of m_F, and as the frequency increases the transition probability becomes vanishingly small. From eqn (3.59) it follows that measurements on transitions of this kind yield the quantities $|(g_\parallel + g_\parallel^{(I)})|$, $|A_\parallel - 2P_\parallel|$, and $|A_\perp|$. If these are combined with observation of transitions of the type $\Delta M = \pm 1$, $\Delta m = 0$, which yield different combinations of the parameters, we can find the quantities $|g_\parallel^{(I)}|$, $|A_\parallel|$, $|P_\parallel|$, the sign of $g_\parallel^{(I)}$ relative to $g_\parallel$, and that of $P_\parallel$ relative to $A_\parallel$. If the sign of $g_\parallel$ is known, then that of $g_\parallel^{(I)}$ is determined (and vice versa); similarly for $P_\parallel$ and $A_\parallel$. In practice it is not usually possible to find $g_\parallel^{(I)}$ because it is $\sim 10^{-3} g_\parallel$, and to obtain sufficiently

accurate measurements observations must be made in fields such that $g^{(I)}\beta H$ is comparable with the line width; then the transitions involved in eqn (3.59) usually have insufficient intensity to be detectable.

Nuclear electric quadrupole interaction—perturbation theory

We now extend the treatment of § 3.8, hyperfine structure in strong external fields, to include the nuclear electric quadrupole interaction. The first-order effects of this interaction have already been evaluated (eqn (3.47)) and shown to produce no effect on the spectrum in this approximation. The second-order effects therefore become unusually important, since it is only through their effect on the spectrum that the size of the nuclear electric quadrupole interaction can be found. In general, the magnitude of this interaction is smaller than that of the magnetic hyperfine interaction, and we make this assumption in applying perturbation theory to treat the case of axial symmetry, without restriction on the value of S.

If an external magnetic field is applied at an angle θ to the symmetry axis (the z-axis) in the xz-plane, and the nuclear coordinate system (x_n, y_n, z_n) is introduced where the z_n-axis makes an angle ψ with the z-axis, the nuclear electric quadrupole interaction

$$P_{\|}\{I_z^2-\tfrac{1}{3}I(I+1)\}$$

becomes

$$\begin{aligned}\tfrac{1}{2}P_{\|}\{I_z'^2-\tfrac{1}{3}I(I+1)\}(3\cos^2\psi-1)-\\ -P_{\|}(I_x'I_z'+I_z'I_x')\cos\psi\sin\psi+\\ +\tfrac{1}{4}P_{\|}(I_+'^2+I_-'^2)\sin^2\psi. \quad (3.61)\end{aligned}$$

The last two terms are off-diagonal and give rise to matrix elements between the states $|m\rangle$ and $|m\pm1\rangle$, $|m\pm2\rangle$ belonging to the same value of the electronic magnetic quantum number M. This gives a complicated energy matrix in which perturbation methods can only be applied if $|P| \ll |AM|$, since AM is the energy difference between successive nuclear levels. If this inequality holds, the strongly allowed transitions are still those in which $\Delta m = 0$, $\Delta M = \pm1$. The first (diagonal) term in eqn (3.61) adds to the energy of the state $|M, m\rangle$ in eqn (3.54) an amount

$$\begin{aligned}\tfrac{1}{2}P_{\|}\{m^2-\tfrac{1}{3}I(I+1)\}\left\{3\frac{g_{\|}^2A_{\|}^2}{g^2A^2}\cos^2\theta-1\right\}\\ = P\{m^2-\tfrac{1}{3}I(I+1)\}, \quad (3.62)\end{aligned}$$

which is just a special case of eqn (3.47). The off-diagonal terms, treated by second-order perturbation theory, add to the energy a

further amount

$$(g_\parallel g_\perp A_\parallel A_\perp/g^2A^2)^2\{P_\parallel^2 \sin^2 2\theta/8AM)\}m\{8m^2+1-4I(I+1)\}+ \\ +(g_\perp A_\perp/gA)^4\{P_\parallel^2 \sin^4\theta/8AM\}m\{2I(I+1)-2m^2-1\}. \quad (3.63)$$

The quantum of energy required for the transition $|M, m\rangle \leftrightarrow |M-1, m\rangle$ is increased by an amount

$$-(g_\parallel g_\perp A_\parallel A_\perp/g^2A^2)^2\{P_\parallel^2 \sin^2 2\theta/8AM(M-1)\}m\{8m^2+1-4I(I+1)\}- \\ -(g_\perp A_\perp/gA)^4\{P_\parallel^2 \sin^4\theta/8AM(M-1)\}m\{2I(I+1)-2m^2-1\}, \quad (3.64)$$

where the term in P (eqn (3.62)) has vanished since it does not depend on M. The second-order terms, unlike those in eqn (3.56), do not vanish in strong fields, since the denominators contain A and not G. In addition to terms in m, which change the spacing of all the hyperfine lines equally, they contain terms in m^3 that make the spacing of the hyperfine lines greater at the outside than at the middle when $\theta = 90°$, with the reverse effect at intermediate angles. This effect vanishes at $\theta = 0°$, where there are no off-diagonal terms if there is axial symmetry. Thus quadrupole effects give a pattern that is symmetrical about the centre, unlike second-order effects of the magnetic hyperfine structure, which produce terms in m^2.

A more important and more easily detectable effect of the off-diagonal elements of the quadrupole interaction is that they give rise to transitions in which the nuclear magnetic quantum number changes by one or two units ($\Delta m = \pm 1, \pm 2$) that would otherwise be forbidden. In a first approximation, where energies of the order $(P/A)^2$ are neglected, these transitions occur as follows (in these equations the value of P, which occurs in the energy, is given by eqn (3.62)). Transitions $|M, k\pm\frac{1}{2}\rangle \leftrightarrow |M-1, k\mp\frac{1}{2}\rangle$:

$$\text{Hyperfine energy} = Ak \pm \{A(M-\tfrac{1}{2})+2Pk-G_I\}. \quad (3.65)$$

The intensities, relative to that of the $\Delta m = 0$ transitions, are:

$$(g_\parallel g_\perp A_\parallel A_\perp/g^2A^2)^2\{P_\parallel \cos\theta \sin\theta/AM(M-1)\}^2 \times k^2\{(I+\tfrac{1}{2})^2-k^2\}. \quad (3.66)$$

Transitions $|M, m\pm 1\rangle \leftrightarrow |M-1, m\mp 1\rangle$:

$$\text{Hyperfine energy} = Am \pm \{A(2M-1)+4Pm-2G_I\}. \quad (3.67)$$

The intensities, relative to that of the $\Delta m = 0$ transitions, are:

$$(g_\perp^2 A_\perp^2/g^2A^2)^2\{P_\parallel \sin^2\theta/8AM(M-1)\}^2 \times \{(I+1)^2-m^2\}\{I^2-m^2\}. \quad (3.68)$$

Here G_I is in general given by eqn (3.55), but if $g^{(I)}$ is isotropic the rather complicated angular dependence of G_I is simply $\cos(\theta-\psi)$, as can be seen from eqn (3.53). If the quantities $g_\parallel A_\parallel$, $g_\perp A_\perp$ are of opposite

sign, G_I may pass through zero, since there is an angle at which $(\theta - \psi)$ is 90°, corresponding to a situation where the electronic magnetic field $\mathbf{H}_e$ at the nucleus is perpendicular to the external magnetic field $\mathbf{H}$.

The general behaviour of the energy levels and transitions is illustrated in Fig. 3.13.

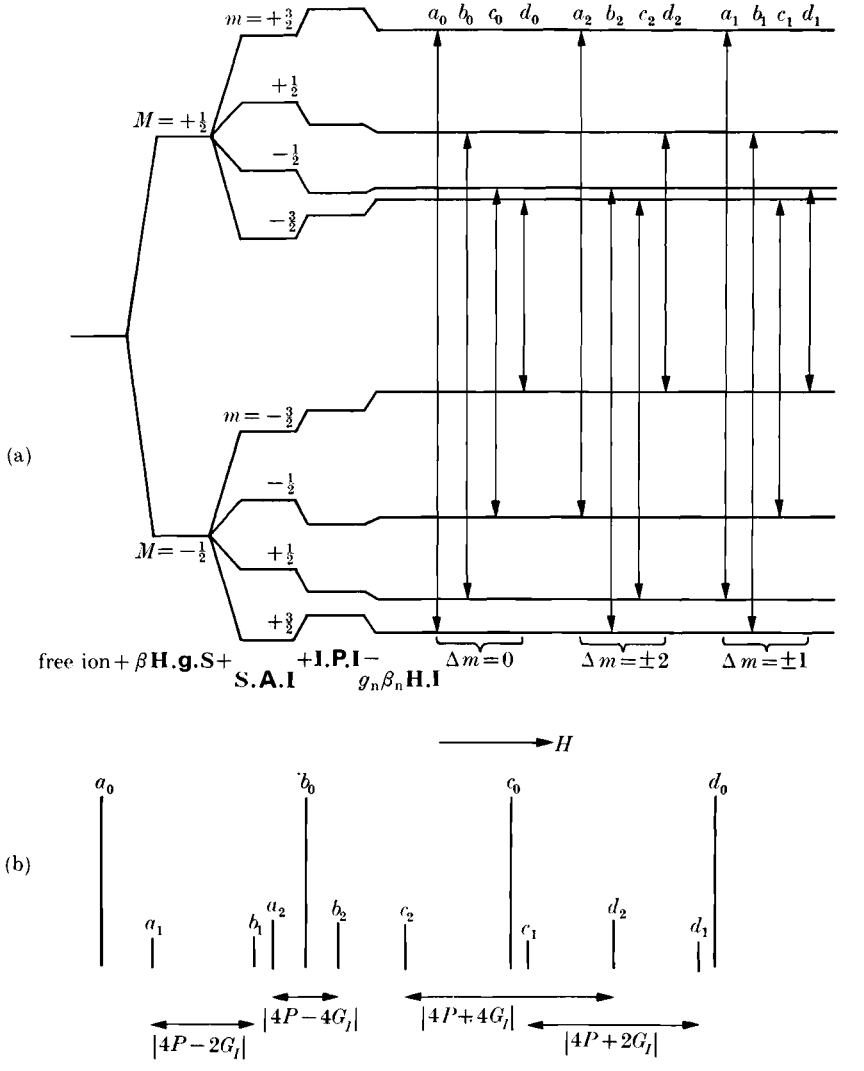

FIG. 3.13. (a) Schematic energy-level diagram for $S = \frac{1}{2}$, $I = \frac{3}{2}$. Of the transitions shown, $\Delta m = 0$ and $\Delta m = \pm 2$ are allowed if the external magnetic field is along a rhombic axis, while $\Delta m = \pm 1$ are allowed only in intermediate directions.
(b) Schematic representation of the spectrum corresponding to (a).
Second-order terms have been neglected; the intensities are not to scale.

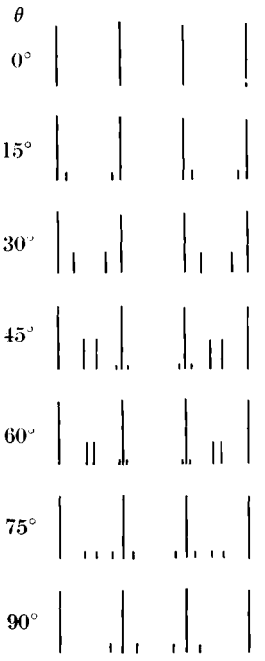

FIG. 3.14. Quadrupole effects in spectrum for $S = \frac{1}{2}$, $I = \frac{3}{2}$, with no anisotropy and $A_{\parallel} = A_{\perp} = 5P_{\parallel}$.

The behaviour of these lines can best be appreciated from a simple example. Figure 3.14 shows the spectrum at various angles for a hypothetical ion for which $S = \frac{1}{2}$, $I = \frac{3}{2}$, $A_{\parallel} = A_{\perp} = 5P_{\parallel}$, $g_{\parallel} = g_{\perp}$. At $\theta = 0$ only the four $\Delta m = 0$ lines are allowed. As θ increases the $\Delta m = \pm 1$ lines appear first, as doublets symmetrically situated about the midpoints between all the $m = 0$ lines except at the centre of the whole spectrum. From (3.65), since $(M - \frac{1}{2}) = 0$ in this case, the splitting of these doublets is $(4Pk - 2G_I)$ and so is greatest at the ends of the spectrum, but is asymmetrical because the terms $4Pk$ and $2G_I$ add at one end and subtract at the other. The intensities (eqn (3.66)) are greatest when $\theta = 45°$, and fall to zero again at 90°. The behaviour of the $\Delta m = \pm 2$ lines is rather similar, except that the doublets have twice as great a splitting (see eqn (3.67)) and are centred on each of the $\Delta m = 0$ lines except the outside lines; the intensity (eqn (3.68)) increases to a maximum at $\theta = 90°$K. Figure 3.14 is drawn for a case of no anisotropy, but the behaviour is qualitatively similar when axial anisotropy is present. The nuclear quadrupole effects then essentially depend on the angle ψ, which may be very much closer than θ to 0

or π if $|(g_\parallel A_\parallel / g_\perp A_\perp| \gg 1$, or closer to $\pm\pi/2$ if this quantity is less than unity. If $|(g_\parallel A_\parallel / g_\perp A_\perp)|$ is much greater than unity, the quadrupole lines appear only at values of θ close to 90°, and the whole of the variation of P (which passes through zero at $\cos\psi = 3^{-\frac{1}{2}}$) occurs over a small range of θ close to 90°. On the other hand, if $|(g_\parallel A_\parallel / g_\perp A_\perp)| \ll 1$, the quadrupole effects are spread over a wide range of the angle θ, and may appear with considerable intensity when θ is quite small.

In principle, observation of these quadrupole lines gives a good deal of extra information, since the doublet splitting yields both $|P|$, from which the nuclear quadrupole moment can be calculated if the electric field gradient is known, and $|G_I|$ from which the nuclear magnetic moment can be obtained directly. Determination of the relative signs of these quantities needs careful analysis.

Since both g and A are positive quantities, the lines for which m or k are positive occur always at the high frequency (low field) end of a group of hyperfine lines. When $S = \frac{1}{2}$, the extra lines due to quadrupole interaction fall into doublets from whose splitting the relative signs of P and G_I can be determined, since the splitting will be smallest at the high frequency (low field) end if P, G_I have the same signs, and vice versa (see Fig. 3.13(b)). Inspection of the expressions for P, G_I shows that observations at different angles then give the sign of $P_\parallel$ relative to the signs of $(A_\parallel g_\parallel / g_\parallel^{(I)})$, $(A_\perp g_\perp / g_\perp^{(I)})$ which occur in G_I (eqn (3.55)), together with the magnitudes of $|P_\parallel|$, $|g_\parallel^{(I)}|$, $|g_\perp^{(I)}|$, $|A_\parallel|$, $|A_\perp|$.

Further information about signs can be obtained from theory or from consideration of second-order effects:

(1) atomic theory of the electronic ground state may give the sign and magnitudes of the quantities $g_\parallel$, $g_\perp$, $(A_\parallel / g_\parallel^{(I)})$, $(A_\perp / g_\perp^{(I)})$, and (P/Q); then the signs of $(A_\parallel g_\parallel / g_\parallel^{(I)})$, $(A_\perp g_\perp / g_\perp^{(I)})$ are known and from the experiments one can deduce the sign of P and hence also of Q, the electric quadrupole moment of the nucleus;

(2) the second-order terms in eqn (3.64) are of fixed sign and if their effect is observable, the actual signs of P and G_I can be found;

(3) the second-order terms in eqn (3.56) are of fixed sign and by observing their effect in intermediate fields the sign of P, and hence of G_I (either directly or from the strong field experiments) can be found;

(4) if $S = 1$ or more, the signs of P and G_I are found from first-order effects through the terms in AM in eqns (3.65), (3.67), provided that the sign of M has been identified for the various electronic transitions; otherwise the first-order terms give only the signs of P, G_I relative to the fine structure terms.

In many cases sufficient resolution may not be available to determine all these quantities. The term G_I is usually rather small so that it cannot be determined accurately unless measurements are made at rather high fields.

It must be stressed that the perturbation methods used above are valid only if $|P/A|$ is quite small. From Fig. 3.14 it can be seen that even for $P/A = 0{\cdot}2$ the $\Delta m = \pm 1$ transitions have an intensity about $0{\cdot}4$ that of the $\Delta m = 0$ transitions at some angles; this reflects the fact that the off-diagonal terms are by no means small compared with the diagonal terms in the energy matrix. The effects of G_I and terms of order A^2/G on the intensity can also be quite important, as is illustrated in Fig. 3.15.

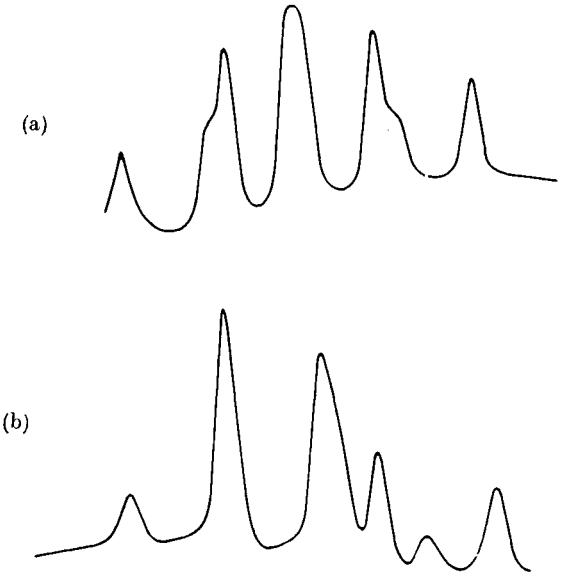

FIG. 3.15. 'Perpendicular' spectrum of $(Mg, Cu)_3La_2(NO_3)_{12}.24D_2O$ in a $\langle 110 \rangle$ direction relative to the local fourfold axes: (a) at $0{\cdot}3$ cm^{-1}, (b) at $0{\cdot}8$ cm^{-1}. The increased asymmetry at the higher frequency is due to the interaction of the larger external magnetic field with the nuclear magnetic moment (Bleaney, Bowers, and Trenam 1955).

3.10. 'Forbidden' hyperfine transitions

In the paramagnetic resonance spectra of ions which have a more than doubly degenerate ground state, split by the crystalline electric field by amounts of the order 10^{-2} to 10^{-1} cm^{-1}, and which also have a hyperfine structure, a number of extra hyperfine lines have often been observed which appear to correspond to transitions in which

the nuclear magnetic quantum m changes by ± 1. These were first reported by Bleaney and Ingram (1951*a*) in manganese ammonium sulphate and manganese fluosilicate (both diluted); they appeared when the external magnetic field was at an angle between parallel and perpendicular to the crystal axis, and were inexplicably large in intensity. They arise from second-order effects due to cross terms in the spin Hamiltonian between the 'fine structure' splitting and the hyperfine structure splitting, as shown by Bleaney and Rubins (1961).

We consider an ion with spin $S(>\frac{1}{2})$ and a fine structure term of the second degree with axial symmetry; for simplicity we shall assume that the spectroscopic splitting factor and the hyperfine structure are both isotropic, as is closely the case for ions such as d^5 and f^7, or d^3 in an octahedral field, where such effects are usually observed. The spin Hamiltonian is then

$$\mathscr{H} = g\beta\mathbf{H}\,.\,\mathbf{S}+D\{S_z^2-\tfrac{1}{3}S(S+1)\}+A\mathbf{S}\,.\,\mathbf{I}-g_I\beta\mathbf{H}\,.\,\mathbf{I}. \quad (3.69)$$

If $\mathbf{H}$ is at an angle θ to the crystal axis, and the Zeeman energy is the largest term, the latter can be diagonalized by choosing the direction of $\mathbf{H}$ as the new z-axis. With axial symmetry this change can be treated as a rotation through an angle θ about the y-axis, and the Hamiltonian then becomes

$$\begin{aligned}\mathscr{H} = {} & g\beta HS_z+\tfrac{1}{2}D\{S_z^2-\tfrac{1}{3}S(S+1)\}\{3\cos^2\theta-1\}+ \\ & +D(S_zS_x+S_xS_z)\cos\theta\sin\theta+\tfrac{1}{4}D(S_+^2+S_-^2)\sin^2\theta+ \\ & +A\mathbf{S}\,.\,\mathbf{I}-g_I\beta\mathbf{H}\,.\,\mathbf{I}. \quad (3.70)\end{aligned}$$

Zero-order wave-functions $|M, m\rangle$ (where M, m are the electronic and nuclear magnetic quantum numbers), which would be appropriate to an ion in a very large magnetic field, are admixed by the off-diagonal terms in this Hamiltonian. The effect on the energy of first-order admixtures due to terms in A and D has been evaluated earlier, but there are important second-order admixtures arising from cross products of the terms in D and A. These consist of products

$$(S_zS_+)(S_-I_+),\ (S_zS_-)(S_+I_-)$$

and other products formed by permutation of the components of S, whose energy coefficients are of order (DA/Zeeman energy). Such terms can be reduced to an equivalent operator

$$\begin{aligned}\tfrac{1}{8}DA\sin 2\theta(I_++I_-)\Big[&\frac{(2S_z-1)\{S(S+1)-S_z^2+S_z\}}{W_M-W_{M-1}}+ \\ &+\frac{(2S_z+1)\{S(S+1)-S_z^2-S_z\}}{W_M-W_{M+1}}\Big] \quad (3.71)\end{aligned}$$

and if $D \ll g\beta H$, we can take the energy denominators as

$$W_{M+1} - W_M = W_M - W_{M-1} = g\beta H,$$

when (3.71) reduces to

$$\frac{3DA \sin 2\theta}{4g\beta H}(I_+ + I_-)\{S_z^2 - \tfrac{1}{3}S(S+1)\}. \tag{3.72}$$

The importance of the terms in (3.71) and (3.72) derives from the fact that they contain operators connecting hyperfine levels with the same M, which differ in energy only by AM. Hence a nuclear state $|m\rangle$ becomes admixed with states $|m \pm 1\rangle$ by amounts of order

$$3D \sin 2\theta / 4g\beta H$$

and transitions of the type $\Delta M = \pm 1$, $\Delta m = \pm 1$ become allowed with intensities of the order of the square of this admixture coefficient, relative to the intensities of the ordinary transitions in which m does not change. Detailed evaluation of these gives for the relative intensity the expression

$$\left(\frac{3D \sin 2\theta}{4g\beta H}\right)^2 \left\{1 + \frac{S(S+1)}{3M(M-1)}\right\}^2 \{I(I+1) - m^2 + m\} \tag{3.73}$$

for the transitions

$$|M, m\rangle \leftrightarrow |M-1, m-1\rangle \text{ and } |M, m-1\rangle \leftrightarrow |M-1, m\rangle.$$

These lines are strongest in the electronic $|+\tfrac{1}{2}\rangle \leftrightarrow |-\tfrac{1}{2}\rangle$ transition, and their angular dependence is such that they vanish parallel or perpendicular to the symmetry axis, being strongest at $\theta = 45°$. Their intensity is surprisingly large, for at this angle they would rival the $\Delta m = 0$ transitions in intensity for a value of $D/g\beta H$ as small as $\frac{1}{12}$.

Under such conditions transitions with $\Delta m = \pm 2$ will also have appreciable intensity. It is readily seen that these arise from admixtures due to the repeated application of the cross-product terms already considered, together with cross-products of the form $(DS_+^2)(AS_-I_+)^2$ and $(DS_-^2)(AS_+I_-)^2$. By means of perturbation theory it can be shown that the relative intensity of the transitions

$$|M, m \pm 1\rangle \leftrightarrow |M-1, m \mp 1\rangle$$

is, assuming D, $A \ll g\beta H$,

$$\left[\frac{1}{2}\left(\frac{3D \sin 2\theta}{4g\beta H}\right)^2 \left\{1 + \frac{S(S+1)}{3M(M-1)}\right\}^2 \pm \frac{3DA \sin^2\theta}{16(g\beta H)^2}\left\{1 + \frac{S(S+1)}{3M(M-1)}\right\}\right]^2 \times$$
$$\times \{I^2 - m^2\}\{(I+1)^2 - m^2\}. \tag{3.74}$$

Positions of lines

The energy of the state $|M, m\rangle$ due to the hyperfine terms is

$$AMm+m(A^2/2g\beta H)\{M^2-S(S+1)\}+M(A^2/2g\beta H)\{I(I+1)-m^2\}-$$
$$-g_I\beta Hm+(D\sin 2\theta/4g\beta H)^2(2Am/M)[\{M^2-S(S+1)\}^2-M^2]+$$
$$+(D\sin^2\theta/4g\beta H)^2(2AmM)\{2M^2+1-2S(S+1)\}, \quad (3.75)$$

where all second-order terms have been included, together with the important third-order terms arising from the cross products considered above. An idea of the appearance of the spectrum is obtained by omitting at first the energy terms which vanish at high frequencies; then for an ion with $S = \frac{3}{2}$, $I = \frac{3}{2}$ and D large enough to separate out the three electronic transitions, the spectrum will be roughly as in Fig. 3.16. For the central transition, the $\Delta m = \pm 1$ lines occur as

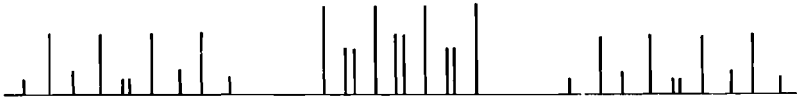

FIG. 3.16. Schematic plot of spectrum for $S = \frac{3}{2}$, $I = \frac{3}{2}$ showing the strong $\Delta m = 0$ lines and the extra $\Delta m = \pm 1$ lines.

doublets, with splitting $2g_I\beta H$, centred on the points midway between the main lines, and with greatest intensity at the centre. For the outer transitions, half of the $\Delta m = \pm 1$ lines are displaced by an amount A towards the higher frequencies, while the other half are equally displaced in the opposite sense; hence one line at each end of a hyperfine set falls outside the main hyperfine structure lines. For an ion with a higher value of S, the displacements are $\pm 2A$ for the $|\pm\frac{5}{2}\rangle \leftrightarrow |\pm\frac{3}{2}\rangle$ transitions, and $\pm 3A$ for the $|\pm\frac{7}{2}\rangle \leftrightarrow |\pm\frac{5}{2}\rangle$ transitions.

To this must be added the second-order displacements. As would be expected, the term in $A(D/g\beta H)^2$ is the most important if D is large. However, for the electronic $|+\frac{1}{2}\rangle \leftrightarrow |-\frac{1}{2}\rangle$ transition this term shifts the two components of the $\Delta m = \pm 1$ doublets equally, and so does not affect the splitting of each doublet, which is

$$|(A^2/g\beta H)\{S(S+1)-\tfrac{1}{4}\}+2g_I\beta H|. \quad (3.76)$$

Measurement of the splitting at different field strengths makes it possible to determine both quantities in (3.76). This is not usually a very precise method of determining g_I, but it may be of use in fixing its sign (strictly only its sign relative to g can be found). If there were a nuclear electric quadrupole interaction (with a corresponding term $P\{m^2-\frac{1}{3}I(I+1)\}$ as in eqn (3.62)), a term $2P(2m-1)$ would have

to be included between the modulus signs in eqn (3.76). This would increase the splitting of the doublets at one end and decrease it at the other. Thus equal spacing in the doublets serves as rather a delicate test of such an interaction, though caution must be observed in using this test, since terms in m^2 which would give similar effects may arise from higher order effects neglected in treatment.

The positions of the $\Delta m = \pm 2$ lines can be easily seen. For the central electronic transition they form doublets spaced by twice the amount given by eqn (3.76), centred on all the main hyperfine lines except the outside ones. For the outer electronic transitions they will be displaced sideways, but by an amount twice that (in first order) for the $\Delta m = \pm 1$ transitions.

These sideways displacements give the sign of A relative to g_I, from observation whether the displacement is added to or subtracted from that due to $g_I\beta H$ in the outer transition with positive M. The sign of M is, however, only identified if that of D is known; otherwise only the sign of the product DAg_I is determined.

The general correctness of this theory has been verified by Bleaney and Rubins (1961) in the spectrum of a single crystal of $ZnSiF_6{,}6H_2O$ containing about 1 per cent of V^{2+}. This ion, $3d^3$, has a singlet ground state with $S = \frac{3}{2}$, and the abundant stable isotope ^{51}V has $I = \frac{7}{2}$. The spin Hamiltonian (3.69) is applicable with the parameters:

$$g = 1{\cdot}971 \pm 0{\cdot}002; \qquad g_I = +0{\cdot}80 \times 10^{-3};$$
$$D = (+808 \pm 1) \times 10^{-4}\ \text{cm}^{-1}; \qquad A = (-84{\cdot}2 \pm 0{\cdot}1) \times 10^{-4}\ \text{cm}^{-1}.$$

The value of D is so large that perturbation theory can be used only for angles where $\sin 2\theta$ is rather small; Fig. 3.17 shows the central electronic transition $|+\frac{1}{2}\rangle \leftrightarrow |-\frac{1}{2}\rangle$, with **H** at 78° to the crystal axis. At the shorter wavelength the $\Delta m = \pm 1$ lines are visible as unresolved doublets, whose intensity at the centre is nearly equal to that of the $\Delta m = 0$ lines. At the longer wavelength the intensity of the 'forbidden' transitions is considerably greater: both $\Delta m = \pm 1$ and ± 2 lines are visible, while the $\Delta m = 0$ lines have sunk to small intensity except at the two ends. Exact diagonalization of the energy matrix using a computer showed that a very complex spectrum would be expected; for example near $\theta = 45°$ the $\Delta m = \pm 3$ and ± 4 transitions should be the most intense.

Graphs showing the computed variation of intensity of the various 'forbidden' transitions with angle are given by Bleaney and Rubins; though applicable only to a special case, they illustrate the fact that

the intensity can be remarkably large, so that the observed spectrum may bear little resemblance to that expected from simple theory. Obviously fine structure terms other than the simple DS_z^2 term can produce similar effects, and these have been analyzed for a cubic term (see, for example, Cavenett (1964) who has compared the theory with the experimental results for Mn^{2+} in cubic ZnSe).

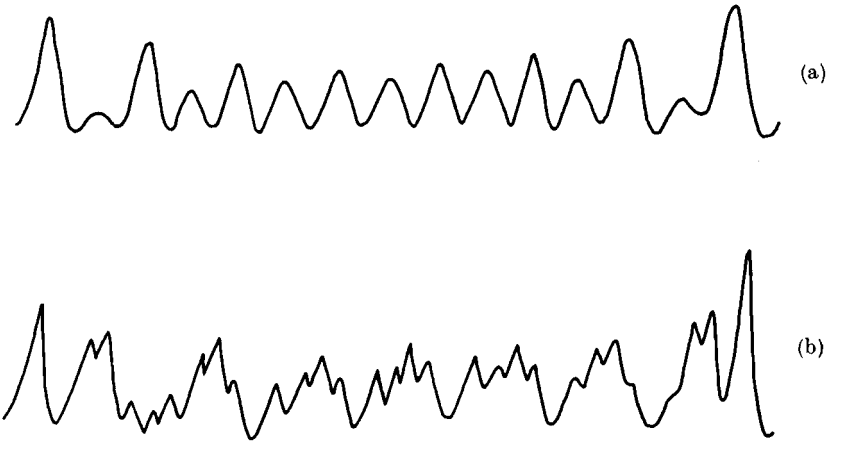

FIG. 3.17. Central $|+\frac{1}{2}\rangle \leftrightarrow |-\frac{1}{2}\rangle$ transition for dilute vanadium fluosilicate, with **H** at 78° from the crystal axis: (a) wavelength 1·3 cm ($H \sim 8200$ G), (b) wavelength 3·2 cm ($H \sim 3400$ G); the line at the extreme right is abnormally intense through an accidental coincidence with a line belonging to an outer electronic transition (Bleaney and Rubins 1961).

Although the appearance and intensity of the 'forbidden' transitions is their most striking feature, they are naturally accompanied by displacements of the $\Delta m = 0$ lines from their expected positions. These displacements must of course be taken into account in calculating values of the spin Hamiltonian parameters from experimental measurements on the spectrum; however, unless the orientation of the magnetic field with respect to the crystal axes is very accurately known it is generally best to make measurements in extreme directions where less accuracy in orientation is required. This rather elementary rule is quite general in its application, but we wish to emphasize that in Endor measurements, where hyperfine structure can be measured with great accuracy, the effects of the off-diagonal terms discussed in this section can become quite remarkably important. In many cases serious errors arising from their neglect can be avoided only by aligning the magnetic field along a crystal axis to a high degree of accuracy.

3.11. Ligand hyperfine structure

When the magnetic electrons are not entirely localized on the central 'magnetic' ion, and their wave-functions include orbitals belonging to the ligand ions, an additional splitting of the paramagnetic resonance lines is observed if the ligand nuclei possess nuclear spins. This ligand hyperfine structure (sometimes known as 'super' hyperfine structure) is described by additional terms in the spin Hamiltonian, which have axial symmetry about the 'bond' axis—the line through the centre of the ligand ion and the centre of the magnetic ion. If this line is the z-axis, the additional terms due to the one ligand ion L are

$$\mathscr{H}_{\mathrm{L}} = A_{\parallel}^{\mathrm{L}} I_z^{\mathrm{L}} S_z + A_{\perp}^{\mathrm{L}}(I_x^{\mathrm{L}} S_x + I_y^{\mathrm{L}} S_y) + \\ + P_{\parallel}^{\mathrm{L}}\{(I_z^{\mathrm{L}})^2 - \tfrac{1}{3} I^{\mathrm{L}}(I^{\mathrm{L}}+1)\} - g_I^{\mathrm{L}} \beta \mathbf{H} \cdot \mathbf{I}^{\mathrm{L}}, \quad (3.77)$$

where $\mathbf{I}^{\mathrm{L}}$ is the spin of the ligand nucleus, $\mathbf{S}$ the fictitious spin of the magnetic ion, and the parameters are analogous to those used to describe the hyperfine structure of the central ion.

In general the magnitude of these parameters is such that when an external field is applied large enough to bring the resonance spectrum into the microwave region, we can treat the ligand interaction by means of perturbation theory retaining only the first-order terms. Then the allowed electronic transitions are those in which the orientation of the ligand nucleus remains unchanged ($\Delta m^{\mathrm{L}} = 0$), and if the external magnetic field makes an angle θ with the bond axis, the transition is displaced by an amount $A^{\mathrm{L}} m^{\mathrm{L}}$, where

$$(A^{\mathrm{L}})^2 = (A_{\parallel}^{\mathrm{L}})^2 \cos^2\theta + (A_{\perp}^{\mathrm{L}})^2 \sin^2\theta \quad (3.78)$$

provided that the central ion has an isotropic g-factor. If the g-factor is anisotropic, and its principal axes coincide with the x, y, z axes appropriate to eqn (3.77) and the z-axis is the bond axis, the value of A^{L} is given by an equation similar to (3.44),

$$g^2(A^{\mathrm{L}})^2 = (l^2 g_x^2 + m^2 g_y^2)(A_{\perp}^{\mathrm{L}})^2 + n^2 g_z^2 (A_{\parallel}^{\mathrm{L}})^2, \quad (3.79)$$

where (l, m, n) are the direction cosines of the magnetic field with respect to the x, y, z axes.

The effect of this additional interaction is to sub-divide each electronic transition, or each hyperfine line if the central ion has a nuclear spin, into $(2I^{\mathrm{L}}+1)$ lines of equal intensity with separation A^{L}. If the number of ligands is n (all identical), then the sub-division is into $(2I^{\mathrm{L}}+1)^n$ lines, which with an ion octahedrally coordinated to six ligand ions of nuclear spin $I^{\mathrm{L}} = \frac{1}{2}$ would give $2^6 = 64$ lines.

Fortunately the problem is not so serious as this calculation suggests, since many of the lines coincide. If the magnetic ion is at a centre of inversion symmetry, the ligand ions will always be identical in pairs, and the line displacement due to such a pair will be $A^{L}(m_1+m_2)$, where m_1, m_2 each take on their $(2I^{L}+1)$ possible values. The ligand hyperfine structure due to such a pair is shown in Fig. 3.18 for values of I^{L}

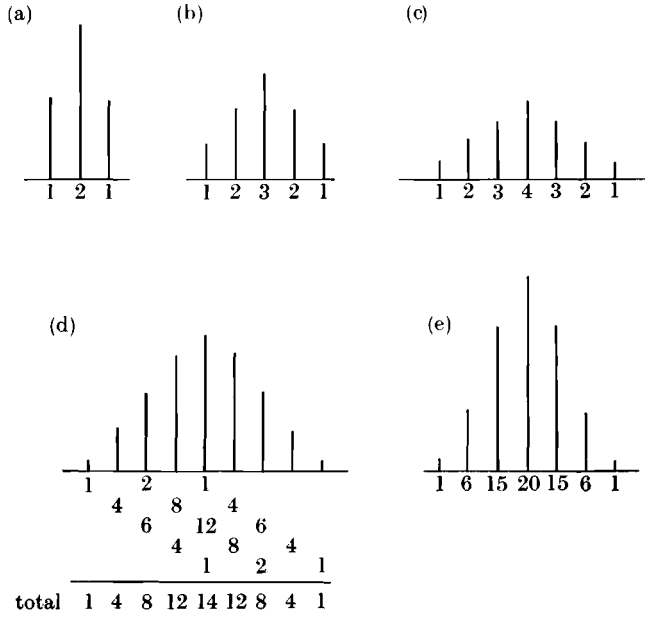

FIG. 3.18. (a)(b)(c) Hyperfine structure due to two identical ligand ions, with nuclear spins (a) $I = \frac{1}{2}$, (b) $I = 1$, (c) $I = \frac{3}{2}$. (d), (e) Hyperfine structure due to 6 ligand nuclei, all with $I = \frac{1}{2}$. In (d) the hyperfine constant is twice as large for two nuclei as for the other four. In (e) all hyperfine constants are identical.

equal to $\frac{1}{2}$, 1, and $\frac{3}{2}$. The structure consists of a set of equally spaced lines of separation A^{L}, but with an intensity which increases in arithmetical progression towards the centre owing to the number of ways in which (m_1+m_2) can sum to a given value. The total intensity in (a), (b), and (c) of Fig. 3.18 is drawn to be identical in each case; the higher the nuclear spin, the greater the number of lines between which the intensity must be divided, and the lower the intensity of individual lines.

Two examples of the ligand hyperfine structure due to six nuclei, where simple numerical relationships between the hyperfine parameters produce a simplification of the patterns, are also shown in Fig. 3.18.

In (d) it is assumed that the hyperfine splitting of two identical ions is twice that of the other four, so that lines from different ligands are superimposed. Each nucleus is assumed to have $I = \frac{1}{2}$, so that two identical ions produce a 1:2:1 intensity pattern, and four identical ions produce a 1:4:6:4:1 pattern. The resultant intensity pattern can be regarded either as a superposition of five 1:2:1 patterns, with relative intensity 1:4:6:4:1, or three 1:4:6:4:1 patterns with relative intensity 1:2:1. These can be identified visually by reading the intensity ratios below the figure horizontally and diagonally, respectively. The case where four ions are identical but different from the other two is typical of a regular octahedron of ligand ions, with the magnetic field in one of the planes of reflection symmetry normal to a twofold axis. The ratio of 2:1 in the hyperfine splittings may occur at some particular orientation of the magnetic field; if the coupling were purely dipolar, it would be numerically twice as large for the two ions whose bond axis is parallel to the magnetic field as for the four ions whose bond axes are normal to the field.

Naturally the simplest pattern is obtained when all ions give the same hyperfine splitting. This is shown in (e) for six ligand ions each with $I = \frac{1}{2}$. The intensity pattern is 1:6:15:20:15:6:1, the same as the binomial coefficients in the expansion of $(x+y)^6$. The rather large intensity ratios, typical of patterns due to a number of nuclei, often make it difficult to see the outermost lines in the spectrum (to bring the total intensity to be the same as in (a), (b), (c) the lines should be smaller by a factor 2 in (d) and (e)). Thus the outside lines in (e) have each an intensity which is only $\frac{1}{64}$ $(= (\frac{1}{2})^6)$ of the total intensity associated with any given electronic transition (which may already be subdivided because of hyperfine structure due to a nuclear moment on the central ion). In the case of eightfold coordination to a regular cube of fluorines (for example, a paramagnetic ion replacing a Ca^{2+} ion in CaF_2) the intensity pattern is 1:8:28:56:70:56:28:8:1 if all ions give the same hyperfine splitting, so that each outside line would have only $\frac{1}{256} = (\frac{1}{2})^8$ of the total intensity.

A situation where all ligand hyperfine parameters are equal normally occurs only for certain directions of the external magnetic field, and also requires high symmetry in the complex. With a regular octahedron of ligand ions, the magnetic field must be directed along a threefold axis; with a regular cube or tetrahedron of ligand ions, the magnetic field must be along a fourfold axis. Of course it will also occur if the hyperfine parameters $|A_{\parallel}^{L}|$, $|A_{\perp}^{L}|$ in eqn (3.77) are equal, in which case

the ligand hyperfine pattern will be independent of the orientation of the magnetic field. Since there are a number of contributions to the ligand hyperfine structure, the condition $A_{\parallel}^{\mathrm{L}} = \pm A_{\perp}^{\mathrm{L}}$ may be fortuitously obeyed; it will also be approximately correct if the contribution from s-electrons on the ligand ion is much larger than the contributions from any other source (including dipolar interaction).

The Hamiltonian for ligand hyperfine structure has been treated above by means of first-order perturbation theory. This implies that the hyperfine parameters are small compared with the electronic Zeeman energy, and this condition is normally fulfilled. The treatment given also implies that the magnetic hyperfine interaction be large compared with the other terms in eqn (3.77), since we have diagonalized the main portion of this term, as in § 3.8; then the allowed transitions are those in which $\Delta m^{\mathrm{L}} = 0$, whose positions are not affected (in first order) by the nuclear electric quadrupole term or the nuclear Zeeman interaction with the external field. Obviously there will be second-order shifts of order $((A^{\mathrm{L}})^2/h\nu)$, but these are not usually important in an electron spin resonance experiment, though they may well be in an Endor experiment where the precision is much higher. For a nucleus whose spin I is greater than $\frac{1}{2}$, the electric quadrupole term $P_{\parallel}^{\mathrm{L}}$ may be comparable with A^{L}, in which case transitions with $\Delta m^{\mathrm{L}} \neq 0$ may have appreciable intensity; this gives a situation similar to that considered in § 3.9, but the hyperfine structure is more complex because of the number of nuclei involved. A further possibility is that the ligand hyperfine structure is rather small, so that A^{L} is comparable with, or smaller than, the nuclear Zeeman term; this needs a rather different treatment, which we give below.

For simplicity we consider only the case where the nuclear electric quadrupole interaction is zero. However our treatment is not necessarily confined to a hyperfine structure due to a ligand nucleus, so that we will omit the superscript L and the restriction to axial symmetry. The hyperfine Hamiltonian including the nuclear Zeeman energy is then

$$\mathscr{H}_{\mathrm{n}} = A_x S_x I_x + A_y S_y I_y + A_z S_z I_z - \beta(g_x^{(I)} H_x I_x + g_y^{(I)} H_y I_y + g_z^{(I)} H_z I_z), \tag{3.80}$$

where the nuclear g-factor may be anisotropic owing to indirect effects as discussed in Chapter 18, but is assumed to have the same principal axes as the hyperfine 'tensor' A. Suppose the external magnetic field has direction cosines (l, m, n) with respect to these axes. Then the electronic Zeeman interaction is diagonalized as in § 3.2, and on

retaining only the terms in S'_z in the magnetic hyperfine interaction the nuclear Hamiltonian becomes

$$\mathscr{H}_n = lI_x\left(\frac{g_x A_x S'_z}{g} - g_x^{(I)}\beta H\right) + mI_y\left(\frac{g_y A_y S'_z}{g} - g_y^{(I)}\beta H\right) + \\ + nI_z\left(\frac{g_z A_z S'_z}{g} - g_z^{(I)}\beta H\right). \quad (3.81)$$

The coefficients of I_x, I_y, I_z may be regarded as the components of an interaction which can be diagonalized by a suitable transformation of the nuclear axes to a set (x_n, y_n, z_n) where the z_n-axis has direction cosines proportional to the coefficients of I_x, I_y, I_z. Then the interaction may be written in the form KI'_z, where

$$K^2 = \sum_{x,y,z} l^2\left(\frac{g_x A_x S'_z}{g} - g_x^{(I)}\beta H\right)^2 \quad (3.82)$$

and the hyperfine energy is simply Km, where m is the nuclear magnetic quantum number defined by the projection of the nuclear spin onto an axis parallel to the vector **K**. The vector **K** may be regarded as the sum of two vectors, one representing the interaction with the electronic magnetic field and the other the interaction with the external field (the latter vector is, of course, parallel to the external field if $g^{(I)}$ is isotropic), as shown in Fig. 3.19. The length of the former vector is proportional to S'_z, and is therefore different in different electronic states; thus the resultant vector **K** is different both in magnitude and direction for different electronic states. In a given state with $S'_z = M$, we denote it by $\mathbf{K}_M$. In a transition $(M, m) \leftrightarrow (M', m')$ the additional energy due to the hyperfine interaction will be $mK_M - m'K_{M'}$, assuming that the state M lies higher in energy than M'. Here there will in general be no restriction relating the allowed values of m' to m; in other words, changes in the nuclear magnetic quantum number are allowed. The reason for this is that m, m' represent the components of nuclear spin along the directions $\mathbf{K}_M$, $\mathbf{K}_{M'}$, which are differently oriented. If we take a given state m referred to the $\mathbf{K}_M$ axis, and transform it by a rotation that takes the z_n-axis from $\mathbf{K}_M$ to $\mathbf{K}_{M'}$, it will be represented by a linear combination of all possible states m' referred to the latter axis. Thus a transition in which the orientation of the nuclear magnetic moment remains fixed in space must be represented by a sum of transitions in which the nuclear magnetic quantum number m, as defined above, changes to all values m' without restriction, though in certain definite proportions that determine the

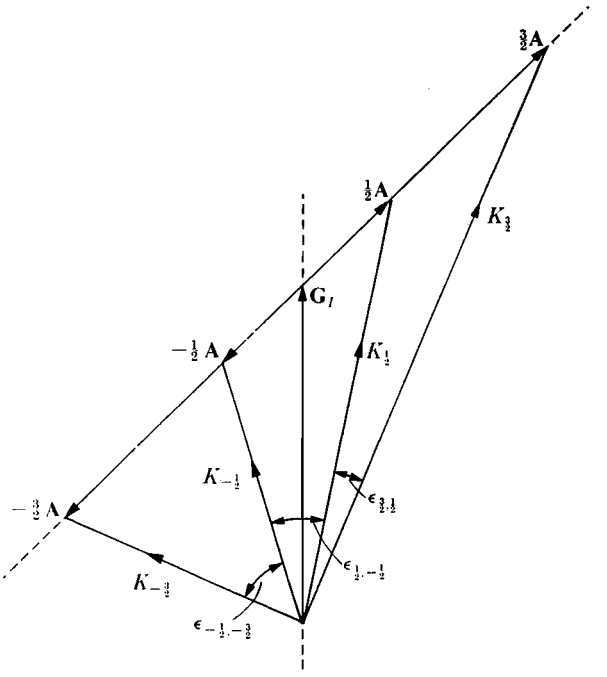

FIG. 3.19. Diagram illustrating the vector addition of the electronic interaction with the nucleus (AS_z') and the nuclear Zeeman interaction ($\mathbf{G}_I$) for the case of $S = \frac{3}{2}$. If the nuclear g-factor $g^{(I)}$ is isotropic the direction of $\mathbf{G}_I$ is the same as that of the external magnetic field. The net hyperfine interaction energy in a state (M, m) is mK_M.

relative amplitudes in the various transitions. These proportions are a function of the angle ϵ between $\mathbf{K}_M$ and $\mathbf{K}_{M'}$, and are shown for the case of $S = \frac{1}{2}$, $I = \frac{3}{2}$ in Fig. 3.20. From this figure it will be seen that when the angle $\epsilon = 0$, the only allowed transitions are those in which $m' = m$; this corresponds to the limit in which the electronic magnetic field at the nucleus is zero ($A = 0$), and the only field is the external field, which remains fixed in direction during a transition. When the angle $\epsilon = 180°$, the only allowed transitions are those in which $m' = -m$; this corresponds (for $S = \frac{1}{2}$) to the case considered earlier, where the electronic magnetic field at the nucleus is much greater than the external field, so that to a good approximation the net field is just reversed in the transition $M = \frac{1}{2} \leftrightarrow -\frac{1}{2}$. (These allowed transitions are of course those which were labelled $\Delta m = 0$ in earlier sections, since the positive direction for m was then considered fixed, instead of reversing when M goes from $+\frac{1}{2}$ to $-\frac{1}{2}$, as in the present treatment.)

The hyperfine displacement $mK_M - m'K_{M'}$ vanishes for the transitions in which $m' = m$ if $K_M = K_{M'}$. The latter holds if $A = 0$, but it may

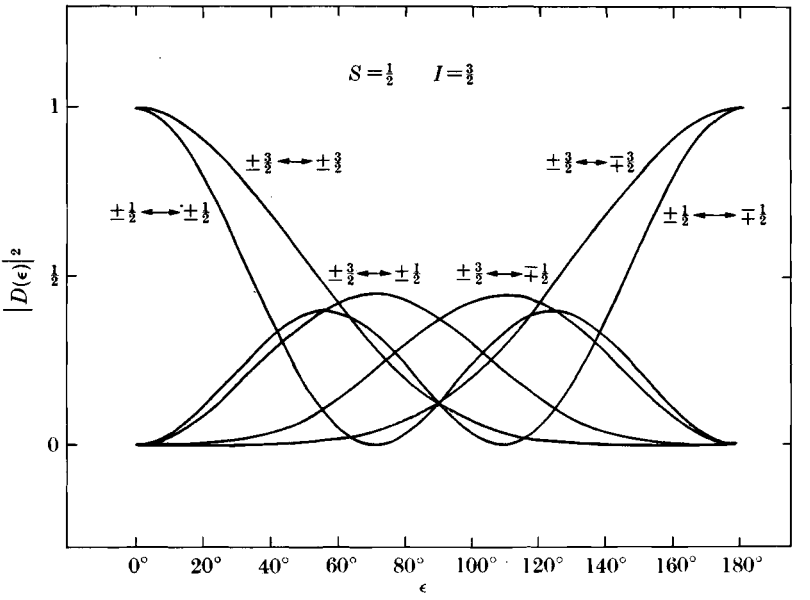

FIG. 3.20. Relative strengths of the various transitions $(+\frac{1}{2}, m) \leftrightarrow (-\frac{1}{2}, m')$ as a function of the angle ϵ between $\mathbf{K}_{\frac{1}{2}}$ and $\mathbf{K}_{-\frac{1}{2}}$ for $S = \frac{1}{2}$, $I = \frac{3}{2}$. $D_{mm'}(0, \epsilon, 0)$ is a matrix element of the three-dimensional rotation operator. (After Weil and Anderson 1961.)

also occur when $A \neq 0$ provided that the hyperfine energy is comparable with the nuclear Zeeman energy. For the transition $M = \frac{1}{2} \leftrightarrow -\frac{1}{2}$ this requires that the direction of $\mathbf{A}$ be normal to that of $\mathbf{G}_I$, as in Fig. 3.21; this will occur only at certain specific orientations of the external magnetic field, and also requires that the principal values $g_x A_x$, $g_y A_y$, $g_z A_z$ do not all have the same sign (or, a less probable alternative, that $g_x^{(I)}$, $g_y^{(I)}$, $g_z^{(I)}$ do not all have the same sign). Cases where the hyperfine structure passes through zero in this way have been observed by Weil and Anderson (1961) and Woodbury and Ludwig (1961).

When $A \gg G_I$ we have a hyperfine structure of the normal kind discussed in earlier sections where the extreme hyperfine lines are displaced by $\pm AI$ in any electronic transition. If transitions occur in which $\Delta m \neq 0$, these lie within these extremes when $S = \frac{1}{2}$. This is not necessarily true for the case discussed in this section, where A may be smaller than G_I. A clear example arises in the situation represented by Fig. 3.21, where the hyperfine transitions $(+\frac{1}{2}, m) \leftrightarrow (-\frac{1}{2}, m)$ are undisplaced, but a transition with $m' \neq m$ occurs at $K(m-m')$, where $K = |K_{\pm\frac{1}{2}}|$. Such transitions appear as 'satellites' either side of the main line; if $A \ll G_I$ they are displaced by an amount almost equal to

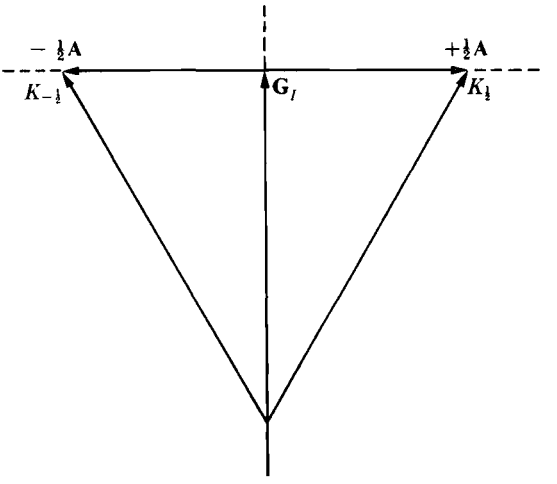

FIG. 3.21. When the vectors **A**, $\mathbf{G}_I$ are perpendicular the values of $K_{\frac{1}{2}}$ and $K_{-\frac{1}{2}}$ are equal, so that the net hyperfine energy for the transition $(+\frac{1}{2}, m) \leftrightarrow (-\frac{1}{2}, m)$ vanishes. From eqn (3.82) this requires that

$$\sum l^2\left\{\frac{g_x A_x}{2g} - g_x^{(I)}\beta H\right\}^2 = \sum l^2\left\{\frac{g_x A_x}{2g} + g_x^{(I)}\beta H\right\}^2$$

or $(lg_xA_x/g)(lg_x^{(I)}) + (mg_yA_y/g)(mg_y^{(I)}) + (ng_zA_z/g)(ng_z^{(I)}) = 0$, or $\mathbf{A} \cdot \mathbf{G}_I = 0$; that is the vectors **A** (direction cosines lg_xA_x/g, etc.) and $\mathbf{G}_I$ (direction cosines $lg_x^{(I)}$, etc.) are mutually perpendicular.

the precession frequency of the nuclear moment in the external field (cf. Fig. 1.39), or a multiple thereof. Such transitions were first explained by Trammell, Zeldes, and Livingstone (1958) as due to 'spin flips' of the proton nuclear moments in the electron magnetic resonance spectrum of various irradiated acids. When the ligand nucleus has $I = \frac{1}{2}$ we would expect only one satellite line on each side of the main line, due to the nuclear magnetic quantum number changing from $+\frac{1}{2}$ to $-\frac{1}{2}$ or vice versa, but when a number of ligand nuclei have nuclear moments, further satellites of smaller intensity can be seen due to 'flips' of more than one nuclear moment. The theory of such transitions has been considered in some detail by Baker, Hayes, and O'Brien (1960), and compared with experiment for a number of lanthanide ions in CaF_2.

In conclusion, we point out that such satellite lines have a simple classical explanation. If the external magnetic field is directed along the z-axis, the Hamiltonian may contain terms such as $A_{zz}S_zI_x$. To take a concrete example, let the magnetic field be parallel to a fourfold axis in CaF_2, with a paramagnetic ion on a Ca^{2+} site surrounded by a cube of eight fluorine ions. The Ca—F bonds lie along the threefold

axes, so that a dipole on a Ca^{2+} site parallel to the fourfold or z-axis produces a magnetic field at a F^- nucleus which is normal to the z-axis. If the direction of this dipolar field at this site is taken as the x-axis, then the interaction of the fluorine nuclear moment with this field will give rise to a term of the form $A_{zx}S_zI_x$, since the x-component of the field is proportional to S_z. Conversely, the x-component of the nuclear moment of the fluorine ion will give rise to a magnetic field at the Ca^{2+} site in the z-direction. If the external field is much larger than the local field of the paramagnetic ion at the F^- site, the fluorine nuclear moment will precess about the external field at a frequency $\nu_n = g_I\beta H/h$, and will give rise to a magnetic field ΔH parallel to H at the Ca^{2+} site which oscillates at this frequency. Thus the electron moment will precess about a field $H+\Delta H\cos 2\pi\nu_n t$, so that the precession may be regarded as frequency modulated, with a carrier frequency ν_e and sidebands separated from this frequency by $\pm\nu_n$ and multiples thereof, with decreasing intensity.

3.12. The spectrum of a powder

If a paramagnetic resonance spectrum is completely isotropic, it can be examined in a powder (under which term we include a polycrystalline specimen) without loss of resolution. For this purpose local cubic symmetry at the ion is a necessary but not a sufficient condition—for example, the spectrum of an ion with a cubic 'fine structure' term of the type discussed in § 3.4 is by no means isotropic. In a powder the spectrum of any ion that is anisotropic will naturally be spread out; to a considerable extent the detail will be lost, and the information extractable from the spectrum may be drastically reduced. Such information as can be retrieved comes usually from the limits of the spread-out spectrum, since these normally appertain to ions whose orientation is such that the magnetic field happens to lie along one of the principal axes of the tensor parts of the spin Hamiltonian.

Little (if any) analysis has been attempted of the powder spectrum of ions with less than axial symmetry, and we shall restrict discussion to this case. The number of ions for which the magnetic field makes an angle between θ and $\theta+\mathrm{d}\theta$ with the unique axis is then proportional to $\sin\theta\,\mathrm{d}\theta$, and since the spectrum is not affected by reversal of the magnetic field we may restrict the range of angles to be considered to lie between 0 and $\pi/2$, in which case the factor of proportionality is unity. Assuming the spectrum is observed at constant frequency and variable magnetic field, we need to relate the angle θ to the magnetic

field at which the spectrum line for an ion at this angle would be observed. For this purpose we consider first an ion with an anisotropic g-factor of axial symmetry, for which (eqn (3.14))

$$g^2 = g_\parallel^2 \cos^2\theta + g_\perp^2 \sin^2\theta.$$

From this relation we have

$$\cos\theta = \left(\frac{g^2-g_\perp^2}{g_\parallel^2-g_\perp^2}\right)^{\frac{1}{2}} = \left(\frac{H^{-2}-H_\perp^{-2}}{H_\parallel^{-2}-H_\perp^{-2}}\right)^{\frac{1}{2}}, \tag{3.83}$$

where the symbols H, $H_\parallel$, and $H_\perp$ refer to the fields at which the lines appropriate to values g, $g_\parallel$, and $g_\perp$ would occur. Differentiation gives

$$\begin{aligned}\sin\theta\,\mathrm{d}\theta &= \frac{H^{-3}\,\mathrm{d}H}{\{(H^{-2}-H_\perp^{-2})(H_\parallel^{-2}-H_\perp^{-2})\}^{\frac{1}{2}}} \\ &= \frac{H_\perp^2 H_\parallel\,\mathrm{d}H}{H^2\{(H^2-H_\perp^2)(H_\parallel^2-H_\perp^2)\}^{\frac{1}{2}}}.\end{aligned} \tag{3.84}$$

This distribution function allows only for the random orientation of the crystallites, and is equivalent to that given by Sands (1955). It must be modified to allow for the fact that the transition probability is also a function of angle (see Bleaney 1960); in other words, to allow for the anisotropy in g_1^2. Equation (3.16) shows that the intensity is a maximum when the microwave field is normal to the steady field, and we shall assume that it is so oriented. Then, in eqn (3.16), $\sin(\theta_1-\theta) = 1$, and on averaging over η for a powder we have $\langle\sin^2\eta\rangle = \langle\cos^2\eta\rangle = \frac{1}{2}$, so that the average value of g_1^2 is

$$g_1^2 = \frac{g_\perp^2(g_\parallel^2+g^2)}{2g^2}. \tag{3.85}$$

This can be related as before to the field at which resonance occurs, and for the sake of obtaining an expression for the distribution of intensity which is non-dimensional we extract only the factor

$$(g_\parallel^2+g^2)/g^2 = (H^2+H_\parallel^2)/H_\parallel^2.$$

On multiplying this by eqn (3.84) we find for the intensity distribution,

$$\text{powder intensity} \propto \frac{H_\perp^2(H^2+H_\parallel^2)\,\mathrm{d}H}{H_\parallel H^2\{(H^2-H_\perp^2)(H_\parallel^2-H_\perp^2)\}^{\frac{1}{2}}}. \tag{3.86}$$

The main feature of this function is the infinity at $H = H_\perp$ (see Fig. 3.22) which arises because no line width mechanism has been included. Attempts have been made to remedy this deficiency (see, for example, Searl, Smith, and Wyard 1961; Ibers and Swalen 1962) which give fair

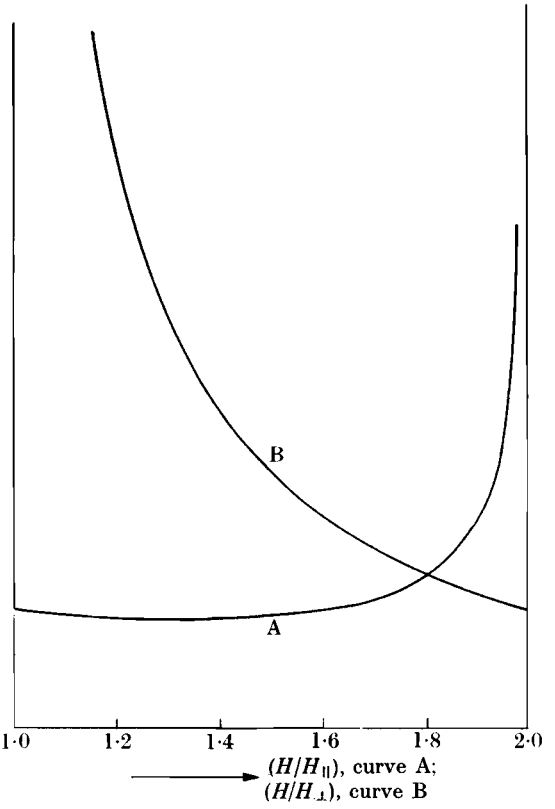

FIG. 3.22. Relative intensity distribution in the spectrum of a powder for an ion with $S = \frac{1}{2}$ and an axially symmetric g-factor, from eqn (3.86).
Curve A, $H_{\|} = H_{\perp}/2$; curve B, $H_{\|} = 2H_{\perp}$.

agreement with experiment for small anisotropy. With large anisotropy a proper knowledge of the line shape (which may be a function of angle) becomes much more important, particularly in concentrated substances.

In some cases effects due to hyperfine structure can be observed in a powder, as each hyperfine line has its own limits for maximum and minimum fields. An example is shown in Sands (1955) for the Cu^{2+} ion in glass, though it should be noted that his conclusion that $A_{\|}$ and $A_{\perp}$ have opposite signs cannot be justified from the observed spectrum, as the hyperfine lines do not invert in order (as assumed by him) in going from the parallel to the perpendicular direction (see § 3.8).

In his work on glass Sands found that a large number of samples

showed lines corresponding to apparent anisotropic g-values of approximately 6 and 4·2, which later work (Castner, Newell, Holton, and Slichter 1960) suggests are due to Fe^{3+} ions with rather large crystal field splittings. If the term DS_z^2 is large compared with $h\nu$, we are in the weak Zeeman effect region. For an ion with $S = \frac{5}{2}$, the spectrum in zero field consists of three well-spaced doublets corresponding to $S_z = \pm\frac{5}{2}$, $\pm\frac{3}{2}$, and $\pm\frac{1}{2}$ respectively. In a weak magnetic field only resonance within the latter doublet is observable, and it behaves like an ion with an apparent $S = \frac{1}{2}$ and $g_\parallel = 2$, $g_\perp = 6$. The latter corresponds to the point of maximum intensity in a powder, and is presumed to give rise to the anisotropic line at $g = 6$. The line at $g = 4{\cdot}2$ has been ingeniously explained by Castner *et al.*, who assume that it is due to a ferric ion with a fine structure term of the form $E(S_x^2 - S_y^2)$. In zero magnetic field this splits the $S = \frac{5}{2}$ levels into three equally spaced doublets, the wave-functions for the middle doublet being $(\frac{9}{14})^{\frac{1}{2}}|\pm\frac{5}{2}\rangle - (\frac{5}{14})^{\frac{1}{2}}|\mp\frac{3}{2}\rangle$. In a weak magnetic field this has an isotropic g-factor of $(15g_s/7) = \frac{30}{7} = 4{\cdot}28$, in good agreement with the value of 4·27 observed by Castner *et al.* This unexpected result of an isotropic weak field g-factor for an ion with a highly anisotropic Hamiltonian shows that great care is often required in the interpretation of a spin resonance spectrum.

For an ion whose effective spin is greater than $\frac{1}{2}$, a number of electronic transitions occur whose position is generally sharply dependent on orientation, owing to the 'fine structure' discussed in §§ 3.3–3.6, even when g is isotropic. A conspicuous exception in such cases is the $|+\frac{1}{2}\rangle \leftrightarrow |-\frac{1}{2}\rangle$ transition, which is not dependent on orientation as far as terms linear in the fine structure parameters, provided that g is isotropic (as is often true in such cases to a good approximation). Thus, if terms of order (fine structure parameter)$^2/g\beta H$ are relatively unimportant, the central transition $|+\frac{1}{2}\rangle \leftrightarrow |-\frac{1}{2}\rangle$ can be observed in a powder without much loss of resolution. If the source of such lines is unknown, the spectrum gives little help in identification unless a characteristic hyperfine structure is present; if g is isotropic the hyperfine structure is usually also isotropic and may be well resolved in the central transition. The spectrum of a sample of modelling clay is shown in Fig. 3.23; at a wavelength of 1·3 cm, six almost equally spaced lines are observed which may be rather confidently attributed to Mn^{2+}, with $g = 2{\cdot}0013 \pm 0{\cdot}0006$ and $|A| = (88{\cdot}7 \pm 0{\cdot}3) \times 10^{-4}$ cm^{-1}. At the longer wavelength of 3·2 cm, the spectrum shows a number of additional lines, which may be identified as the 'forbidden' hyperfine

FIG. 3.23. Spectrum of modelling clay at (a) 1·3 cm, (b) 3·2-cm wavelength. The spectrum is attributed to the $|+\frac{1}{2}\rangle \leftrightarrow |-\frac{1}{2}\rangle$ transition of a trace of $^{55}Mn^{2+}$. High field is towards the right (Bleaney and Rubins 1961).

lines discussed in the previous section. Their intensity may be used to estimate a value of D, which cannot be determined directly, by using eqn (3.73) averaged over all values of θ from 0 to $\pi/2$, with a weighting factor of sin θ. This results in $\sin^2 2\theta$ being replaced in eqn (3.73) by $\frac{8}{15}$.

An independent estimate of D in such a specimen or a powder can be obtained from the splitting of the hyperfine lines $\Delta m = 0$ shown in Fig. 3.23(b). This results from the combination of higher-order effects of two kinds: shifts of order $D^2/g\beta H$, which can be found from eqn (3.35) and are the same for all hyperfine lines; and shifts of order $D^2A/(g\beta H)^2$, which arise from the last terms in eqn (3.75), which are proportional to the distance of the hyperfine line from the centre of the spectrum. On combining all the terms that depend on the angle θ, we find that the position of the transition $|+\frac{1}{2}, m\rangle \leftrightarrow |-\frac{1}{2}, m\rangle$ is shifted by an amount

$$\Delta H = x(y\cos^2\theta - z\sin^2\theta)\sin^2\theta, \tag{3.87}$$

with $x = (D^2/16g\beta H)\{4S(S+1)-3\}$ and $y = 8(1-\delta)$, where

$$\delta = (Am/4g\beta H)\{4S(S+1)+1\},$$

and $z = 1+(Am/g\beta H) = 1+\epsilon$. The number of ions whose spectrum lies in the range of field H to $H+\Delta H$ is proportional to

$$\Delta n = \sin\theta(\mathrm{d}\theta/\mathrm{d}H)\,\Delta H,$$

and intensity peaks occur in the line shape when $(\Delta n/\Delta H)$ is infinite. From eqn (3.87) the quantity $\sin\theta(\mathrm{d}\theta/\mathrm{d}H)$ is inversely proportional to $\cos\theta\{(y+2z)\sin^2\theta - y\cos^2\theta\}$ and thus becomes infinite at $\theta_1 = \pi/2$ and at θ_2 where $\tan^2\theta_2 = y/(y+2z)$. Peaks in the spectrum corresponding to the two values of θ will therefore occur at fields which differ by

$$\delta H = x\left\{z+\frac{y^2}{4(y+z)}\right\}. \tag{3.88}$$

Since y is a function of m, the splitting of the hyperfine components varies within the central electronic transition. When δ is small, eqn (3.88) reduces to

$$\delta H = \left(\frac{25x}{9}\right)\left\{1 - \frac{32\delta - 13\epsilon}{45}\right\} \tag{3.89}$$

and since δ, ϵ are proportional to m, the splitting varies linearly from one end of the hyperfine structure to the other. In fact the splitting is always greatest at the high field end (as in Fig. 3.23(b)), since this corresponds to negative values of m if A is positive (and vice versa), and δ, ϵ are proportional to (Am).

In making a similar calculation for the 'forbidden' hyperfine lines allowance must be made for the fact that the transition probability is proportional to $\sin^2 2\theta$ (see eqn (3.73)) so that there is no intensity peak at $\theta_1 = \pi/2$. Hence the forbidden lines are not split, though they will be broadened.

In the modelling clay specimen examined by Bleaney and Rubins, the average separation of the 'forbidden' $\Delta m = \pm 1$ lines at the shorter wavelength was 16 ± 1 G, in good agreement with the value calculated from (3.76) using the known nuclear moment of ^{55}Mn. The difference in splittings at either end was less than 2 G, suggesting that any nuclear electric quadrupole term P was less than 10^{-5} cm^{-1}. The value estimated for $|D|$ by the methods outlined above is about 0·01 cm^{-1}. This value was confirmed by the observation of two asymmetrical lines, assigned to the electronic transitions $|\pm\frac{3}{2}\rangle \leftrightarrow |\pm\frac{1}{2}\rangle$, which move as $\pm D(3\cos^2\theta - 1)$, with intensity peaks at $\theta = \pi/2$.

3.13. Effects of crystal imperfections

We have hitherto assumed that all parameters have sharp values, which might be true in a perfect crystal but is seldom the case in practice. In this section we consider the broadening of resonance lines due to crystal imperfections (broadening due to spin-spin interaction and spin-lattice relaxation is discussed in Chapters 9 and 10).

We distinguish between two effects:

(a) mosaic structure, in which the crystal is not truly single but consists of a multitude of small crystallites with slightly different orientations. The spin Hamiltonian parameters are the same in each crystallite, so that no broadening is observed in the resonance lines in zero magnetic field, but the lines become broadened in a magnetic field because (with a few obvious exceptions) the positions of the

resonance transitions depend on the angle that **H** makes with the individual crystal axes. Such broadening is a minimum at directions (such as the principal axes) where the resonance lines reach extreme positions in the spectrum, and their first-order dependence on crystal mis-orientation by a small angle vanishes.

(b) impurities, dislocations, and other defects set up stresses within a single crystal, which may change the point symmetry at the paramagnetic ion, or preserve the point symmetry but change the crystal field parameters slightly. The changes in the parameters are not independent of each other, since for any given ion they are linked to a specific deviation in its ligand field. Simple examples illustrating this point abound in Chapter 5, where it is shown that under axial symmetry the values of $g_{\|}$, $g_{\perp}$ can often be related to a single parameter (see for example, eqn (5.12)); thus even a strain preserving axial symmetry may produce changes in $g_{\|}$, $g_{\perp}$ that are simply related to one another.

Whatever the cause, the effect of a variation in g differs from that of variations in other spin Hamiltonian parameters because $H = (h\nu/g\beta)$, so that at constant frequency ν we have

$$\langle \delta H^2 \rangle = (h\nu/g^2\beta)^2 \langle \delta g^2 \rangle, \tag{3.90}$$

and the root mean square width in field increases linearly with the resonance frequency. On the other hand, for any parameter that splits the spectrum lines as in fine or hyperfine structure effects, we have $h\nu = g\beta H + X$, or $H = (h\nu/g\beta) - (X/g\beta)$, and

$$\langle \delta H^2 \rangle = (1/g\beta)^2 \langle \delta X^2 \rangle, \tag{3.91}$$

showing that $\langle \delta H^2 \rangle$ from this cause will not be frequency dependent.

We now consider briefly the effect of mosaic structure. Variation of orientation of the crystallites means that instead of **H** being along a specific direction (l, m, n) with respect to the principal axes for all ions, we have a spread in the values of l, m, n. For small variations, since $(l^2 + m^2 + n^2) = 1$, we have

$$l\,\delta l + m\,\delta m + n\,\delta n = 0, \tag{3.92}$$

and if **H** is along a principal axis for the median point of the distribution (say along [100]) we have $m = n = 0$ and hence $\delta l = 0$. Then from a formula such as (3.5) we have

$$g\,\delta g = l\,\delta l g_x^2 + m\,\delta m g_y^2 + n\,\delta n g_z^2 \tag{3.93}$$

and clearly $\delta g = 0$ when **H** is along a principal axis. Since all spin Hamiltonian parameters such as D'', A, P (see eqns (3.30), (3.44), (3.47))

appropriate to a strong external field vary in a manner dependent on l^2, m^2, n^2, the spread in field $\langle \delta H^2 \rangle$ due to mosaic structure also vanishes in first order when **H** is along a principal axis.

For simplicity we now restrict discussion to the case of axial symmetry. Then, from eqn (3.14), writing $g_\parallel$, $g_\perp$ for g_z, g_x, we have

$$g(\partial g/\partial\theta) = (g_\perp^2 - g_\parallel^2)\sin\theta\cos\theta$$

and hence, using (3.90),

$$\langle \delta H^2 \rangle = (h\nu/g^3\beta)^2(g_\perp^2 - g_\parallel^2)^2 \sin^2\theta\cos^2\theta\langle\delta\theta^2\rangle, \tag{3.94}$$

which obviously vanishes always if $g_\parallel = g_\perp$ (no anisotropy), but otherwise only at the extrema $\theta = 0$ and $\pi/2$. Similarly we have for the second degree fine structure parameter in strong magnetic field ($g\beta H \gg D''$),

$$D'' = D\{(3g_\parallel^2/g^2)\cos^2\theta - 1\}$$

from which

$$\partial D''/\partial\theta = -2D(3g_\parallel^2/g^2)\sin\theta\cos\theta, \tag{3.95}$$

which again vanishes at $\theta = 0$ and $\pi/2$. For fine structure splittings of higher degree there may be intermediate positions where the splitting parameter is independent of small angular variations. For example, in a cubic field the splitting parameter $p = 1 - 5(l^2m^2 + m^2n^2 + n^2l^2)$ has stationary values (independent of small variations in three mutually perpendicular directions) along the fourfold, threefold, and twofold axes, as can be verified from the formulae in § 3.4. Hence we would expect spreading in the resonance line to vanish when **H** is along any of these axes, as far as small random variation in crystallite orientation is concerned. This has been verified by Shaltiel and Low (1961) for Gd^{3+} in ThO_2, where the splitting is predominantly due to the fourth-degree cubic field parameter (in fact the splitting due to the sixth-degree parameter has extrema along the same axes).

Whatever the cause of the variation in the fine structure parameters, the resulting line widths in strong external magnetic fields are largest for lines furthest from the centre of the spectrum, being just proportional to the distance from the centre (the same is true for hyperfine lines). Since the fine structure parameters involve only even powers of the magnetic quantum number M, a transition such as $|M\rangle \leftrightarrow |-M\rangle$ is not broadened in first order, though it may be in second or higher order. Thus for an ion with half-integral spin, the 'allowed' transition $|+\tfrac{1}{2}\rangle \leftrightarrow |-\tfrac{1}{2}\rangle$ is not broadened in first order, nor are 'forbidden' transitions such as $|+\tfrac{3}{2}\rangle \leftrightarrow |-\tfrac{3}{2}\rangle$; for integral spin this holds for a

'forbidden' transition such as $|+1\rangle \leftrightarrow |-1\rangle$. In either case $\Delta M = \pm 1$ transitions (except $|+\frac{1}{2}\rangle \leftrightarrow |-\frac{1}{2}\rangle$) are broadened in first order, and the variation in line width for different transitions within the spectrum gives a measure of the variation in the fine (or hyperfine) structure parameters.

Attempts have been made (see Feher 1964, McMahon 1964, Stoneham 1966) to relate the excess line width (which is not necessarily isotropic even in a cubic crystal such as MgO) to strain fields within the crystal. When present, excess line width due to variations in the fine structure parameters is generally larger than that due to variation in the g-value, though both are strongly dependent on the amount of orbital momentum in the ground state. Representative values of the excess width (which may vary of course from crystal to crystal) are given in Table 3.12, for the ions Mn^{2+}, Fe^{2+}, Ni^{2+} in MgO. In the latter two cases the

TABLE 3.12

Measured line widths for three ions in MgO, showing the variation between different lines for each ion, and the large variation from ion to ion. Since the excess line width is due to strains, variations between crystals are to be expected, and the values given here must only be regarded as representative order of magnitude results

Ion	g	Transition	Line width (G)	Reference
Mn^{2+}, $3d^5$, $S = \frac{5}{2}$	2·0014	$\|+\frac{1}{2}\rangle \leftrightarrow \|-\frac{1}{2}\rangle$	0·7	Feher (1964)
		$\|\pm\frac{3}{2}\rangle \leftrightarrow \|\pm\frac{1}{2}\rangle$	0·9 to 2·4	
		$\|\pm\frac{5}{2}\rangle \leftrightarrow \|\pm\frac{3}{2}\rangle$	1·4 to 4·5	
Ni^{2+}, $3d^8$, $S = 1$	2·1728	$\|\pm 1\rangle \leftrightarrow \|0\rangle$	50	Orton *et al.* (1960*a*)
		$\|+1\rangle \leftrightarrow \|-1\rangle$	3	Smith *et al.* (1969)
Fe^{2+}, $3d^6$, $\tilde{S} = 1$	3·428	$\|\pm 1\rangle \leftrightarrow \|0\rangle$	10^3	McMahon (1964)
		$\|+1\rangle \leftrightarrow \|-1\rangle$	20	

$|+1\rangle \leftrightarrow |-1\rangle$ transition (which would be forbidden in the absence of strains) is much narrower than the $|\pm 1\rangle \leftrightarrow |0\rangle$ transitions; coincident with the latter a narrow line has also been observed which is attributed to a 'double quantum' transition. This is essentially a $|+1\rangle \leftrightarrow |-1\rangle$ transition (hence its small line width) which involves the absorption or emission of two quanta instead of one. Thus it occurs at the point where the $|\pm 1\rangle \leftrightarrow |0\rangle$ transitions would occur in the absence of strain, whereas the ordinary $|+1\rangle \leftrightarrow |-1\rangle$ 'forbidden' single quantum transition occurs at twice the frequency at constant field strength, or at half the field strength at constant frequency.

3.14. The weak-field Zeeman interaction for non-Kramers ions

Specific formulae for the weak-field Zeeman effect, where the Zeeman splitting is small compared with fine structure splittings, have not so far been considered except in the cases (see § 3.4) of ions with $S = \frac{5}{2}, \frac{7}{2}$ in a cubic field. In a ligand field of axial symmetry a manifold of $(2S+1)$ states will split into $(S+\frac{1}{2})$ doublets if S is half-integral, or S doublets and one singlet if S is integral. If the ligand field splitting is large compared with the Zeeman (and other, such as hyperfine) interactions, each doublet can be treated using an effective spin Hamiltonian with an effective spin $\tilde{S} = \frac{1}{2}$. For a set of Kramers doublets this was illustrated in § 1.8 by the example of a $4f^1$ ion in its ground state $J = \frac{5}{2}$. The position for non-Kramers ions is rather different, and we first illustrate the problem by means of another simple example.

Assume we have an ion with $S = 2$, subject to a strong axial splitting represented by a term $D\{S_z^2 - \frac{1}{3}S(S+1)\}$. Then, if a magnetic field $\mathbf{H}$ is applied at an angle θ to the symmetry axis (the z-axis) in the zx-plane, the spin Hamiltonian is

$$\mathscr{H} = D\{S_z^2 - \tfrac{1}{3}S(S+1)\} + g_{\parallel}\beta H S_z \cos\theta + g_{\perp}\beta H S_x \sin\theta. \quad (3.96)$$

Under the conditions $g\beta H \ll D$, the energy levels and states are in first order (see Fig. 3.24(a) and (b))

$$\begin{aligned} |\pm 2\rangle \quad & W_{\pm 2} = +2D \pm 2g_{\parallel}\beta H \cos\theta, \\ |\pm 1\rangle \quad & W_{\pm 1} = -D \pm g_{\parallel}\beta H \cos\theta, \\ |0\rangle \quad & W_0 = -2D, \end{aligned}$$

with no allowed transition in either doublet. In second-order perturbation theory the calculation is complicated because the states $|\pm 1\rangle$, which are degenerate when $\cos\theta = 0$, each has a matrix element of $g_{\perp}HS_x \sin\theta$ with the state $|0\rangle$. Similar difficulties arise if a small rhombic splitting term $E(S_x^2 - S_y^2) = \frac{1}{2}E(S_+^2 + S_-^2)$ is present; not only does this split the $|\pm 1\rangle$ states in first order, but it also splits the $|\pm 2\rangle$ states in second order through their matrix element with $|0\rangle$. A useful trick in such cases is to use as the basis states $|2^s\rangle$, $|2^a\rangle$, $|1^s\rangle$, $|1^a\rangle$ which are simple linear combinations of the form

$$|2^s\rangle = \frac{1}{\sqrt{2}}\{|+2\rangle + |-2\rangle\}, \qquad |2^a\rangle = \frac{1}{\sqrt{2}}\{|+2\rangle - |-2\rangle\}$$

The energy matrix and energy levels for the spin Hamiltonian (3.96) together with the term $E(S_x^2 - S_y^2)$ are given in Table 3.13, correct to

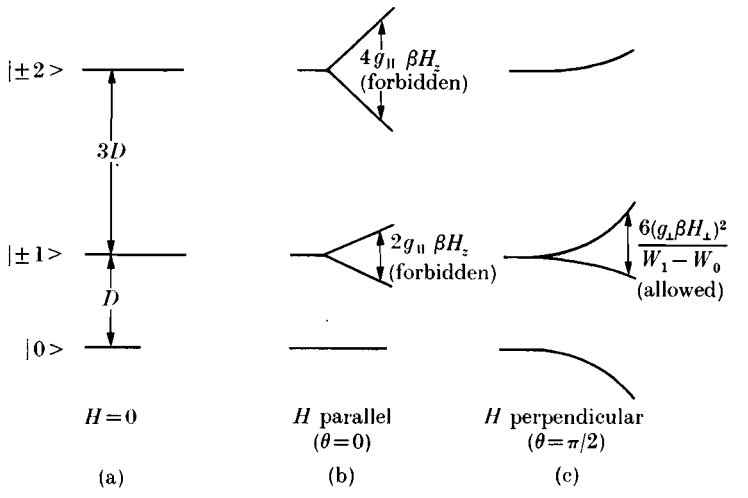

FIG. 3.24. Energy levels corresponding to $S = 2$ for the spin Hamiltonian (3.96) with (a) $H = 0$, (b) H parallel to z-axis (the symmetry axis), (c) H perpendicular to the z-axis.

second order in perturbation theory. This shows the following:

$E = 0$.

No allowed transition within the $|\pm 2\rangle$ doublet, but for the $|\pm 1\rangle$ doublet each state is an admixture of the form $|+1, 0, -1\rangle$ for an arbitrary value of θ, and a transition is weakly allowed except when **H** is along the z-axis ($\theta = 0$) through the second-order Zeeman effect, as shown in Fig. 3.24(c). (The splitting of the $|\pm 1\rangle$ doublet states due to the second-order Zeeman effect can also be seen in Fig. 1.7 for $S = 1$.)

$E \neq 0$.

The states are again admixed, but both for $|\pm 1\rangle$ and for $|\pm 2\rangle$. However, if either $\theta = 0$ or we can neglect the small splitting of order $(g_\perp \beta H \sin\theta)^2/(W_1 - W_0)$ of the $|\pm 1\rangle$ states, we have for both doublets energy levels of the form (see Fig. 3.25)

$$W_\pm = \pm\tfrac{1}{2}\{(\tilde{g}_\parallel \beta H \cos\theta)^2 + \Delta^2\}^{\frac{1}{2}}, \tag{3.97}$$

where for the $|\pm 2\rangle$ doublet $\tilde{g}_\parallel = 4g_\parallel$, $\Delta_2 = 12E^2/(W_2 - W_0)$, and for the $|\pm 1\rangle$ doublet $\tilde{g}_\parallel = 2g_\parallel$, $\Delta_1 = 6E$, neglecting small corrections to $\tilde{g}_\parallel$ that arise from admixtures of the other states. In each case the states can be written in the form

$$\left.\begin{aligned} |+'\rangle &= \cos\alpha\,|+\rangle + \sin\alpha\,|-\rangle, \\ |-'\rangle &= \sin\alpha\,|+\rangle - \cos\alpha\,|-\rangle, \end{aligned}\right\} \tag{3.98}$$

TABLE 3.13

Energy matrix and energy levels for $S = 2$ with the spin Hamiltonian

$$\mathscr{H} = D\{S_z^2 - \tfrac{1}{3}S(S+1)\} + E(S_x^2 - S_y^2) + g_{\parallel}\beta H S_z \cos\theta + g_{\perp}\beta H S_x \sin\theta.$$

The perturbation denominators are written $(W_2 - W_1)$, etc., because this indicates the origin of the second-order terms and allows the displacement of the energy levels by a diagonal fourth degree term of the form $B_4^0 O_4^0$ to be easily included if present

Energy matrix

	$\|2^s\rangle$	$\|2^a\rangle$	$\|1^s\rangle$	$\|1^a\rangle$	$\|0\rangle$
$\|2^s\rangle$	$2D$	$2g_{\parallel}\beta H\cos\theta$	$g_{\perp}\beta H\sin\theta$	0	$\sqrt{(12)}E$
$\|2^a\rangle$	$2g_{\parallel}\beta H\cos\theta$	$2D$	0	$g_{\perp}\beta H\sin\theta$	0
$\|1^s\rangle$	$g_{\perp}\beta H\sin\theta$	0	$-D+3E$	$g_{\parallel}\beta H\cos\theta$	$\sqrt{(3)}g_{\perp}\beta H\sin\theta$
$\|1^a\rangle$	0	$g_{\perp}\beta H\sin\theta$	$g_{\parallel}\beta H\cos\theta$	$-D-3E$	0
$\|0\rangle$	$\sqrt{(12)}E$	0	$\sqrt{(3)}g_{\perp}\beta H\sin\theta$	0	$-2D$

Energy levels

$$W_{\pm 2} = 2D + \frac{(g_{\perp}\beta H\sin\theta)^2}{W_2 - W_1} + \tfrac{1}{2}\Delta_2 \pm \{(2g_{\parallel}\beta H\cos\theta)^2 + (\Delta_2/2)^2\}^{\frac{1}{2}},$$

$$W_{\pm 1} = -D + \frac{(g_{\perp}\beta H\sin\theta)^2}{W_1 - W_2} + \frac{3(g_{\perp}\beta H\sin\theta)^2}{2(W_1 - W_0)} \pm$$

$$\pm\left[(g_{\parallel}\beta H\cos\theta)^2 + \left\{3E + \frac{3(g_{\perp}\beta H\sin\theta)^2}{2(W_1 - W_0)}\right\}^2\right]^{\frac{1}{2}}$$

$$W_0 = -2D + \frac{12E^2}{W_0 - W_2} + \frac{3(g_{\perp}\beta H\sin\theta)^2}{W_0 - W_1}$$

where $\Delta_2 = \dfrac{12E^2}{W_2 - W_0}$.

where $\tan 2\alpha = \Delta/(\tilde{g}_{\parallel}\beta H\cos\theta)$, and $|+\rangle$, $|-\rangle$ are the states in the limit $(\Delta/H) = 0$, while in the opposite limit of $(H/\Delta) = 0$ the states are $(1/\sqrt{2})\{|+\rangle \pm |-\rangle\}$. The states (3.98) have a matrix element linking them of $\langle +'|\, \tilde{g}_{\parallel}\beta S_z\, |-'\rangle = \frac{1}{2}\tilde{g}_{\parallel}\beta\sin 2\alpha$, so that transitions are allowed between the two levels for an oscillating magnetic field along the z-axis whose probability is given by (cf. eqn (2.51))

$$|\mu_{ij}|^2 = |\mu_z|^2 = \tfrac{1}{4}\tilde{g}_{\parallel}^2\beta^2\frac{\Delta^2}{(\tilde{g}_{\parallel}\beta H\cos\theta)^2 + \Delta^2}$$

$$= \tfrac{1}{4}\tilde{g}_{\parallel}^2\beta^2\frac{\Delta^2}{(\hbar\omega)^2} \tag{3.99}$$

and which require a quantum

$$\hbar\omega = h\nu = \{(\tilde{g}_{\parallel}\beta H\cos\theta)^2 + \Delta^2\}^{\frac{1}{2}}. \tag{3.100}$$

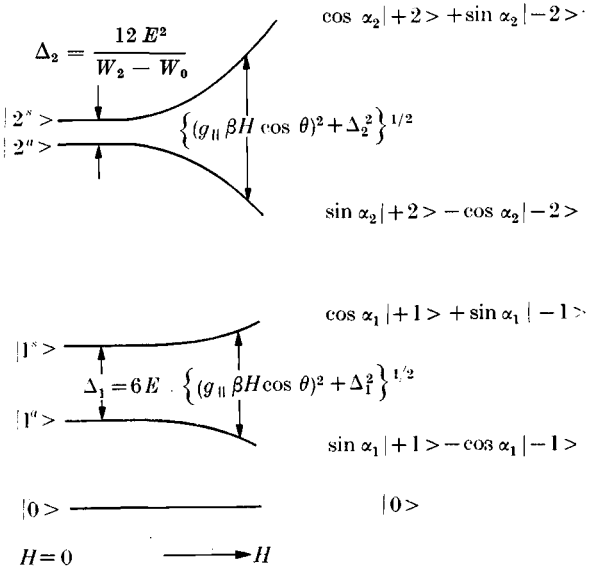

FIG. 3.25. Energy levels and states corresponding to Table 3.13, but neglecting terms of order $(g\beta H)^2/\Delta W$, where ΔW equals $W_2 - W_1$ or $W_1 - W_0$. The states in zero magnetic field are shown on the left, the modified states in a field **H**, with a component $H\cos\theta$ along the z-axis, on the right.

An example of such a transition occurs in the ground doublet ($S_z = \pm 2$) of Fe^{2+}, $3d^6$, $S = 2$ in ZnF_2 which has rhombic symmetry (Tinkham 1956*a*). Such transitions are allowed transitions, though from eqn (3.99) their probability diminishes with the inverse square of the frequency, and the line shape is normal. The value of Δ will obviously be larger for the $|\pm 1\rangle$ doublet than for the $|\pm 2\rangle$ doublet, depending on E in the former case and on $E^2/(W_2 - W_0)$ in the second case. These conclusions are not substantially altered by the presence of fine-structure terms of the fourth degree, such as $B_4^0 O_4^0 + B_4^2 O_4^2 + B_4^4 O_4^4$. The first of these is diagonal, the second has matrix elements between states differing by 2 in S_z and thus behaves similarly to

$$B_2^2 O_2^2 = \tfrac{1}{2} B_2^2 (S_+^2 + S_-^2) = E(S_x^2 - S_y^2),$$

while the last connects states differing by 4 in S_z and thus splits the $|\pm 2\rangle$ levels in first order.

When $E = 0$, and H is zero, we are in the anomalous position that if we take the doublet states as $|\pm 2\rangle$, $|\pm 1\rangle$ there appear to be no allowed transitions within either doublet, but if we take any linear combinations (which should be equally valid as basis states) such as

$|2^s\rangle$, $|2^a\rangle$, $|1^s\rangle$, $|1^a\rangle$ for which there are matrix elements

$$\langle 2^s|\, S_z\, |2^a\rangle = 2\langle 1^s|\, S_z\, |1^a\rangle$$

we expect to find allowed transitions if the oscillatory magnetic field is along the z-axis. In practice there will always be some perturbation, such as a component H_z due to the external or the local field, or a deviation from axial symmetry, which lifts the degeneracy and gives properly defined states.

In this situation strains that upset the axial symmetry (e.g. strains corresponding to $E \neq 0$) play a special role for non-Kramers doublets. In the absence of any strain, and neglecting second and higher-order Zeeman effects, we see that a field **H** with a component H_z along the z-axis splits such a doublet, giving states such as $|\pm 2\rangle$, $|\pm 1\rangle$ with no allowed transitions, corresponding to $\tilde{g}_\perp = 0$ in the effective spin Hamiltonian with $\tilde{S} = \frac{1}{2}$ for each doublet. A rhombic strain will give rise to a small splitting Δ when $H = 0$, and even for a finite H_z the states will be of the form (3.98) for which weak transitions are allowed. If the strains are random, we do not expect sharp energy levels and the resonance line will be broadened. A suitable spin Hamiltonian under these conditions (see § 18.5) is, with $\tilde{S} = \frac{1}{2}$ for each doublet,

$$\mathscr{H} = \tilde{g}_\parallel \beta H_z \tilde{S}_z + \Delta_x \tilde{S}_x + \Delta_y \tilde{S}_y \tag{3.101}$$

for which the energy levels and transition frequency are given by eqns (3.97), (3.100) and the transition probability by (3.99), with

$$\Delta^2 = \Delta_x^2 + \Delta_y^2.$$

The resonance line lies wholly on the high-frequency side of $h\nu = \tilde{g}_\parallel \beta H_z$ at constant H, or on the low-field side of $H_0 = (h\nu/\tilde{g}_\parallel \beta)$ at constant frequency, the displacement being determined by the value of Δ^2. If the line shape is dominated by the spread in Δ^2 rather than by any other source of line width, we have, in place of eqn (2.51), for an oscillatory field $(H_1)_\parallel$ along the z-axis

$$w\, \mathrm{d}(\Delta^2) = \frac{\pi}{2\hbar^2} \{|\mu_z|^2\, (H_1)_\parallel^2\} P(\Delta^2)\, \mathrm{d}(\Delta^2) \tag{3.102}$$

where $P(\Delta^2)$ is the normalized probability distribution in Δ^2. If we assume a random Gaussian distribution for Δ_x, Δ_y we have

$$P(\Delta^2)\, \mathrm{d}(\Delta^2) = \exp\left\{-\frac{\Delta^2}{\Delta_0^2}\right\} \mathrm{d}\left(\frac{\Delta^2}{\Delta_0^2}\right), \tag{3.103}$$

where Δ_0^2 is the most probable value of Δ^2. On inserting eqn (3.103) into (3.102) and using eqn (3.99) we see that the transition rate is zero for $\Delta = 0$ and for $\Delta = \infty$, with an asymmetrical line shape. If the resonance is observed at constant frequency and variable field, and $\Delta_0 \ll (\hbar\omega)$, we can write $H_z = H_0 - h$ where

$$\frac{\Delta^2}{(\hbar\omega)^2} = \frac{2\tilde{g}_{\parallel}\beta h}{(\hbar\omega)}, \tag{3.104}$$

and instead of a frequency distribution we have

$$P(\Delta^2)\,\mathrm{d}(\Delta^2) = \exp(-h/h_0)\,\mathrm{d}(h/h_0), \tag{3.105}$$

where $\tilde{g}_{\parallel}\beta h_0 = \frac{1}{2}\Delta_0^2/(\hbar\omega)$. Then the transition rate is, as a function of field strength,

$$w(h)\,\mathrm{d}h = \frac{\pi}{2\hbar^2}\{\tfrac{1}{2}\tilde{g}_{\parallel}\beta(H_1)_{\parallel}\}^2\left\{\frac{2\tilde{g}_{\parallel}\beta h}{\hbar\omega}\right\}\exp\left(-\frac{h}{h_0}\right)\mathrm{d}\left(\frac{h}{h_0}\right), \tag{3.106}$$

for which a typical line shape is shown in Fig. 3.26(a), with maximum intensity at $h = h_0$.

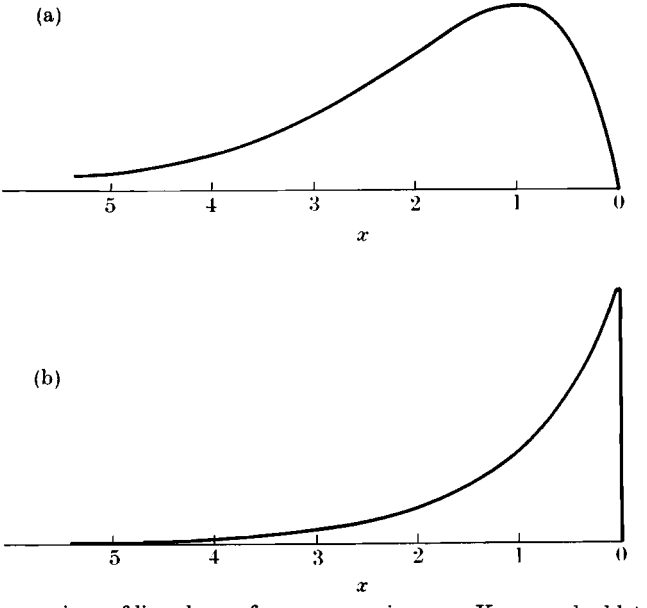

FIG. 3.26. Comparison of line shapes for resonance in a non-Kramers doublet (a) due to an oscillating magnetic field $(H_1)_{\parallel}$ along the symmetry axis, (b) due to an oscillating electric field $(E_1)_{\perp}$ normal to the symmetry axis. The quantity $x = (h/h_0)$, where h,h_0 are defined in the text; $h = H_0 - H_z = (\hbar\omega/\tilde{g}_{\parallel}\beta) - H_z$, so that increasing h (or x) means decreasing field strength H_z at constant frequency. The units for intensity are arbitrary and not the same in (a) and (b).

If the paramagnetic ions occupy sites whose point symmetry is such that there are one or more planes that are not planes of reflection symmetry, there may be an electric dipole moment normal to any such plane (see § 15.10). For a non-Kramers ion in a ligand field of axial symmetry, the important term in the (anisotropic) interaction of such an electric dipole moment with an applied electric field, which we may write in the form

$$\mathscr{H}_E = \beta(\tilde{\mathbf{S}} \cdot \mathbf{g}^{(E)} \cdot \mathbf{E}) \tag{3.107}$$

where $\mathbf{E}$ is the local applied field (which may be different from the external field), will be

$$g_\perp^{(E)}\beta(\tilde{S}_x E_x + \tilde{S}_y E_y). \tag{3.108}$$

Such a term is allowed if the site symmetry lacks reflection symmetry in planes containing the z-axis, and is thus possible, for example, for C_{3h} symmetry but not for C_{3v}. If an oscillatory electric field $(E_1)_\perp$ is applied normal to the z-axis, transitions can be induced within the doublet, and instead of (3.102) we have for the transition rate

$$w\,\mathrm{d}(\Delta^2) = \frac{\pi}{2\hbar^2}\{|\mu_x|^2 + |\mu_y|^2\}(E_1)_\perp^2 P(\Delta^2)\,\mathrm{d}(\Delta^2) \tag{3.109}$$

where

$$|\mu_x|^2 + |\mu_y|^2 = (\tfrac{1}{2}g_\perp^{(E)}\beta)^2\left\{1 - \left(\frac{\Delta}{\hbar\omega}\right)^2\right\} \tag{3.110}$$

This differs from (3.99) in the important respect that it is a maximum at $\Delta^2 = 0$, leading to a different line shape in which maximum intensity occurs at the undisturbed frequency $\hbar\omega = \tilde{g}_\parallel \beta H_0$, since a strain ($\Delta^2 \neq 0$) is no longer needed to produce an allowed transition. Under these circumstances we have instead of eqn (3.106) a transition rate as a function of magnetic field strength $h = H_0 - H_z$ at constant frequency given by

$$w(h)\,\mathrm{d}h = \frac{\pi}{2\hbar^2}\{\tfrac{1}{2}g_\perp^{(E)}\beta(E_1)_\perp\}^2\left\{1 - \left(\frac{h}{H_0}\right)\right\}^2 \exp\left(-\frac{h}{h_0}\right)\mathrm{d}\left(\frac{h}{h_0}\right) \tag{3.111}$$

The line shape as a function of h when transitions are due to a perpendicular oscillatory electric field only is shown in Fig. 3.26(b), the maximum intensity now falling at $h = 0$.

In a resonant cavity at microwave frequencies a sample can be placed in a position of maximum $(H_1)_\parallel$ or of maximum $(E_1)_\perp$, and (if sufficiently small) it can experience one field without the other. The results of an experiment (Williams (1967)) on yttrium ethylsulphate

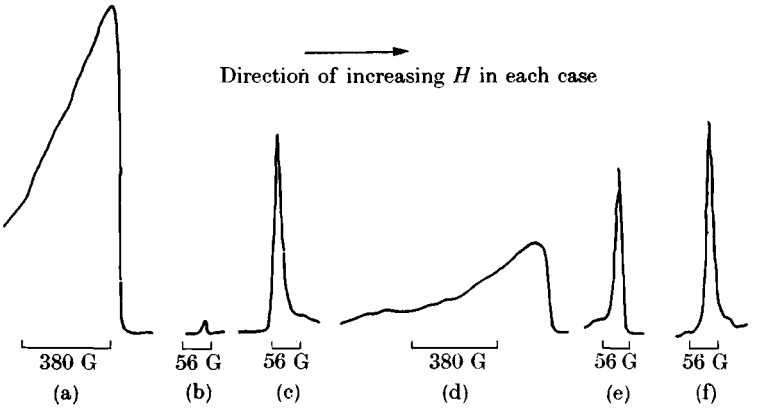

FIG. 3.27. Comparison of absorption intensities due to oscillatory 'electric' and 'magnetic' fields for the non-Kramers doublet ground state of Pr^{3+} in yttrium ethylsulphate. The purely 'magnetic' resonance of Nd^{3+} ions in the sample and in another crystal is used as a reference signal.

(a) Pr^{3+}
(b) Nd^{3+} } in sample at position of maximum $(E_1)_\perp$ and minimum $(H_1)_\parallel$;
(c) Nd^{3+} in second crystal used as reference signal for (a), (b);
(d) Pr^{3+}
(e) Nd^{3+} } in sample at position of minimum $(E_1)_\perp$ and maximum $(H_1)_\parallel$;
(f) Nd^{3+} in second crystal used as reference signal for (d), (e).
(After Williams (1967).)

(symmetry C_{3h}) containing small amounts of Pr^{3+} and Nd^{3+} ions, whose ground states are a non-Kramers and a Kramers doublet respectively, are shown in Fig. 3.27. This shows from the comparison of intensities that the transition in the non-Kramers doublet is primarily due to $(E_1)_\perp$ rather than to $(H_1)_\parallel$, with a corresponding line shape in which the maximum is close to $h = 0$.